

Ulm University Hospital

Institute of Virology

Director: Prof. Dr. med. Thomas Mertens

**HCMV enters into M1- and M2- macrophages
via macropinocytosis in a pH-dependent manner**

Dissertation

To obtain the Doctoral Degree of Human Biology (Dr. Biol. Human) at the

Faculty of Medicine, University of Ulm

Presented by

Li Wang

from Beijing

2012

Dean of the Faculty: Prof. Dr. Thomas Wirth

1. Reviewer: Prof. Dr. Thomas Mertens

2. Reviewer: Prof. Dr. Paul Walther

Day doctorate awarded: 24.05.2013

| | |
|---|-----------|
| Abbreviations: | I |
| 1. Introduction: | 1 |
| 1.1 Pathways of virus entry into cells | 1 |
| 1.1.1 Clathrin-mediated endocytosis | 4 |
| 1.1.2 Caveolin/raft-mediated endocytosis..... | 4 |
| 1.1.3 Macropinocytosis..... | 5 |
| 1.1.4 Phagocytosis | 5 |
| 1.1.5 Viral entry by membrane fusion | 7 |
| 1.2 The human cytomegalovirus | 7 |
| 1.2.1 Morphology of virus particles..... | 8 |
| 1.2.2 Viral life-cycle | 9 |
| 1.2.3 Pathogenesis | 11 |
| 1.2.4 Entry into target cells | 12 |
| 1.3 The Macrophages | 13 |
| 1.3.1 M1- and M2- macrophages | 13 |
| 1.3.2 Macrophages and HCMV | 14 |
| 1.4 Aim of the study | 15 |
| 2. Materials and methods | 16 |
| 2.1 Instruments | 16 |
| 2.2 Chemicals | 17 |
| 2.3 Antibodies | 19 |
| 2.4 Viruses | 20 |
| 2.5 Cells | 20 |
| 2.6 Cell media | 20 |
| 2.7 Cell buffer | 21 |
| 2.8 Inhibitors stock solutions | 23 |
| 2.9 Production of cell free virus and titration | 24 |
| 2.10 Production of monocytes derived macrophages | 25 |
| 2.11 Cultivation of HFFs | 26 |
| 2.12 Indirect Immunofluorescence assay (IIF) | 27 |
| 2.13 Sample preparation for Transmission Electron Microscopy | 27 |
| 2.14 Sample preparation for Scanning Electron Microscopy | 30 |
| 2.16 Flow cytometry analyses (FACS) | 31 |
| 3. Results: | 32 |
| 3.1 HCMV enters into M2-Mϕ more efficiently than into M1-Mϕ | 32 |
| 3.1.1 Mock- and HCMV-infected M1- and M2-M ϕ have similar morphology | 32 |
| 3.1.2 HCMV localizes in the periphery of M1-M ϕ , but accumulates closed to nucleus in M2-M ϕ | 33 |

| | |
|--|-----------|
| 3.1.3 Internalization of HCMV into M1- than M2-M ϕ | 36 |
| 3.2 Cytoskeleton remodeling is required for HCMV infection..... | 38 |
| 3.2.1 Morphology of cytoskeleton remodeling in M1- and M2-M ϕ | 38 |
| 3.2.2 The cytoskeleton interacts with HCMV particles during entry in M1- and M2-M ϕ | 41 |
| 3.2.3 The viral gene expression is inhibited by actin cytoskeleton inhibitor | 43 |
| 3.2.4 Latrunculin A does not interfere with the metabolic activity of M1- and M2- M ϕ | 46 |
| 3.3 HCMV internalization into M1- and M2-Mϕ occurs via a macropinocytosis-like pathway..... | 48 |
| 3.3.1 Morphology of vesicles containing virus particles in M1- and M2- M ϕ | 48 |
| 3.3.2 HCMV internalization into M1- and M2- M ϕ is impaired by EIPA | 50 |
| 3.4 HCMV infection of M1- and M2-Mϕ depends on endosomal acidification | 53 |
| 3.4.1 Neutralization of the endosomal pH inhibits HCMV internalization into M1- and M2- M ϕ | 53 |
| 3.4.2 Lysosomotropic agents do not alter metabolic activities of M1- and M2-M ϕ | 56 |
| 3.5 HCMV viral particles do not co-localize with late endosomes but only with early endosomes | 58 |
| 3.5.1 HCMV do not co-localize with late endosomes in M1- and M2-M ϕ | 58 |
| 3.5.2 HCMV does not co-localize with gold labeled vesicles representing late endosomes | 59 |
| 4. Discussion | 63 |
| 5. Summary | 69 |
| 6. Reference..... | 71 |

Abbreviations:

| | |
|--------|-------------------------------------|
| Ab | Antibody |
| AEC | 3-amino-9-ethycarbazole |
| AIDS | acquired immunodeficiency syndrome |
| bp | base pair |
| BSA | bovine serum albumin |
| CSF | colony-stimulating factor |
| DC | dendritic cells |
| DMSO | Dimethyl sulfoxide |
| dpi | day(s) post infection |
| ds | double-stranded |
| EDTA | ethylene diamine tetraacetic acid |
| EGFR | epidermal growth factor receptor |
| EtOH | ethanol |
| EM | electron microscopy/microscope |
| EIPA | 5-(N-ethyl-N-isopropyl)-amiloride |
| FACS | fluorescence –activated cell sorter |
| FCS | fetal calf serum |
| FIP | fusion inhibitory peptide |
| FITC | fluorescein isothiocyanate |
| FIG. | Figure |
| GM-CSF | granulocyte-macrophage CSF |
| g | glycoprotein |
| HCMV | human cytomegalovirus |
| HFF | human foreskin fibroblast |
| HIV | human immunodeficiency virus |
| HSPGs | heparan sulphate proteoglycans |

| | |
|-------|--|
| HSV | herpes simplex virus |
| HUVEC | human umbilical vein endothelial cells |
| IE | immediate early |
| IIF | indirect immunofluorescence assay |
| Ig | immunoglobulin |
| LPS | lipopolysaccharide |
| mAb | monoclonal antibody |
| mA | milli Ampere |
| MACS | magnetic-activated cell sorting |
| M-CSF | macrophage CSF |
| MDM | monocytes-derived macrophages |
| MEM | minimum essential medium |
| MeOH | methanol |
| MHC | major histocompatibility complex |
| moi | multiplicity of infection |
| MVB | multivesicular body |
| NIEPs | noninfectious enveloped particles |
| ORF | open reading frame |
| µg | microgram |
| µl | microliter |
| PBMC | peripheral blood mononuclear cells |
| PBS | phosphate buffered saline |
| PBG | 0.2% gelatin and 0.5% BSA in PBS |
| PCR | polymerase chain reaction |
| PFA | phosphonoformic acid |
| PFU | plaque-forming unit(s) |
| pUL | protein encoded by the UL... ORF |

| | |
|-------|---|
| RNA | ribonucleic acid |
| rpm | revolutions per minute |
| rt | room temperature |
| SEM | scanning electron microscopy/microscope |
| TEM | transmission electron microscopy/microscope |
| TRITC | Tetramethylrhodamine-5-(and 6-) - Isothiocyanate |
| WT | wild-type HCMV |

1. Introduction:

1.1 Pathways of virus entry into cells

Entry of virus

Viruses are intracellular parasites that rely on the host cell machinery for their life cycle, because they lack metabolic or motile activities. In order to infect host cells and organisms the virus has to transfer its genome into target cells. Viral entry is the first step to viral infection and replication within cells. During this process viral particles first bind to cell surface structures, this can be proteins, lipids or carbohydrates. In contrast to such unspecific and reversible binding to carbohydrate structures, binding to high affinity receptors is specific and actively promotes viral entry; thereby initiating conformational a cell in the virus and activating cellular signaling. These signaling activities induce specific endocytotic mechanisms [47]. Various endocytotic pathways are offered by host cells, as shown in (Fig. 1). It has been demonstrated that some viruses can penetrate into the cytosol by fusing their membranes directly with the host plasma membrane e.g. Herpes simplex virus 1, (HSV-1) [9], but most virus enter into target cells by endocytosis. One advantage of endocytosis is that the vesicles carrying the viral particles can easily cross the cytoplasm to the perinuclear space, by passing barriers, such as the actin cortex and by exploiting molecular motors recruited to the vesicles [18,51]. In addition, viruses use endocytosis and penetrate intracellular organelles to avoid viral protein exposure on the host membrane in order to delay immune detection [Smith and Helenius 2004]. Another advantage of endocytotic uptake of virus is the possibility to use the special conditions within maturing endosomes, e.g. lower pH, specific proteases for optimal penetration and uncoating of viral particles [51,94]. On the other hand endocytosis of virus particles might lead to degradation upon fusion of the endosome with the lysosomal compartment. By utilizing entry pathways and the trafficking machinery of host cells, a virus can reach its replication site within the target cells, so that it completely progresses throughout the infectious life cycles [85].

Endocytosis

Endocytosis is defined as the process in which a substance gains entry into the cell without diffusing through the plasma membrane. Endocytosis has many physiological roles and it is used to ingest essential nutrients, remove dead or damaged cells from the body, and protect against microorganisms. It is also required for cell adhesion, morphological changes, such as establishment of cellular asymmetry or migration, antigen presentation and mitosis [17]. The process of endocytosis is very complex and a diversity of endocytotic pathways has been discovered in mammalian cells so far (Fig. 1).

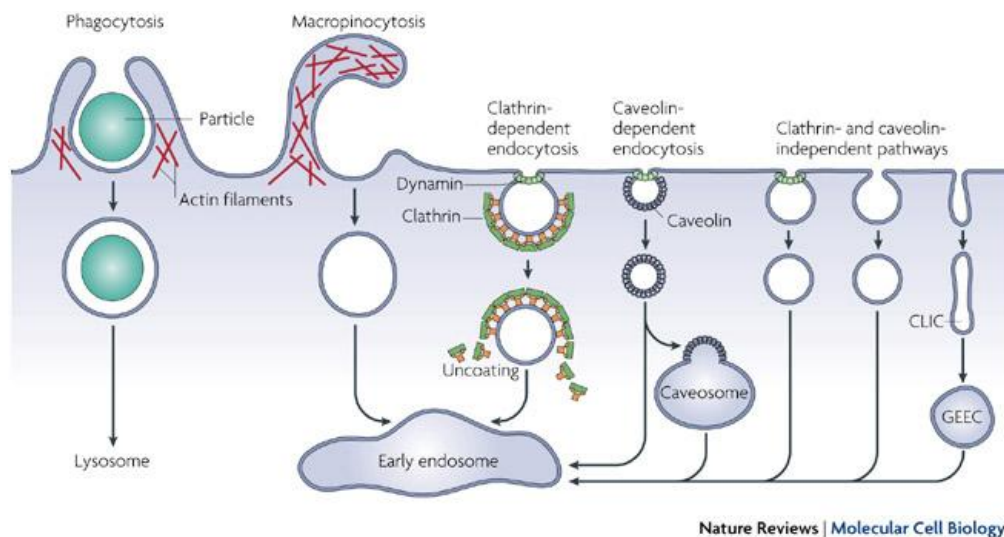


Figure 1: Endocytic uptake into cells. Large particles are taken up by phagocytosis, whereas fluids are taken up by macropinocytosis. Numerous cargos can be endocytosed by clathrin- or caveolin-dependent and independent mechanisms. By some pathways, cargos may first traffic to intermediate compartments such as the caveosome or the glycosyl phosphatidylinositol-anchored protein-enriched early endosomal compartment (GEEC), then they route to the early endosomes (modified from Nature publishing group Parton, R.G. and Simons, K.).

In general, endocytosis starts with the formation of primary endocytotic vesicles, which are converted into heterogeneous endosomal vesicles. These vesicles or endosomes undergo molecular changes that are responsible for sorting, recycling, degradation, storage and transcytosis of cargo. For sake of simplicity, endosomal organelles are divided into early endosome, which are the first and main sorting station for cargo, late endosome, lysosome and recycling endosomes. Early endosomes (EE) are mainly dispersed throughout the cytosol, whereas recycling endosomes (RE) and late endosome (LE) are mainly located

perinuclearly (Fig. 2). Endosomal organelles contain different membrane domains often enriched in different Rab GTPases and their effectors, or phosphoinositides, e.g. Rab 5 on EE, Rab 4 and Rab11/12 on RE (divided into fast and slow recycling, respectively), Rab7 on LE, and finally Rab9/retromer on the trans-Golgi-network. In general, cargo is moved quickly through the endosomal compartments: after internalization, the cargo remains in EE for 2 to 5 minutes, it is delivered into LE in 10 to 15 minutes, and it reaches the lysosomes in 30-60 minutes [36,43,58]. All of the vesicular traffic occurs along cytoskeleton microtubules.

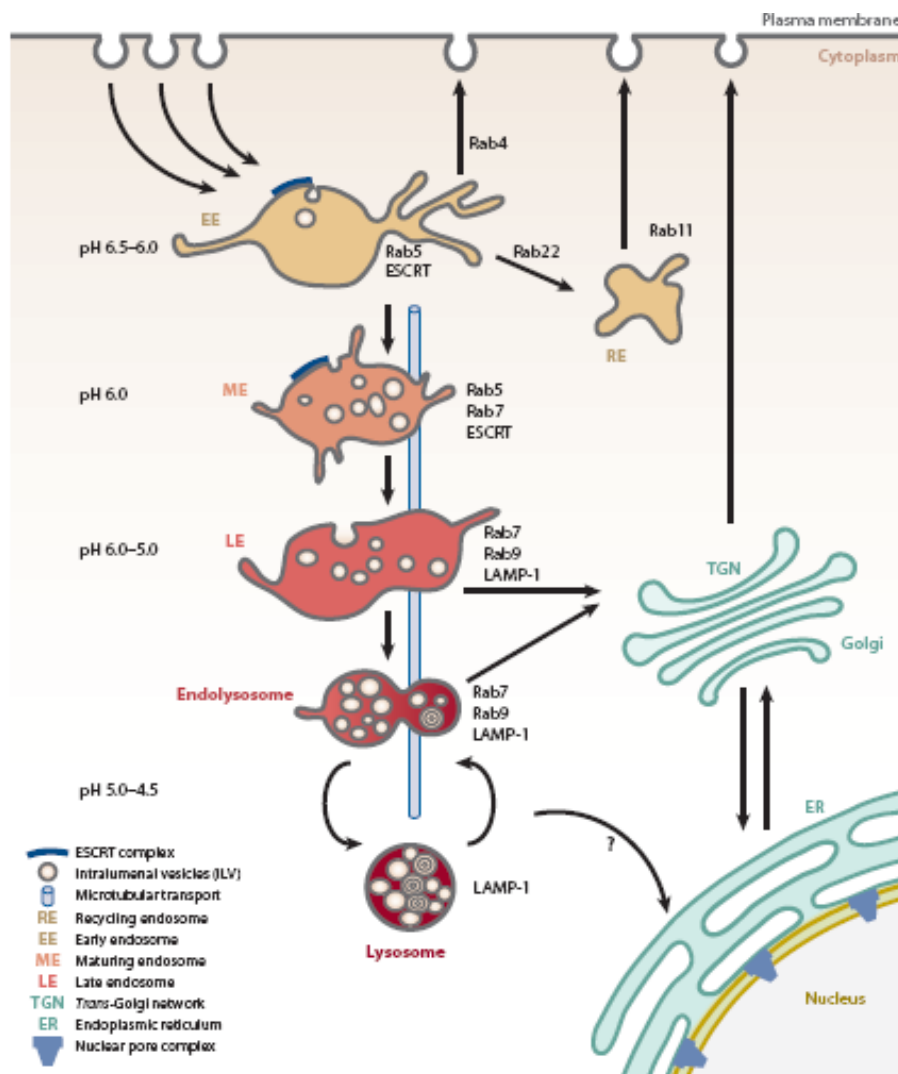


Figure 2: Overview of the various endosomal compartments. After internalization of cargo into endosomal organelles the vesicular traffic and movement of endosomes occur along microtubules and depend on the different acidification of the vesicles (Modified from Mercer et al. 2010).

Viruses employ various endocytotic routes that are distinguished by i) the mode of how the material is engulfed at the cell surface, ii) the cellular proteins involved in the membrane curvature and pinching-off of vesicles and iii) the final destination of the vesicles. Several common endocytotic pathways observed during uptake of virus particles into host cells are described in detail below.

1.1.1 Clathrin-mediated endocytosis

Clathrin-mediated endocytosis is the best- understood endocytotic pathway [17] and is characterized by formation of clathrin-coated pits, namely invaginations of the cytoplasmic face of the plasma membrane associated to aggregates of clathrin [33,80]. Cargo, such as a virus, can induce the formation of clathrin-coated pits that are pinched out from the plasma membrane and released free in the cytosol by the action of the GTPase dynamin. This process is highly regulated and many proteins are also involved and interact with clathrin. Typically, PI4, 5P₂ as regulator protein for the recruitment of the adaptor protein AP2, further adaptors such as AP180 and Eps15 are required for cargo selection and immobilization [105]. Clathrin mediated endocytosis is a fast constitutive process and since it takes about 1 minute to form individual pits, this pathway provides an efficient route for virus entry. After viruses are taken up by clathrin-coated endocytosis, they are transported to early or late endosomes where the acidic pH leads to conformational changes in the particles and triggers the fusion of the viral and the endosomal membranes [47]. The first virus described to enter cells via clathrin-coated vesicles was Semliki Forest Virus (SFV) [29]. Up to now, this mechanisms of viral entry has been described for many other viruses, such as Adenovirus 2 and 5, Hepatitis C virus, Denguevirus, influenza A virus , SARS, Coronavirus, and Vesicular Stomatitis Virus (VSV) [47,51,54,99].

1.1.2 Caveolin/raft-mediated endocytosis

The caveolin/raft mediated endocytosis is different from clathrin-mediated endocytosis since it is lipid raft-dependent. Lipid rafts are specialized membrane microdomains characterized by different lipid compositions (enriched in cholesterol and sphingolipids) as compared to the plasma membrane from which they are derived. These domains contain caveolin proteins and appear by the electron microscopy as flash shaped invaginations of the plasma membrane [16,66-68,86]. Caveolins form the shape and structure of these

invaginations, which have usually a diameter of 50-80 nm [48]. Viruses such as Simian virus 40 (SV40), Echo 1 virus and Papilloma viruses as well as certain bacteria make use of this uptake mechanism [38,66,94]. The internalized viruses are either routed to acidic early endosomes or to caveosomes from where they are further transported to their replication sites [47,48].

1.1.3 Macropinocytosis

Macropinocytosis has diverse biological functions ranging from nutritional uptake in amoebas [39], to extensive sampling of soluble antigens in immature dendritic cells. Unlike other endocytotic pathways such as clathrin-coated and caveolin-mediated endocytosis, macropinocytosis requires extensive actin cytoskeletal reorganization [51], so that the plasma membrane forms large membrane extensions that surround and enclose large amounts of extracellular fluids. Macropinocytosis is a nonspecific internalization process to uptake large amount of fluids and solutes and it does not rely on ligand binding to a specific receptor [41,50,85]. However, in most situations, macropinocytosis is a transient mechanism induced upon growth-factor stimulations of the cells [62,85]. The macropinosomes are relatively large in size with diameter of up to 10 μm [17,51,85]. The activation of macropinocytosis and formation of primary endosome vesicles requires cellular factors such as sodium/proton exchanger and the Rho GTPases Rac1 and/or cdc42, various cellular kinases, CtB1 and cholesterol [35,50]. The macropinosomes can be recycled to the plasma membrane, undergo intraluminal acidification, and either homotypic or heterotypic fusion with early endosomes [30,74,100]. A variety of viruses use macropinocytosis to enter their host cells such as: Vaccinia virus and Kaposi's sarcoma-associated Herpesvirus [50,75].

1.1.4 Phagocytosis

Phagocytosis is an endocytotic pathway specific for the uptake of large pathogens with diameter of more than 1 μm [48,50]. While in lower organisms phagocytosis assures nutrient acquisition [1], in mammalian cells phagocytosis is mainly relevant for the degradation of large particles, such as apoptotic cell debris and pathogens [1,14]. During phagocytosis many cellular factors such as actin, RhoA, tyrosine kinases, cholesterol and dynamin-2 are involved in formation of primary endosomal vesicles and vesicular

trafficking in the cytosol. After ligand binding to a receptor, the receptor activation drives the formation of local actin-protrusions of the plasma membrane that extend until the particle is completely enclosed into a phagosome [1,51]. The phagosome undergoes maturation by fusing and fissioning with other endosomal compartments so that gradual acidification takes place and allows particle degradation [1]. The best characterized example of virus uptake by phagocytosis is mimivirus. In addition amoebal pathogens and HSV-1 enter into fibroblasts also through phagocytosis [25,102].

An overview of the cellular factors involved in the four endocytosis pathways, is provided in the following Table 1.

Table 1: Overview of the main cellular endocytotic pathways and the relative key cellular factors

| Endocytosis | Clathrin-mediated | Caveolin-mediated | Macropinocytosis | Phagocytosis |
|---------------------------|--|---|--|--|
| Coat proteins | Clathrin | Caveolin-1 | None | None |
| Adaptors | AP2, eps15, epsin1 | none | Unknown | AP2 |
| Scission factors | Dynamin-2 | Dynamin-2 | Unknown | Dynamin-2 |
| Regulatory factors | PI(3,4), PI(4,5)P2, cholesterol, cortactin, Arp2/3 | Tyrosine kinase, phosphatases, PKC, RhoA, cholesterol | Tyrosin kinase, Na ⁺ /H ⁺ exchange, PAK1, PI(3)K, PKC, Ras, Rac1, Cdc42, Rab34, CtBP1, cholesterol | Tyrosine kinases, PI(3)K, PKC, Ras, RhoA, RhoG, Rac1, Cdc42, Arf6, cholesterol |
| Cytoskeleton | Actin, microtubules | Actin, microtubules | Actin, microtubules, myosins | Actin, microtubules, myosins |
| Trafficking | Rab5, Rab7, Rab4, Rab11, Rab22 | Rab5 | Rab5, Rab7, Arf6 | Rab5, Rab7 |

Membrane fusion

Even though virus entry into host cells seems to occur mainly by endocytosis, the uptake of enveloped virus can also occur by direct fusion between the plasma membrane and the viral lipid bilayer forming the envelope. The merging of viral and cellular membranes is a

multistep process that can be facilitated by several viral proteins (Fig. 3). Viral proteins can acquire open up conformations and form a bridge between the two bilayers (Fig. 3 a-b), the bridge collapses so that the two membranes comes in close proximity (Fig. 3 c-d); the membranes make a conformational change to reduce the energy barrier and form a fusion pore (Fig. 3 e). The viral capsid can then pass through the fusion pore and reach the cytosol of the target cell [27]. As a result of this process the viral capsids are directly released into the cytoplasm of the host cells as naked capsids.

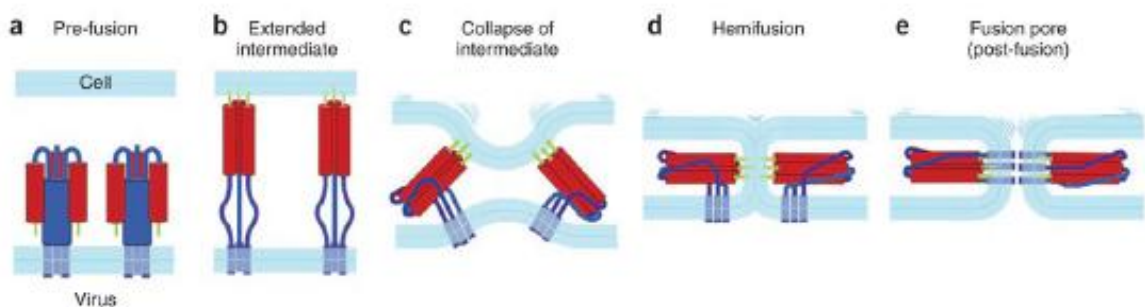


Figure 3: Structural changes of the membrane driven by a viral fusion protein. A) pre-fusion B) extended intermediate. C) collapse of intermediate. D) hemifusion. F) formation of the fusion pore (modified from Harrison et al. 2008).

1.1.5 Viral entry by membrane fusion

The influenza viral protein hemagglutinin is the best characterized viral fusion protein [8,11,110,111]. Flavivirus E and vesicular stomatitis virus G enter their host cells also through membrane fusion [59,77,109]. In addition, depending on the specific cell type HIV and Herpes virus can directly fuse with the plasma membrane and release the capsid into the cytoplasm.

1.2 The human cytomegalovirus

The human cytomegalovirus (HCMV) belongs to the Herpesviridae family, which is divided into three subfamilies: α - , β - , γ -Hepersvirinae, based on special biological

characteristics such as host range, cell tropism, duration of the replication cycle, spread in cell culture and the establishment of latency in different cells types [57,78].

The human α -herpesviruses include herpes simplex virus type 1 (HSV-1 and HSV-2) and the varicella zoster virus (VZV), which are characterized by a fast replication cycle and a rapid spread of infection in cell culture. Latency is established in sensory ganglia. The herpes simplex virus has a broader host range; however varicella zoster virus has a narrow host range restricted to humans and selected cell types of primate and guinea pig origin.

The human cytomegalovirus (HCMV), human herpesvirus type 6 (HHV-6) and 7 (HHV-7) belong to the human β -herpesvirus subfamily. They are characterized by their restricted host range, a slow replication cycle and a slow spread of infection in culture. The typical cytopathic effect induced by HCMV is the enlargement of the host cells and the formation of characteristic nuclear inclusions. The true site of latent infection has not been defined yet but several anatomical locations such as in kidney, secretory glands and lymphoreticular cells have considered as potential sites.

The viruses of the γ -herpesvirus subfamily include Epstein Barr virus (EBV) and human herpesvirus type 8 (HHV8) that replicate *in vitro* only in lymphoblastoid cells.

1.2.1 Morphology of virus particles

The enveloped HCMV particles has a diameter of 150-200 nm and is therefore one of the biggest animal viruses known [76]. The HCMV virion is composed of the nucleocapsid, tegument layer and the surrounding envelope (Fig. 4). The nucleocapsid consists of a linear 230 kbp double-stranded DNA genome and capsid proteins, which are surrounded by at least 25 different viral proteins forming a tegument protein layer [60]. The tegument proteins play important roles for viral replication, immune evasion and transcription. The virus particle is surrounded by an envelope formed by lipid bilayer originated from the producer cell and enclosing at least three viral glycoprotein complexes. The glycoprotein complex I (gCI) is composed of homodimers of the glycoprotein B (UL75), which is an integral membrane protein. The glycoprotein complex II (gCII) consists of two glycoproteins, gM (UL-100) and gN (UL73). In recent research the composition of the third complex (gCIII) has been extensively discussed. As [44] and [12] describe it, gCIII contains glycoprotein gH (UL75), gL (UL115) and gO (UL74). Other groups [2,108] have

described alternative compositions of this glycoprotein complex, namely together with gH and gL, the viral proteins pUL28, pUL130 and pUL131A instead of gO. All three glycoprotein complexes are important for HCMV entry and virus spread. Especially gM and gN contribute to the attachment of virus on host cells, while gB and gH/gL with other components allow viral and host membrane fusion.

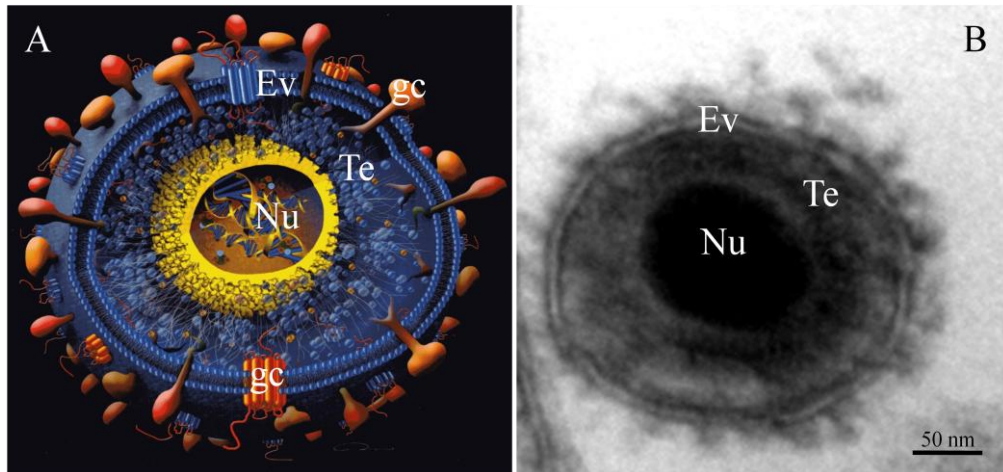


Figure 4: Morphology of HCMV particle. Ev: envelope; Te: tegument; Nu: nucleocapsid; gc: glycoprotein complex. A) Schematic showing the components of a typical HCMV virion: envelope, tegument layer and nucleocapsid (Modified from Streblow et al. 2006) Ultra structural image of HCMV virion obtained at the transmission electron microscope.

HCMV infected cells can produce three types of particles including infectious mature virions (Fig. 4), non-infectious enveloped particles (NIEPs) and dense bodies (DBs). Under electron microscopic observation NIEPs lack an electron dense DNA core compared to mature virions. DBs are amorphous aggregates of mainly the tegument protein pp65 (pUL83) surrounded by a membrane envelope. They are not infectious but play an important role for transcription during HCMV infection in host cells.

1.2.2 Viral life-cycle

In *vivo* HCMV can infect different cell types: epithelial cells, endothelial and hematopoietic cells, fibroblast and smooth muscles cells [88]. In all cell types the infection begins with HCMV entry into the target cells. Notably, the entry mechanism of HCMV is cell type dependent [83], while as example HCMV enters into fibroblast (HFF) by

membrane fusion [12,37], in endothelial and epithelial cells HCMV enters by receptor mediated endocytosis [7,81].

Once in the cytosol, the capsids are transported toward the nuclear pore along microtubules, (mirroring the model proposed for HSV-1 [96]), where the viral genome is released into the nucleus in order to initiate the viral gene expression. HCMV gene expression is strictly temporarily regulated in three phases: immediate-early (IE), early (E), and late (L) [5] phases. Since HFF represent the prototypical cell type infected by HCMV in vitro; the replication cycle in HFF is described here. The IE proteins are the first product after infection and independent of other viral gene expression. IE proteins have important regulatory functions in the host cell and activate the expression of early genes in the nucleus. The products of early genes are frequently enzymes that exert crucial mechanism. Concomitantly with the synthesis of the DNA, late genes, with mainly structural functions, are expressed. The replicated viral DNA is then encapsulated in capsids that are assembled in the nucleus [34] (Fig. 5).

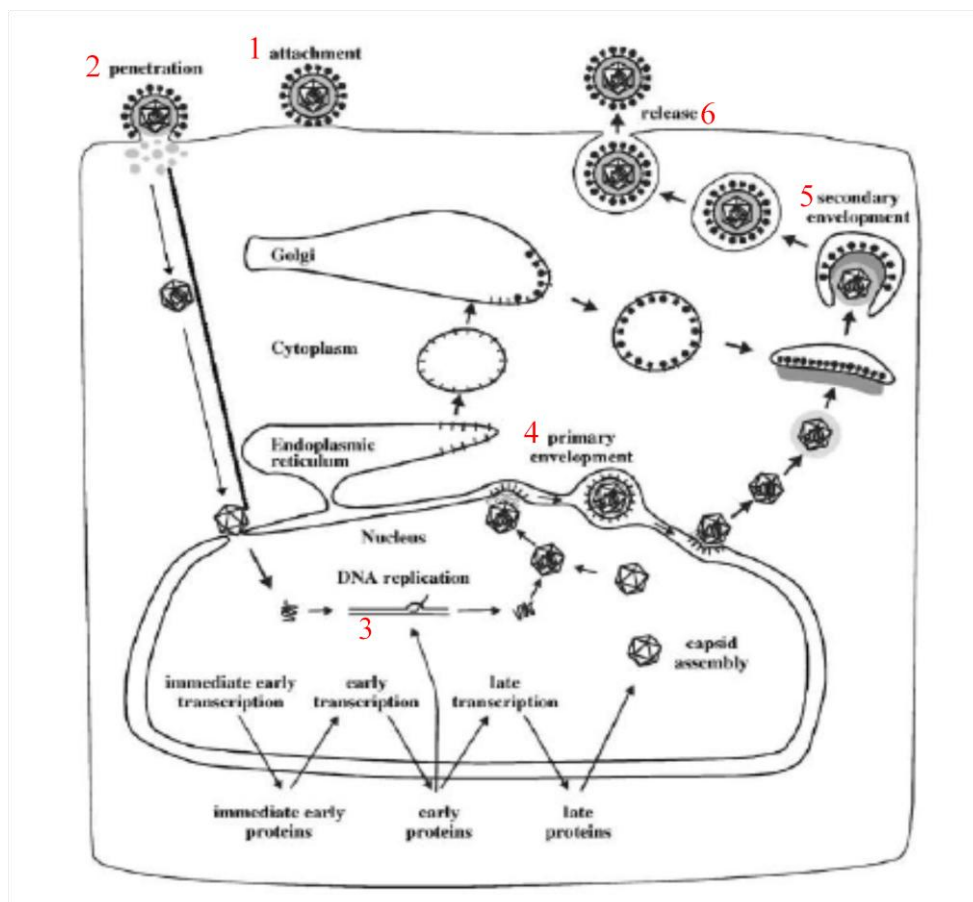


Figure 5: Viral life cycles, the schema shows the subsequent phases of the viral replicative cycle: 1) viral attachment. 2) viral penetration. 3) viral gene expression and genome replication. 4) primary

envelopment. 5) secondary envelopment and 6) release from host cells (modified from Mettenleiter et al. 2004).

Maturation starts in nuclear inclusions, where nucleocapsids mature within a nuclear fibrillar network consisting of viral structural proteins adjacent to a DNA replication compartment. Particles with and without electron-dense DNA cores undergo maturation: A-capsids, lacking a scaffold or DNA core; B-capsids, containing a scaffold but not DNA and C-capsids, containing a DNA core. Progeny nucleocapsids locate to thickened concave patches in the inner nuclear membrane, where they bud into the perinuclear cisternae. The nuclear membrane is modified by viral glycoproteins that are also present on the mature viral envelope. Thus, the initial site of viral envelopment is at the inner nuclear membrane, but the site of final envelopment has not been unambiguously determined and may occur at cytoplasmic membranes through a process of de-envelopment/re-envelopment best characterized in HSV-1 [52,53] (Fig. 5). After membrane fusion with the outer nuclear membrane, the capsids are released into the cytosol of the host cells and obtain the final envelope, consisting either of Golgi-derived membranes [31] or endosome-derived vesicles [104]. Then, as last step, the vesicles containing the viral particles fuse with the plasma membrane and release the viral progeny by exocytosis.

1.2.3 Pathogenesis

HCMV is a common opportunistic human pathogen. In lower socio-economic conditions, up to 90% of human population results HCMV sero-positive [56]. During adult life HCMV infection is transmitted through contact with saliva, tears, blood, urine, semen and cervical secretions. During childhood an additional source of infection is the breast milk and transmission from mother to child, during breastfeeding is a common event. Because of the hormonal changes during pregnancy as Knowles et. Al. 1982 reported, HCMV reactivation often takes place thus leading to vertical transmission. This primary infection of the fetus can cause severe damage of the eyes and liver, or lead to deafness and mental retardation. Primary infection as well reactivation from latency, contributes to pathogenesis. Pathogenesis of HCMV disease is directly linked to the immune status of the host. Immunocompetent individuals control the infection and only rarely show clinically relevant symptoms, On the contrary, immunosuppressed subjects such as organ or bone

marrow transplant recipients and human immunodeficiency virus (HIV)-patients are at risk of severe disease and disseminate multi-organ infections. Typical HCMV associated complications after transplantation are pneumonitis, gastrointestinal lesions, hepatitis, retinitis and dysfunction or rejection of the transplanted organs [15,84]. And in AIDS patients the infection with HCMV can result in retinitis, colitis and esophagitis encephalitis, pneumonitis, hepatitis and gastrointestinal ulceration [15,56] even so directly to death in 20%-30% of these patients.

1.2.4 Entry into target cells

The entry mechanism of HCMV is cell type dependent and so far two different mechanisms have been described: HCMV enters into fibroblast cells by direct fusion at the plasma membrane and into endothelial cells by endocytosis [83]. While HCMV entry into fibroblasts is a pH-independent fusion event leading to a first deposition of naked capsids into the cytosol [12], HCMV entry into endothelial cells requires receptor mediated endocytosis [28,81] and is pH-sensitive. Only under low pH conditions, viral nucleocapsids can be released from the vesicles and reach the nucleus of the host cell. The initial step of virus adhesion to the cell surface is in both cell types mediated by a non-specific, low-avidity interaction of the virus envelope with heparan sulfate proteoglycans (HSPGs) [12]. The stable viral attachment to the cellular surfaces is then promoted by some cellular receptor/factors that have not been so far unequivocally identified. β 2-microglobulin [49], EGFR [109], Annexin II [112], the human aminopeptidase N CD13, [26,97] or integrins [108] have been described as necessary and dispensable by competing authors. It is still confusing whether the interaction of viral components with some cellular receptor/factors activates the entry process directly, by mediating fusion or endocytosis or instead indirectly by triggering intracellular signaling pathways that prepare the cell to the infection. In literature, it has been reported that β 1-integrins and Annexin II [70] can interact with glycoprotein B of HCMV and although this binding did not have a direct effect on HCMV entry of HCMV into fibroblast cells it is likely that it triggers intracellular signaling that indirectly enhances HCMV entry and cell-cell spread [20]. Alternatively the activation of EGFR receptor has been described as a pre-requisite for HCMV entry [10].

1.3 The Macrophages

Macrophages are a heterogeneous population of terminally differentiated myeloid cells; these cells are disseminated in all tissues of the human body and are members of the mononuclear phagocyte system. Macrophages play a crucial role in innate and adaptive immune responses against pathogens, because they can recognize non-self entities, professionally present their antigenic structure to lymphocytes and secrete pro-inflammatory cytokines [65]. The life –span of macrophages ranges from 6 to 16 days.

1.3.1 M1- and M2- macrophages

Two antithetic groups of primary human monocyte-driven macrophages (M ϕ) have been described so far: classically activated M1-M ϕ , which are pro-inflammatory effectors, and alternative activated M2-M ϕ , which exhibit anti-inflammatory properties. In *vitro*, while the hematopoietic growth factor granulocyte-macrophages colony-stimulating factor (GM-CSF) elicits differentiation of monocytes into M1-M ϕ , the macrophages colony-stimulating factor (M-CSF) leads to differentiation of monocytes into M2-M ϕ [22,46,72]. The morphology of these two types of macrophages are almost identical, however they are distinct in their cell surface antigen expression and functions including Fc-gamma receptor mediated-phagocytosis, H₂O₂ production, H₂O₂ sensitivity, catalase activity, susceptibility to HIV-1 and mycobacterium tuberculosis infection and immune suppressor activity [3,4]. M1-M ϕ are able to secrete high amount of interleukin (IL)-12, and IL-23, and therefore M1-M ϕ are responsible for control of intracellular parasites and tumors. In contrast, M2-M ϕ can release high amounts of the anti-inflammatory IL-10, thus driving tissue repair, remodeling and tumor progression. Fig. 6 illustrates the main differences between M1- and M2-M ϕ [46].

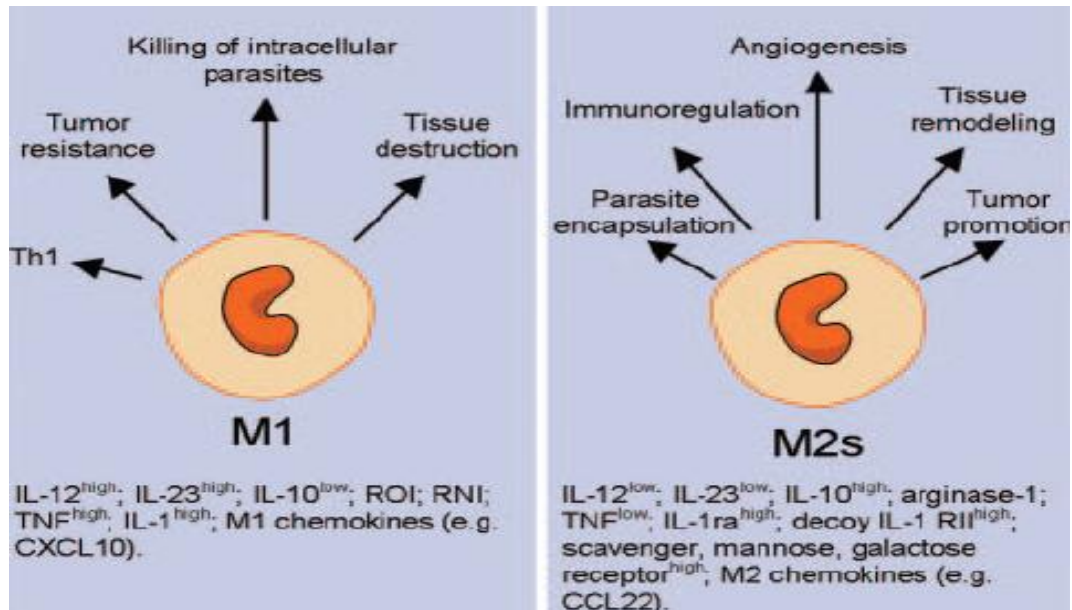


Figure 6: Key properties and functions of polarized M1- and M2-M ϕ . The primary pro-inflammatory M1- and anti-inflammatory M2-M ϕ contribute to immune responses against intracellular and extracellular pathogens. (Modified from Mantovani et al. 2006).

1.3.2 Macrophages and HCMV

Macrophages play opposite roles in the host's antiviral immune reactions and in the viral mechanisms of immune evasion. In *in vivo*, circulating monocytes and tissue macrophages are the predominant cell types harboring HCMV in the peripheral blood as well as in infected organ [90,101]. Macrophages have been described as responsible for HCMV dissemination in the peripheral blood [95], which is possibly mediated by a direct interaction between macrophages and HCMV-infected endothelial cells [24,89]. In healthy HCMV sero-positive subjects, monocytes and macrophages have been described as sites of HCMV persistence/latency and replication, respectively. The actual model hypothesizes that monocytes maintain the HCMV genomes mainly transcriptionally inactive and without release of infectious virus. However inflammatory conditions driving monocytes differentiation into macrophages concomitantly reactivate the "sleeping virus" and lead to completion of the viral cycle and production of infectious viral progeny that can reach different tissues and organs [97].

1.4 Aim of the study

Two distinct types of macrophages (M ϕ) can be produced *in vitro* starting from primary monocytes, namely, the pro-inflammatory M1- and anti-inflammatory M2-M ϕ . Although these cells can be infected by the endotheliotropic strain of HCMV TB40/E, the susceptibility of M1-M ϕ is significantly lower than the susceptibility of M2-M ϕ [23]. Others and we have indeed shown that at 24 hours post infection 30% of M1-M ϕ initiate the viral replication cycle as compared to roughly 70% of M2-M ϕ . The identification of the cellular factors defining the high or low susceptibility to viral infection is an important aim of virological research. Since it has been recently shown that the efficiency of HCMV infection depends on the specific pathway of virus entry and on the efficiency of translocation of the viral capsids to the nucleus [87], we attempted to identify relevant differences between M1- and M2-M ϕ . Starting from the already characterized pathways of HCMV entry, namely the direct fusion of the viral envelope with the cell plasma membrane (mechanisms used to enter fibroblasts) and the pH-dependent endocytosis (mechanism used to enter endothelial cells), we wanted to address whether M1- and M2-M ϕ use differentially/preferentially one of these pathways.

2. Materials and methods

Materials:

2.1 Instruments

| | |
|---------------------------------------|--|
| Aluminium cups for EM | Engineering office M Wohland GmbH, Sennwald, CH |
| Cell scraper 25c | Sarstedt, Nümbrecht, Germany |
| Cellstra tissue culture flask | Greiner Bio-one, Germany |
| Centrifuge tubes | Beckman, Paolo Alto, CA, USA |
| Centrifuges: | |
| Beckmann coulter TM Allegra Tm6 | Beckmann, Munich, Germany |
| Eppendorf Centrifuge 5417C | Eppendorf, Hamburg, Germany |
| Heraeus Megafuge 1.0R | Heraeus, Hanau, Germany |
| Ultracentrifuge Beckmann L7-65 | Beckmann, Munich, Germany |
| Incubator | Heraeus, Hanau, Germany |
| FACS Calibur | Becton Dickinson, Germany |
| High Pressure Freezer: HPF compact 01 | Engineering office M Wohlland GmbH, Sennwald, Switzerland |
| Luminescence Spectrometer LS50B | Peking Elmer, Norwalk, USA |
| MACS separation columns | Miltenyibiotec, Bergisch Gladbach, Germany |
| Commercially available Kits: | |
| CD14 Microbeads human | Miltenyibiotec, Bergisch Gladbach, Germany |
| Microscope and equipment | |
| Fluorescence microscope Axiovert 200 | Zeiss, Jena, Germany |
| Fluorescence microscope Axioskop | Zeiss, Jena, Germany |
| Pipetboy plus | Integra Bioscience Swiss |
| Pipettes Eppendorf | Eppendorf, Munich, Germany |

Rotators:

| | |
|---|---|
| Rotator | Heidolph, Germany |
| REAX2 | Heidolph, Germany |
| Sapphire discs (Φ 3mm) | Wohlwend GmbH, Sennwald, CH, Switzerland |
| Serological pipettes | Sarstedt, Nürbrecht, Germany |
| Polyvinylpyrrolidone-free polycarbonate filters | |
| With 5 μ m pores | Neuroprobe, Pleasanton, CA |
| Scalpels | Greiner Bio-one,,Germany |
| Tubes | |
| Falcon Tubes | Becton Dickinson, NJ, USA |
| Falcon FACS | Becton Dickinson, NJ, USA |
| PCR Tubes | Biozym, Heissisches Germany |
| Safe lock tubes 1,5ml | Eppendorf, Germany |
| Whatman Filter paper 3MM | Whatman, Maidstone, GB, UK |

2.2 Chemicals

| | |
|--|--|
| Ammoniumchlorid (NH ₄ Cl) | Sigma-Aldrich, Germany |
| Acridin orange | Sigma-Aldrich, Germany |
| Aceton | Prolabo, VWR international GmbH, Darmstadt, Germany |
| 30% BSA (Bovin serum albumin) | Sigma Aldrich, Germany |
| Bafilomycin A1 | Sigma Aldrich, Germany |
| DMSO | Merck, Darmstadt, Germany |
| Dynasore | Sigma-Aldrich, Germany |
| EDTA (ethylenediaminetetraacetic acid) | Fluka Sigma Aldrich, Germany |
| EIPA | Sigma-Aldrich, Germany |
| Epon 812 | Fluka Chemie AG, Buchs, CH |
| FCS (fetal calf serum) | Gibco BRL,Germany |

| | |
|--|---|
| FITC-dextran | Sigma-Aldrich, Germany |
| Isopropanol | VWR, Darmstadt, Germany |
| L-Glutamin (200mM) | Biochrom KG, Berlin, Germany |
| Glycerin | Roth, Karlsruhe, Germany |
| Glycin | AooliChem Bio Chemika, Darmstadt, Germany |
| 15 nm gold particles | Aurion, Wageningen, The Netherlands |
| 1-Hexadecen | Merck, Darmstadt, Germany |
| Human Immunoglobulins (Ig) | Taleceris Biotherapeutics, Germany |
| KH ₂ PO ₄ (potassic hydrogenphosphate) | Merck, Darmstadt, Germany |
| Lymphoprep | PAA laboratories, Germany |
| Methanol | Sigma-Aldrich, Germany |
| Monensin | Sigma-Aldrich, Germany |
| NaCl | AppliChem Bio, Chemika, Darmstadt, Germany |
| Na ₂ HPO ₄ | Merck, Darmstadt, Germany |
| Osmiumtetroxide | Merck, Darmstadt, Germany |
| Penicillin | Invitrogen, Germany |
| PFA | Fluka Chemie AG, Buchs Switzerland |
| Poly-L-Lysin | Sigma-Aldrich, Germany |
| RITC-dextran 70S | Sigma-Aldrich, Germany |
| Streptomycin | Invitrogen, Germany |
| Sulphuric acid, H ₂ SO ₄ | Merck, KGaA, Germany |
| Triton 100 | Serva, Heidelberg, Germany |
| Trypan Blue 0.5% (w/v), seromed | Biochrom KG, Berlin, Germany |
| Trypsin | Fa.Gibco, Darmstadt, Germany |

Uranylacetat Merck, Darmstadt, Germany

2.3 Antibodies

Primary Antibodies:

| | |
|---|--|
| Anti-human cytomegalovirus pp65 (pUL83) Cinapool mouse, monoclonal | Argene SA, Varilhes, France |
| Anti-human cytomegalovirus IE1/2, mouse, monoclonal | Argene SA, Varilhes, France |
| Anti-Tublin, mouse, monoclonal | MolecularProbes, Leiden, Netherland |
| Anti-Actin, mouse, monoclonal | Sigma, St.Louis, Missouri, USA |
| Anti-human CD14, mouse, monoclonal | BD Pharmingen, NJ, USA |
| Hybridom gB, mouse, monoclonal | |
| Anti-EEA1 (early endosome antigen) mouse, monoclonal | BD Pharmingen, NJ, USA |
| Anti-Human CD107a (LAMP-1) mouse, monoclonal | BD Pharmingen, NJ, USA |
| Anti-Rab7, mouse, monoclonal | Sigma-Aldrich,Steinheim, Germany |
| Anti-Rab5, mouse, monoclonal | Sigma-Aldrich, Steinheim Germany |
| Anti-CD8, mouse, monoclonal | BD Pharmingen, NJ, USA |
| Secondary antibodies: | |
| Goat-anti mouse, Alexa Fluor 488 conjugated | molecular Probes, Oregon, USA |
| Goat-anti mouse, Alexa Fluor 555 conjugated | molecular Probes, Oregon, USA |

2.4 Viruses

TB40/E: an endothliotropic strain of human cytomegalovirus, which initially was isolated from a throat swab of a bone marrow transplant recipient [88,92,106].

pUL32-EGFP: a recombinant endothliotropic strain of human cytomegalovirus, which was generated from HCMV strain TB40E. It was obtained from Christian Singzer, University of Ulm [42].

2.5 Cells

M1- and M2 –M ϕ : pro- and anti-inflammatory monocytes-derived macrophages (M ϕ); these cells were produced from fresh buffy coat.

HFF-cells: human foreskin fibroblasts, these cells were used until passage 30

HUVEC-cells: human umbilical vein endothelial cells, these cells were used until passage 10.

2.6 Cell media

Macrophages medium:

RPMI 1640 (PAA Laboratories GmbH), 10% (v/v) FCS, 1% (v/v) streptomycin/penicillin, 1% (v/v) L-glutamine

HFF medium:

MEM (Invitrogen), 10% (v/v) FCS, 1 % (v/v) streptomycin/penicillin, 1% (v/v) L-glutamine

HUVEC medium:

EBM+EGM Single Quots (Lonza, USA), final concentration of FBS 2%

2.7 Cell buffer

Phosphate buffer:

0.01 M PBS: 150 mM NaCl, 1 mM KH_2PO_4 , adjusted to pH 7.8 with NaOH, ad l l aqua bidest

0.01M PBS/EDTA: 0,01MPBS, 1% EDTA stock solution

Buffer of isolation monocytes from buffy-coat:

MACS wash buffer:

Dulbecco's PBS, 10ml EDTA w/o $\text{Ca}^{2+}/\text{Mg}^{2+}$ (Biochrom AG)

Miltenyi buffer:

500ml Dulbecco's PBS (PAA Laboratories GmbH), 10 ml 1% EDTA in PBS w/o $\text{Ca}^{2+}/\text{Mg}^{2+}$ (Biochrom AG), 8.3 ml 30% BSA (Sigma Aldrich)

Solution for electron microscopy:

Standard freeze substitution solution:

0.2% (w/v) OsO_4 , 0.1% (w/v), uranylacetate, 5% (v/v), aqua bidest, in acetone

Epon stock solution I:

155 g Epon 812,250g dodecenylsuccinic anhydride

Epon stock solution II:

200 g Epon 812.178 g methyl nadic anhydride

Epon working solution:

60 ml stock solution I, 40 ml stock solution II, 1.5 ml tris (dimethyl aminomethyl) phenol

Fixative:

2.5% glutaraldehyde, 1% sucrose, PBS (pH 7.3), aqua bidest

PBS 0.01M:

0.2 M Na₂HPO₄, 0.2 M NaH₂PO₄, 9 g NaCl, 0.3 g Thimerosal

PBG solution:

PBS 0.01 M, 0.5% Bovine Serum Albumin, 0.2 % cold Water Fish Skin Gelatine

Solution for gradient purification of virus

Sucrose (saccharose)-phosphate buffer:

76.62 g sucrose, 1.218 g K₂HPO₄, 0.52 g KH₂PO₄, ad 1l aqua bidest, autoclave at 110 °C

0.04 M sodium phosphate buffer pH 7.4

Solution A: 1.1 g sodiumdihydrogenphosphate x1 H₂O, in 196 ml aqua bidest

Solution B: 11.5 g dinatriumhydrogenphosphate x12H₂O, in 804 ml aqua bidest

Mix sol. A and sol. B, bring pH to 7.4 and autoclave

35% sodium tartrate: (dihydrat)

Dissolve 35 g sodium tartrate in 65 g of 0.04 M sodium phosphate pH 7.4, autoclave and store at RT

15% sodium tartrate /30% glycerol (glycerin)

Dissolve 15 g sodium tartrate in 55 g of 0.04 M sodium phosphate pH7,4, autoclave and store at RT

Autoclave 30 g glycerol

Mix glycerol and 15% sodium tartrate and store at RT

2.8 Inhibitors stock solutions

Bafilomycin A1 (100 μ M) in DMSO

Ammoniumchlorid (100 mM) in media

Monensin (50 mM) in ethanol

Dynasore (0.8 mM) in DMSO

Latrunculin A (800 μ M) in DMSO

EIPA (100 mM) in DMSO

Sucrose buffer (3 M) in Wather

Methods:

2.9 Production of cell free virus and titration

Production of TB40/E and pUL32-EGFP virus stocks

The human cytomegalovirus (HCMV) clinical isolate TB40/E was obtained from throat swab of a bone marrow transplant recipient by 22 passages in endothelial cells [92,106]. In order to produce a highly concentrated virus stock, HFF cells were passaged and grown to about 90% confluence. At this condition HFF cells were infected with TB40/E with a low MOI (0.05-0.01 PFU/cell) and further cultivated until cytopathic effect became evident in about 90% of cells. Then the supernatants containing virus were harvested, centrifuged for 10 min at 4000 rpm to remove cell debris and afterward concentrated by ultracentrifugation at 23.000 g for 90 min in a Beckman ultracentrifuge. The viral pellet was resuspended in about 250 µl of sucrose phosphate buffer to ensure high titers and cyroprotect the virus during storage at -80 °C. Depending on the size of the viral pellet the final volume was adjusted with HFF culture medium.

The recombinant virus strain pUL32-EGFP was originated from TB40/E [42] and kindly provided by Prof. Sinzger (Institute of Virology, University of Ulm). Firstly, HUVEC cells were infected with pUL32-EGFP and maintained in culture until 80-90% of the cells expressed the green fluorescent protein pUL32-EGFP. At that time, the cells were collected and frozen in small aliquots (1 cryotube = 1/6 of a T75) preserved in liquid nitrogen (-135 °C). To produce highly concentrated virus stock, 4 T75 flasks confluent HFF were co-split with 1 cryotube containing pUL32-EGFP infected HUVEC. When the cytopathic effect reached in 90%, supernatants containing virus particles were collected and processed as described above for the production of TB40E virus stock.

Gradient purification of virus stock

To enrich the virions and eliminate dense bodies and not infectious viral particles (NIEPs), the three fractions were separated by gradient centrifugation. Briefly, 2 ml of virus stock were layer on a sodium tartrate (35%/15%) gradient prior centrifugation at 23.000 rpm for 45 min with break to 800 rpm. Afterward the band corresponding to the virions was recovered; the virions pelleted at 23.000 rpm for 45 min with maximal break,

resuspended in sucrose-phosphate buffer, aliquoted into steril Eppendorf tubes and stored at -80 °C until titration.

Titration of virus stock

The infectious titer of the different HCMV preparations was determined by plaque titration assay in HFF. HFF cells were infected with 10-fold dilutions of virus stocks. At one day post infection the cells were fixed for 10 min at -20 °C with pre-cooled methanol-acetone (1:1). After removal of methanol- acetone, the cells were completely dried, then washed one time with 0.01M PBS and stained with a monoclonal antibody (Mab) raised against the immediate early proteins 1-2 (IE1-2). The cells were then washed three times with PBS and incubated with a secondary anti-mouse Ab conjugated to HRP. After additional washing steps, cells were incubated with AEC as substrates of the peroxidase.

Viral infectivity was determined by counting the number of IE1-2 nuclei at the lowest serial dilution and expressing the titer of each virus stock as plaque forming unit (PFU) per ml.

2.10 Production of monocytes derived macrophages

PBMC Isolation

Peripheral blood mononuclear cells (PBMC) were isolated from buffy-coat of HCMV-seronegative blood donors (provided by the Institute für Klinische Transfusionsmedizin und Immunogenetik Ulm GmbH, Ulm Germany) by Ficoll-Paque density centrifugation following standard procedure. Briefly, buffy-coats were diluted with 50ml endotoxin free D-PBS (Dulbecco`s PBS) prior careful stratification on 15 ml of Lymphoprep Falcon tubes were centrifuged at 1650 rpm for 25 min without break in order to collect PBMC at the interface between the different phases. PBMC were then washed with MACS PBS/EDTA wash buffer at 300 g with maximal break to remove the potential residues of Lymphoprep. The cell pellet was twice resuspended with MACS wash buffer and centrifuged at 200 g for 10 min with maximal break, to discard the platelets which could interfere with the selection procedure. Prior monocyte isolation, PBMC were resuspended in 30 ml of Miltenyi buffer, conveniently diluted with Trypan blue and then counted using a Neubauer counting chamber.

Monocyte Isolation

A positive magnetic selection based on CD14 MicroBeads was applied to purify circulating monocytes starting from PBMC. 150×10^6 PBMC were transferred into 50 ml falcon tubes, pelleted and then resuspended with 1200 μ l Miltenyi buffer prior addition of 300 μ l CD14 MicroBeads. Then the suspension was incubated at 4 °C for 15 min prior cells washing with Miltenyi buffer. In the meanwhile, a MACS LS column was fixed in the magnetic field of a MACS separator and rinsed with 3 ml of Miltenyi buffer for priming. The pellet was resuspended in 1200 μ l Miltenyi buffer and the cell suspension was applied on the column. CD14⁺ monocytes were retained into the column, washed and finally eluted into a new tube by adding 5 ml Miltenyi buffer in column. The purification of the eluted monocytes was verified by FACS and was always higher than 90%.

Cultivation M1- and M2- macrophages *in vitro*

6×10^6 monocytes were cultivated on hydrophobic lummo dishes at 37 °C for seven days in RPMI 1640 complete medium supplemented with 100 ng/ml of either GM-CSF or M-CSF driving monocytes differentiation into M1 macrophages (M1-M ϕ) or M2 macrophages (M2-M ϕ), respectively. At the third day of culture, half medium was replaced and the growth factors completely replenished. At the seventh day of culture, M ϕ were completely differentiated. M ϕ detachment from the dishes was performed by addition of 1 ml of D-PBS to the dishes, incubation at 37 °C for 5 min, followed by pipetting. Detached M ϕ were collected into a new 15 ml falcon tube, centrifuged for 7 min at 1200 rpm and finally resuspended with 2 ml RPMI 1640 complete medium for cell counting.

2.11 Cultivation of HFFs

Human foreskin fibroblasts (HFF) were cultivated in MEM complete medium with 10% (v/v) FCS supplemented with 2mM L-glutamine, 100U/ml penicillin and 100U/ml streptomycin. The cells were grown in T75 cell flasks and when confluent they were split 1 to 2.

2.12 Indirect Immunofluorescence assay (IIF)

Depending on the specific experiments 1.2×10^5 or 1.0×10^5 M ϕ were seeded in ibidi slides or 96-well plates, respectively. After attachment, M ϕ were infected with the indicated virus and at the desired points of time after infection, the cells were washed with 0,01M PBS, fixed with 4% PFA for 10 min at RT and permeabilized by treatment with 0.01% (v/v) Triton in PBS. Primary antibodies raised against different viral proteins were routinely diluted in 1% (v/v) BSA in PBS and incubated for 45 min at 37 °C. Following two washes with 0,01M PBS the secondary antibodies Alex Fluor488-or Alexa Fluor555-conjugated goat anti-mouse immunoglobulins diluted in 1% (v/v) BSA in PBS were added for 45 min at 37 °C. When indicated the cells were counterstained with Evan`s blue diluted 1% (v/v) BSA. Nuclear staining was performed by incubation of the cells with DAPI. Before observation using Zeiss`s software AxioVision LE4.8.2 the ibidi slides or plates could be stored in PBS at 4 °C.

2.13 Sample preparation for Transmission Electron Microscopy

Preparation of Sapphire Discs

M ϕ were grown on sapphire discs (diameter 3 mm), that were used for TEM and SEM. Sapphire discs were cleaned by sonication for 15 min in 60% sulphuric acid. After rinse with water the discs were sonicated again with soapy water and acetone for 15 min. Then, sapphire discs were stored in acetone until usage. Since cells grow better on carbon coated sapphire discs, the discs were allowed to dry and then coated with a carbon layer of approximately 15 nm thicknesses by electron beam evaporation in a BAF 300 freeze etching device (Bal-Tec, Principality of Liechtenstein). To stabilize the carbon layer, the discs were baked in an oven at 120 °C for 8 hours. Then, by carving the number “2” into the carbon layer, the orientation of the discs was made visible. In order to better attach the cells on the sapphire discs, the discs were glow discharged to increase the hydrophilicity (Edwards High Vacuum, Leica Microsystems GmbH). Afterward, the discs were sterilized under UV-light.

Seeding of cells

Four sapphire discs were put into one well of ibidi slide with 150 μ l complete medium. Then 1.5×10^5 cells were drop-wise seeded into the well. After one night incubation at 37 °C, M ϕ were infected with the indicated virus strains and incubated at 37 °C for desired time, before processing for the high pressure freezing.

Colloidal gold labeling of lysosomes

24 hours prior to infection, lysosomes were pre-loaded by feeding M1- and M2-M ϕ with BSA-colloidal gold (25 or 50 μ l of BSA-colloidal gold solution to 200 μ l of cell culture medium). Fixation was performed by high pressure freezing at defined point of time after infection.

High pressure freezing

By high pressure freezing with a HPM01 (Engineering Office M. Wohlwend, Switzerland) biological samples were fixed within milliseconds in native conditions without ice crystal artifacts. Sapphire discs covered with a virus infected monolayer of adherent cells were inserted into the high pressure freezing holder between a lower flat aluminum planchette and an upper one with a cavity of 100 μ m, which firstly were immersed into 1-hexadecene. Then, the high pressure freezing holder with the sample was put into the high pressure machine, where it was cryofixed with liquid nitrogen at a pressure of approximately 2100 bar. After high pressure freezing, the samples were immediately transferred into liquid nitrogen until further.

Freeze substitution and epoxy resin embedding

During freeze substitution water in biological samples is substituted with organic solvents. For this purpose, Eppendorf tubes were filled with 500 μ l of the freeze substitution solution consisting of acetone, Uranlyacet and OsO₄ and pre cooled to -90 °C in the freeze substitution machine. Then the frozen sapphire discs were put into the pre-cooled Eppendorf tube, which was pre-cooled for 30 min. The process lasted over 16 to 18 hour, during this time the temperature was slowly raised from -90 °C to 0 °C with an exponential temperature profile. After freeze substitution the Eppendorf tubes were kept at 0 °C for 1

hour followed by 1 hour at RT. Then the remaining aluminum planchettes were picked out of the tubes, before the sapphire discs were washed 3 times with acetone. For better infiltration with 100% epoxy resin over night, the sapphire discs were pre-incubated with 50% epoxy resin in 50% acetone for two hours at RT. On the next day, the sapphire discs, which point the engraved number “2” to top of Eppendorf tube, were transferred into 500ml Eppendorf tubes containing fresh pure epoxy resin. Finally, the samples were incubated at 60 °C for 3 days for epoxy resin polymerization before thin sectioning.

Thin sectioning for transmission electron microscope

For standard application of transmission electron microscopy the samples were cut to 70nm ultra thin sections by using a Leica Ultracut UCT Microtom (Leica, Germany). The samples in epoxy resin were first immersed in liquid nitrogen to remove the sapphire discs. Then, the samples were trimmed with a razor blad. Then 3 or 4 thin sections were transferred on a 200 mesh copper grid. Then, the samples were post stained 2 minutes with lead citrate and washed 3 times with water. After drying of the samples, they were imaged with a JEOL TEM-1400 transmission electron microscope at an acceleration voltage of 80kV.

Preparation of samples for STEM Tomography

For imaging in a Titan (FEI, Eindhoven) 300 kV field emission transmission electron microscopes by the scanning transmission mode using a high-angle annular dark field detector special samples were prepared. 500 nm thick sections were mounted on copper grids, which were pretreated with poly- L-lysine. After increasing of hydrophilicity by glow discharge for 10 seconds the samples were immersed in a suspension of 15 nm colloidal gold. Afterward samples were dried at 60 °C for 10 min, followed by coating with a 5 nm carbon layer on both sides by electron beam evaporation in a BAF 300. For a tomographical set 71 images were taken at tilt angles in the range from -70 ° to 70 °. The tomography reconstruction was made by weighted back projection using the IMOD software [40]. For segmentation and data display, the AMIRA and IMOD software were used.

2.14 Sample preparation for Scanning Electron Microscopy

Sapphire discs cleaning and seeding of M1- and M2-Mφ was performed as described above.

Chemical fixation and dehydration

For scanning electron microscopy, samples were prepared vacuum stable and dry. After chemical fixation with 2.5% glutaraldehyde for 1 hour at RT, samples were washed with PBS for 3 times. Then they were fixed with 2% osmiumtetraoxid diluted in PBS, which furthermore stabilizes the structure of cells. To reduce surface tension and enhance structure preservation of samples, the water in biological tissue is then first replaced with a graded series of propanol.

Critical point drying

To dry samples for scanning electron microscopy, the organic solutions in biological samples were substituted with CO₂ as translational medium for critical point drying. After cooling the machine to 8 °C, the specimens mounted inside little containers were 8 times flushed with CO₂ 8 to exchange the organic solution. Then the machine was heated to 37 °C which cause the pressure to increase above the critical point of CO₂. Then, the gas was slowly release. To increase the electrical conductivity, a thin layer (3nm) of platinum was coated onto the samples by electron beam evaporation in a BAF 300.

Immunogold labeling of HCMV virus particles

The sapphire discs, on which infected cells were grown, were incubated with PBG for 10 min at RT and with Fc-blocking for 30 minutes at RT to block unspecific binding sites. Then, the first antibody specific against viral particles were added and incubated at 37 °C for 45 min. The sapphire discs were afterwards washed 6 times with PBG (2% gelatine and 0.5% BSA in PBS) and subsequently incubated with the secondary antibody anti –mouse conjugated to 10 nm colloidal gold (Aurion), which is diluted to 50 times with PBG.

Afterward the sapphire discs were repeatedly washed (for 6 times), before they were fixed with 2.5% glutaraldehyde for 10 min at RT followed by washing with 0.01% PBS for 3 times. No post fixation with osmiumtetroxid was performed, since the backscattered electron signal from the osmium would interfere with the signal from the gold particles. Then the samples were dehydrated in a series of alcohol till 70% and stored at RT until they were completely dehydrated and critical point dried as described above. Instead of platinum –coating a very thin layer (approximately 5 nm) of carbon was coated on the samples before observation under the scanning electron microscopy.

Imaging in the SEM and image processing

For conventional SEM, samples were imaged in a Hitachi S-5200 in lens SEM at an acceleration voltage of 10kV. The immune gold labeled samples were also analyzed with the backscattered electron image in addition to the conventionally used secondary electron image. The backscattered electron signal is mass-dependent and shows the distribution of the colloidal gold markers in contrast to the surface signal of secondary electrons [107].

2.16 Flow cytometry analyses (FACS)

FACsCalibur, (Becton Dickinson, San Jose, CA) was used for quantitative uptake of TRITC-dextran into M1- and M2-M ϕ .

After harvest, 2×10^5 M1- and M2-M ϕ were pelleted by centrifugation at 1200 rpm for 7 minutes, resuspended in 500 ml medium containing different concentration of EIPA and incubated for 30 minutes at 37 °C. 3 mg/ml TRITC-dextran were added into each tube and incubated for 20 minutes at 37 °C. Cells were washed with cold PBS 3 times, fixed with 1% PFA and resuspended in 200 μ l cold PBS for FACS acquisition und analysis. Sample incubated for 30 minutes at 4 °C instead than 37 °C served as negative control.

3. Results:

3.1 HCMV enters into M2-M ϕ more efficiently than into M1-M ϕ

In *vivo* human macrophages are important target cells for HCMV infection and host sentinels against virus replication. Primary human M1- and M2- monocyte-derived-macrophages (M ϕ) can be generated and infected *in vitro* in order to investigate the initial steps of HCMV infection. In our previous work we have infected M1- and M2-M ϕ with the highly endotheliotropic and leukotropic HCMV strain called TB40E [88] and observed that the expression of the immediate early genes (IE1-2) is significantly higher in M2-M ϕ than into M1-M ϕ [23]. To explain this difference in permissiveness we hypothesize that TB40E uses different entry mechanisms into the two types of M ϕ . To gain more knowledge about the efficiency and pathways of HCMV infection in M1- and M2-M ϕ , we applied electron microscopy and indirect immune fluorescence microscopy in order to trace the localization of viral particles at different time after infection.

3.1. 1 Mock- and HCMV-infected M1- and M2-M ϕ have similar morphology

M1-M ϕ and M2-M ϕ obtained after 7 days of monocytes stimulation with growth factors exhibit almost identical morphologies when observed by SEM (Fig. 7, upper panels). Both types of M ϕ are adherent and show a rough surface provided of abundant actin filopodia which have contact with neighboring cells. M ϕ shape is about 21 μm diameter, spherical, ovoid or lobulated and measures about 21 μm in diameter.. 30 minutes after contact with TB40/E, the surface of M1- and M2-M ϕ becomes more complex and rougher than the surface of mock- infected M ϕ . To increase the visibility of the viral particles on the cell surface, the samples were unidirectional “shadowed” with platinum and then imaged with the backscattered electron signal [107] (Fig. 7, lower panels). The viral particles appear as small bright spheres (highlighted by the red arrows) whose distribution on the membrane of M1- and M2-M ϕ looks rather similar.

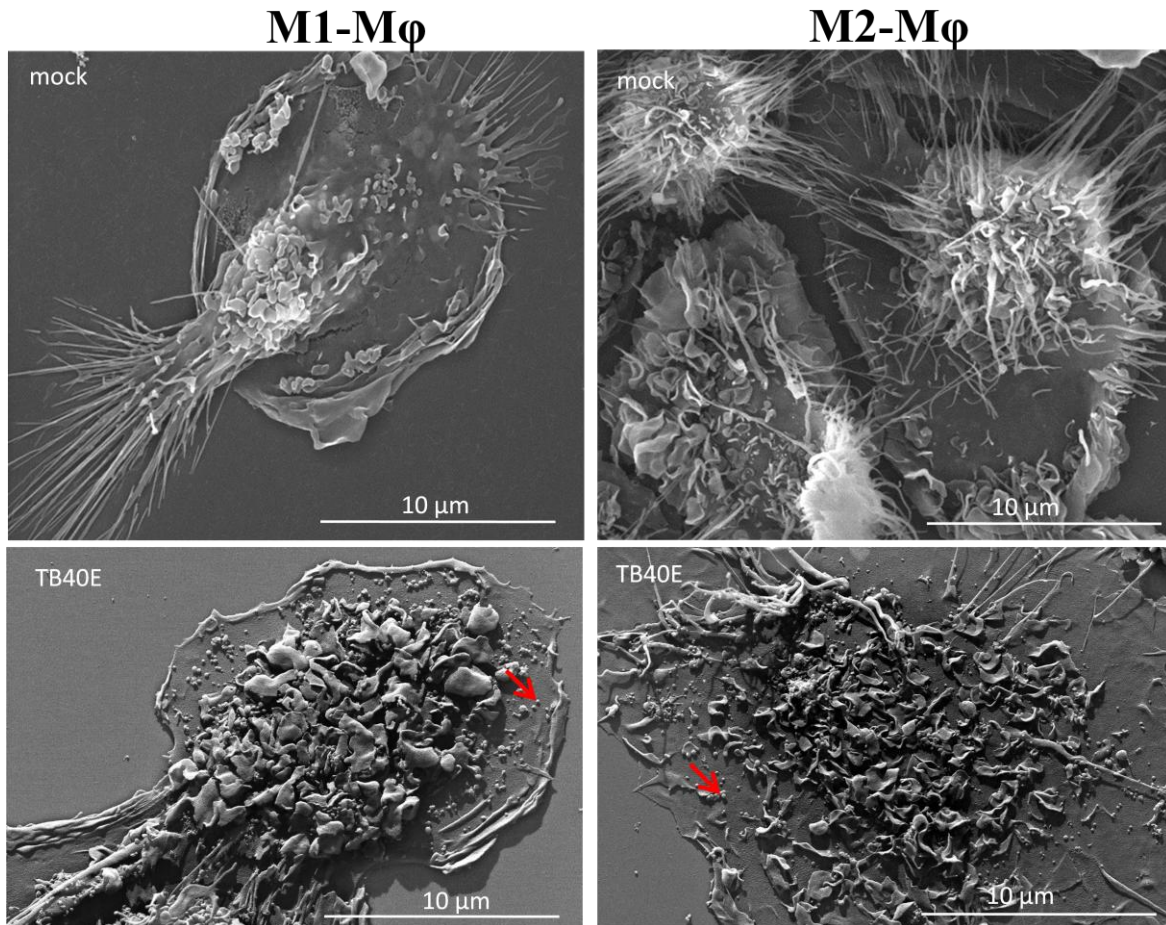


Figure 7: Morphology of mock and HCMV infected M1- and M2-Mφ. Monocytes were stimulated with the growth factors GM-SCF and M-CSF and differentiated into M1- and M2- Mφ, respectively. M1- and M2-Mφ were inoculated with TB40/E (MOI of 5) for 30 minutes. Then prepared for the SEM and imaged with the backscattered electron signal. The viral particles of HCMV spread on the surface of M1 –and M2-Mφ are highlighted by the red arrows.

3.1.2 HCMV localizes in the periphery of M1-Mφ, but accumulates closed to nucleus in M2-Mφ.

In order to follow the intracellular distribution of the viral particles we used indirect immune fluorescence microscopy on both permeabilized and intact cells. Since the treatment with triton enhances membrane's permeability and allows antibody penetration into the cytoplasm of cells, we could distinguish between viral proteins located extra- or intra-cellularly, We chose to investigate the distribution of the glycoprotein B (gB), the major constituent of the gCI on the envelope of HCMV, because it would give two different expression patterns. While gB would locate on the cell surface if the virions fuse

at the plasma membrane, gB would locate intracellularly if the entire virions are taken up by endocytosis. M1- and M2-M ϕ were infected with TB40/E (MOI of 5) and at 90 minutes after infection cells were fixed and either permeabilized with triton or left intact. As shown in Fig. 8, gB could only be detected after permeabilization of the cells, thus indicating, that gB was inside the cell and not on the external surface and therefore suggesting, that the viral particles were not fusing at the plasma membrane. Additionally, while in M1-M ϕ gB accumulated in the cell periphery, in M2-M ϕ , the signal was proximal closed to the nucleus

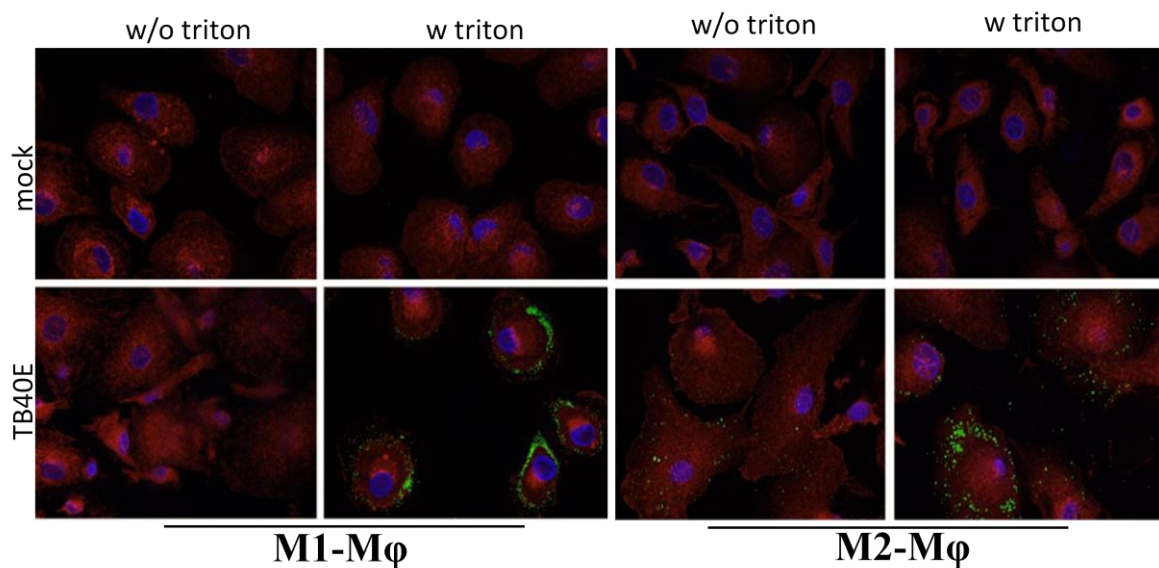


Figure 8: gB distribution on the periphery of M1- M ϕ , but closed to M2-M ϕ . M1- and M2-M ϕ were infected with TB40/E (MOI of 5) for 90 min. Cells were fixed with 4% PFA in PBS, either permeabilized (w triton) or left intact (w/o triton) and then incubated with antibodies raised against the envelope glycoprotein gB. Viral proteins were visualized by secondary antibodies conjugated to Alexa Fluor 488 (green signal). Cells nuclei were counterstained with DAPI and the cytoplasm with Evans blue (blue and red signals, respectively). All pictures (original magnification, 63x) are representative of 5 donors.

In the actual model, virions taken up by endocytosis reach primary endosomes where the viral particles are uncoated and the envelope dissociates from the capsid thus allowing the migration of the capsid in the proximity of the nucleus and the diffusion of pp65 in the whole cytoplasm [103]. Therefore, we analyzed the intracellular distribution of the phosphoprotein pp65 as the major component of the viral tegument. In order to reduce staining background due to non-infectious viral particles (NIEPs) and the dense bodies, we gradient purified the virus stocks and obtained enriched fractions of infectious virions. M1- and M2-M ϕ were infected with gradient purified TB40/E for 90 minutes with an MOI of 5 and then fixed with 4% PFA, permeabilized or left untreated prior staining with antibody

raised against pp65. As shown in Fig. 9, pp65 could only be detected after permeabilization of the cells thus indicating that pp65 was inside. Similarly to gB, while in M1-M ϕ pp65 accumulated in the cell periphery, in M2-M ϕ the signal was distributed in the whole cytoplasm.

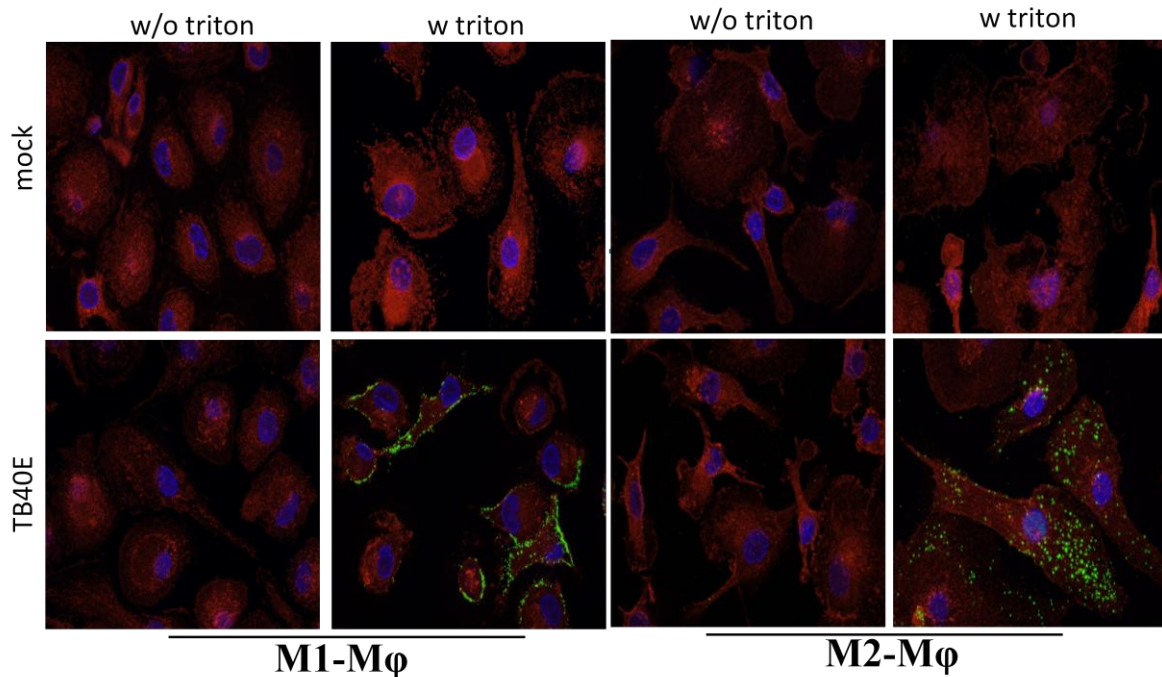


Figure 9: pp65 distribution into M1- and M2- M ϕ . M1- and M2- M ϕ were infected with gradient purified TB40/E (MOI of 5) for 90 minutes. Cells were fixed with 4% PFA in PBS, either permeabilized (w triton) or left intact (w/o triton) and then incubated with antibodies raised against the tegument phosphoprotein pp65. Viral proteins were visualized by secondary antibodies conjugated to Alexa Fluor 488 (green signal). Cell nuclei were counterstained with DAPI and the cytoplasm with Evans blue (blue and red signals, respectively). All pictures (original magnification 63X) are representative of 5 donors.

All together our findings indicate that 90 minutes after infection the majority of the viral particles are inside M1- as well as M2-M ϕ . Due to the lack of gB surface staining we propose that HCMV enters into human primary M ϕ by endocytosis. Since in the two types of M ϕ the viral particles show opposite distributions remaining peripheral in M1-M ϕ and accumulating perinuclearly in M2-M ϕ , we hypothesize that HCMV enters into M1-M ϕ much more efficiently than into M2-M ϕ .

3.1.3 Internalization of HCMV into M1- than M2-M ϕ

Since immune fluorescence investigations of the localization of viral particles in M ϕ suggested a more efficient translocation to the nucleus in M2-M ϕ than in M1-M ϕ , we wanted to confirm this phenomenon by using transmission electron microscopic analysis (TEM). For this aim, M1- and M2-M ϕ were seeded on carbon coated sapphire discs and infected with TB40/E by using an MOI of 30. At 3 hours post infection the cells were cryofixed by high pressure freezing, freeze substituted and embedded in epon resin. Ultrastructural analysis of M ϕ at this early time point of HCMV infection allowed a detailed insight into the distribution of viral particles in the cytoplasm of M ϕ . As shown in Fig. 10 A, in M1-M ϕ the majority of viral particles remained under membrane protrusion while only few viral particles were identified in cytoplasmatic vesicles. In contrast, in M2-M ϕ the majority of viral particles entered in vesicles ubiquitously distributed in the cytoplasm, whereas no viral particles were visible in proximity of the plasma membrane. The amounts of viral particles associated with the plasma membrane or with cytoplasmatic vesicles were quantified in 22 pictures of HCMV infected M1- and M2-M ϕ obtained from 3 different donors and as shown in Fig. 10 B much more HCMV particles were counted into M2-M ϕ as compared to M1-M ϕ .

The ultrastructural analysis confirmed the results of indirect immune fluorescence and showed with more clarity the different distribution of viral particles in M1- and M2-M ϕ . The size and cytoplasmatic location of the vesicles in M2-M ϕ as compared to M1-M ϕ suggested that the virus accumulated in different endocytotic vesicles with varying phenotypes and most likely distinct properties. The high resolution power of the TEM allowed also to identify naked capsids in the cytoplasm of M2-M ϕ , thus indicating that for some viral particles the process of uncoating had already occurred and the viral envelopes successfully dissociated from the viral capsids. Many dense bodies were also observed mixed with infectious particles. It was not surprising that they might behave like infectious virions during entry, since their enveloping membrane is similar to those of infectious virions.

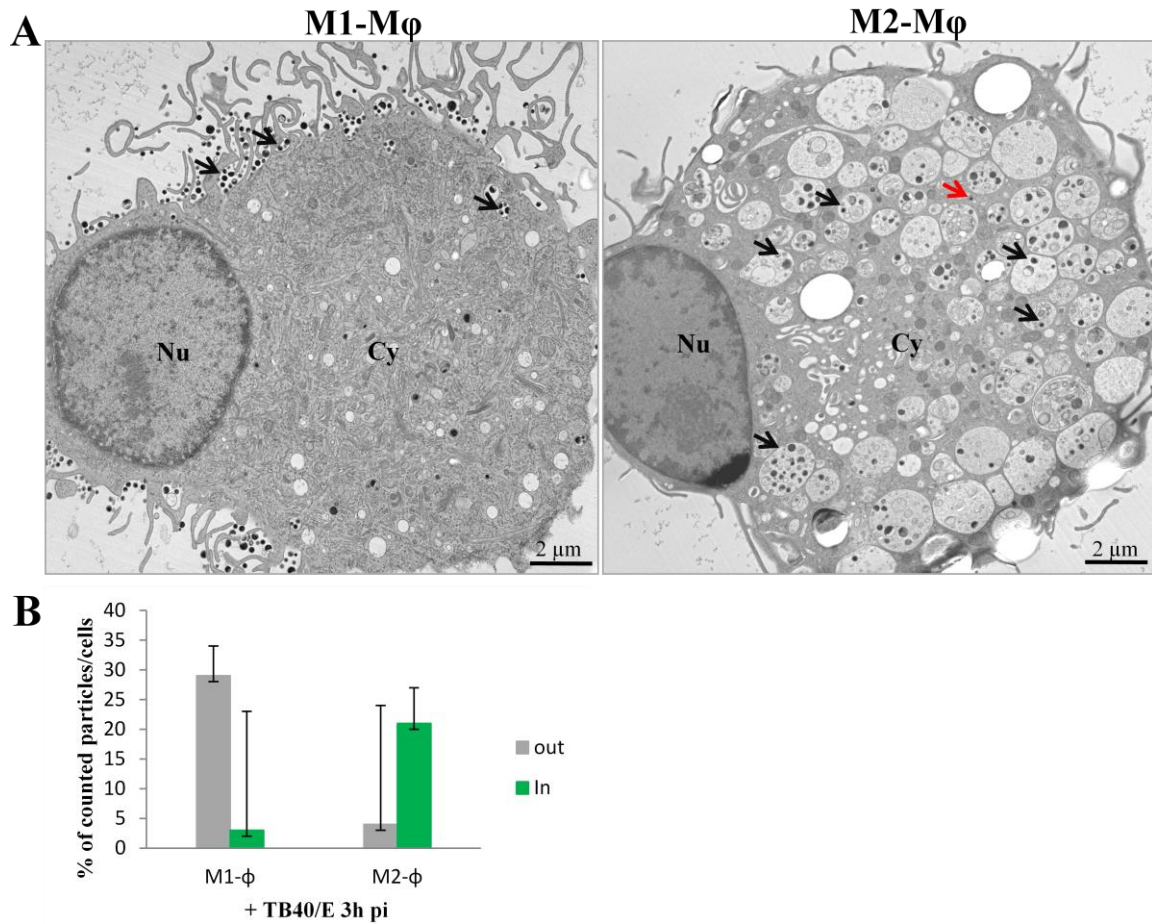


Figure 10: Different distribution of HCMV in M1- and M2- M ϕ . A) M1- and M2-M ϕ were infected with strain TB40/E with an MOI of 30 for 3 hours. Ultra structural analysis of infected M1 - and M2- M ϕ by TEM was performed by high pressure freezing of the samples. B) Quantification of HCMV particles by TEM immobilized in proximity of the plasma membrane (OUT, grey bars) or internalized into vesicles (IN, green bars). These data are obtained from 3 independent experiments.

Since there is an ongoing debate whether circular structures visible in 2D electron microscopy images do really represent (spherical) closed vesicles and not deep extracellular infoldings, we imaged these structures by 3D electron tomography (Fig. 11). The 3D data prove that we imaged a closed vesicle.

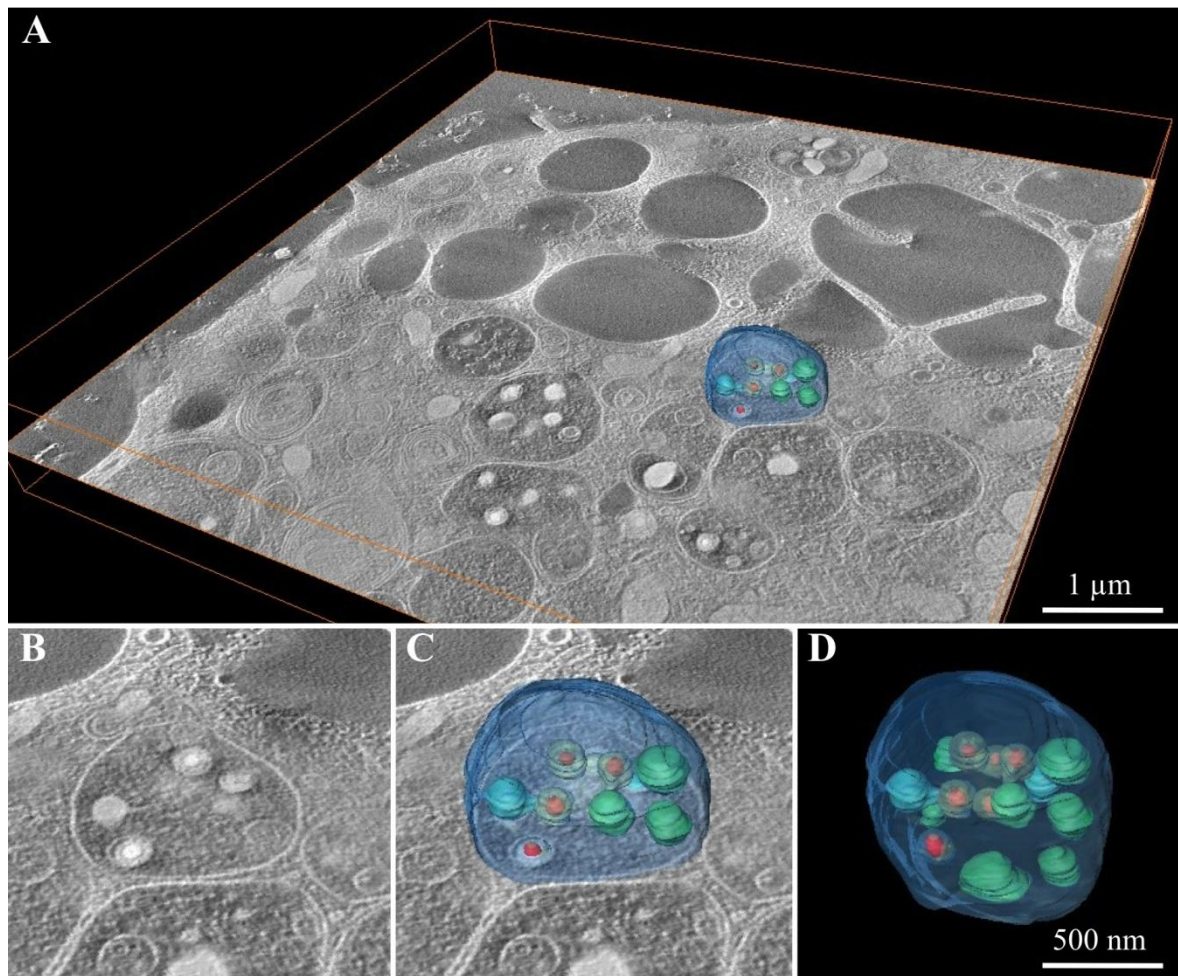


Figure 11: 3D electron tomography. M2-M ϕ were infected with the strain TB40/E with an MOI of 30 for 3 hours. A) An overview of a computed section of a tomogram. B) An endosome with virions. C) Segmentation of the endosome. D) 3D-model of the endosome (transparent blue), containing six virions; capsid (red), tegument (yellow), dense bodies (blue) and vesicles (green). A movie of this tomographic reconstruction can be found on the attached CD.

3.2 Cytoskeleton remodeling is required for HCMV infection.

3.2.1 Morphology of cytoskeleton remodeling in M1- and M2-M ϕ .

Since the previous data would exclude the possibility that the virus envelope fuses directly at the plasma membrane and indicate instead a virus uptake by endocytosis, we aimed to characterize the specific type of endocytotic uptake by M ϕ . Macropinocytosis and phagocytosis are both endocytotic pathways largely used by M ϕ to engulf and eliminate different pathogens. Actin polymerization plays an important role in phagocytosis and macropinocytosis and is required to create and maintain the protrusion of the plasma

membrane surrounding the viral particles. Since actin polymerization is a very fast process, M ϕ were infected with TB40/E (MOI 30) for 5 minutes and then processed for transmission electron microscopy.

As shown in Fig. 12 A, many viral particles distributed around M1- M ϕ and remained mainly located under protrusions of the plasma membrane. In some areas, such as the tail of the cell, the viral particles accumulated in the extracellular space. The structural details corresponding to the insets drawn in Fig. 12 A highlighted that HCMV particles and small debris were under one sided very long extensions (Fig. 12 B). This structural feature may suggest that the uptake of HCMV in M1-M ϕ takes place by unspecific macropinocytosis. Panel C shows details of the cytoplasm of M1-M ϕ containing one big vesicle with a diameter of about 1 μ m containing viral particles consisting of dense bodies, virions, and NIEPs. A smaller vesicle, containing a dense body is also visible nearby.

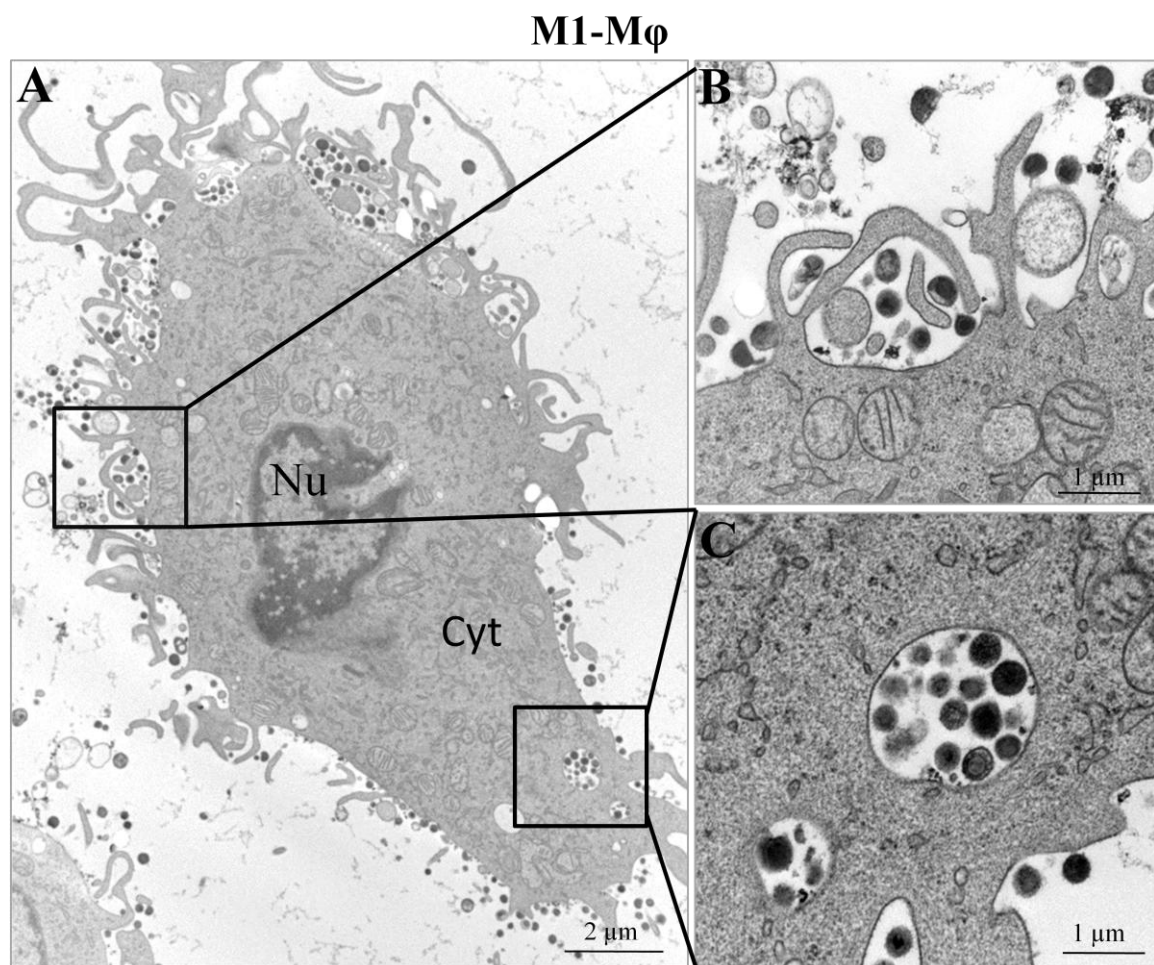


Figure 12: Ultrastructural analysis of HCMV infected M1-M ϕ . M1-M ϕ were infected for 5 minutes with TB40/E with an MOI of 30. Then the cells were fixed by high pressure freezing and the samples imaged with

a transmission electron microscope as described in the methods section. The images are representative of 4 independent experiments. Nu= nucleus; Cyt= cytoplasm

As shown in Fig. 13, 5 minutes after virus TB40/E infection, the cytoplasm of M2-M ϕ contained several virions (point out by red arrows) distributed either inside vesicles or under open membrane extensions. The two virions and several dense bodies are visible under the extreme long membrane protrusion in the lower part of the image. Directly below this area, a big vesicle seems to be located intracellularly; containing smaller vesicles (green arrow), virions, and dense bodies. The diameter of this vesicle is about 1 μ m. The other round intracellular vesicles also contains many virions (red arrows) and dense bodies. Two dense bodies appear in the structure close to the nucleus. This structure, either represents a vesicle, or could be the attachment site of the membrane to the supporting sapphire discs as indicated by the grid shaped membrane.

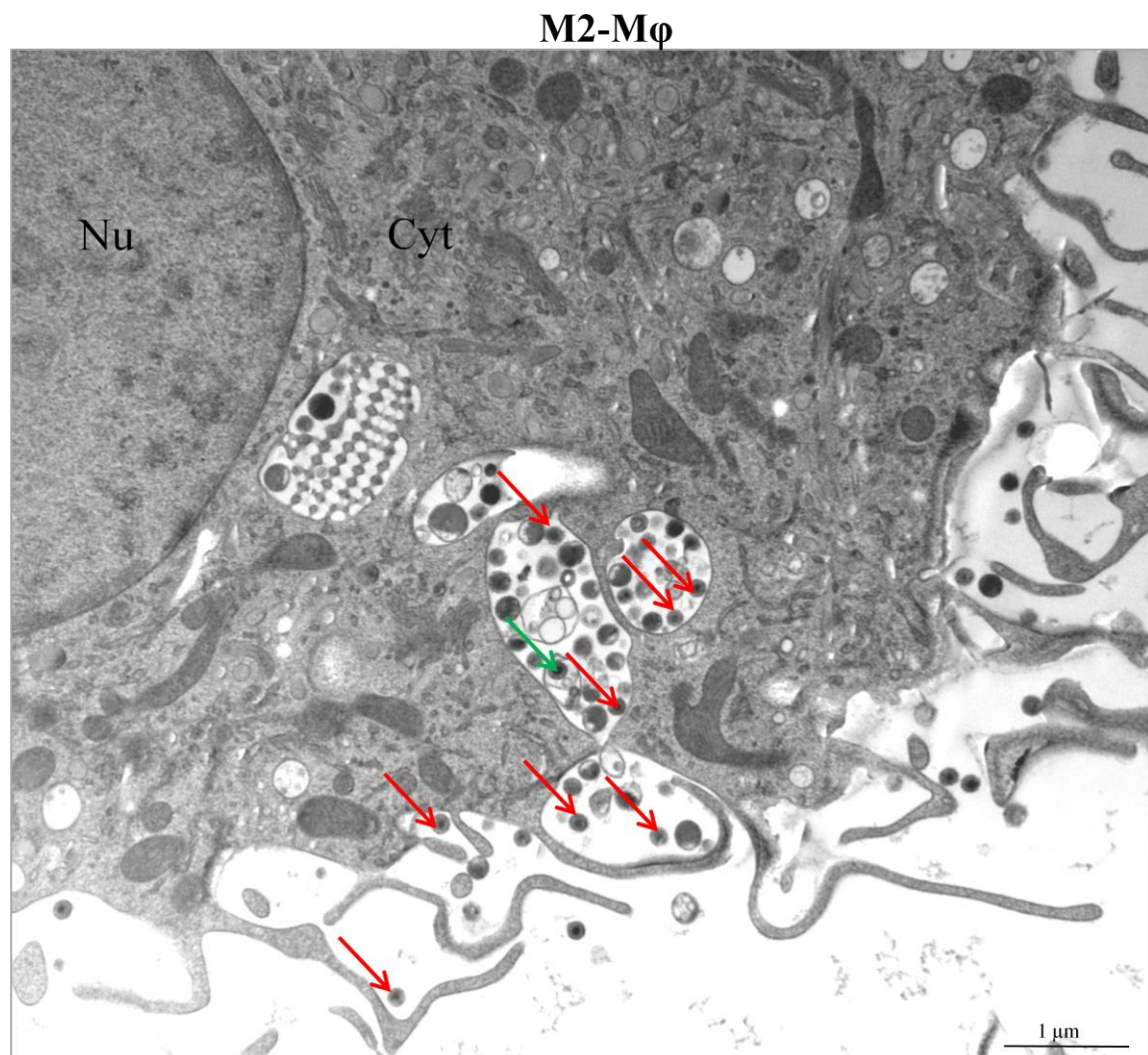


Figure 13: Ultrastructural analysis of HCMV infected M2- ϕ . M2-M ϕ were infected for 5 minutes with HCMV strain TB40/E with an MOI of 30. Then the cells were fixed by high pressure freezing and the samples imaged with a transmission electron microscope as described in the methods section. The images are representative of 4 independent experiments. Nu= nucleus; Cyt= cytoplasm

In summary, the TEM images of HCMV-infected M1- and M2- M ϕ show the cellular cytoskeleton changing after a short time of infection with HCMV. The viral particles are usually under only one asymmetric membrane protrusion that is formed immediately after virus inoculum. The very fast appearance of these protrusions could indicate that actin polymerization is needed to allow membrane remodeling and the engulfment of HCMV virions M ϕ .

3.2.2 The cytoskeleton interacts with HCMV particles during entry in M1- and M2-M ϕ .

Because the section of a TEM sample has only 70 nm thickness and the information from one section is limited, we could not directly observe the interaction between the cell and the whole virus particle. By using Tomography, we increased to 330 nm the thickness of our section/samples and we could observe the interaction between entire virus particles and the surface of the M ϕ . Fig. 15 shows several viral particles attached to tubular protrusions of the M ϕ membrane. Few virions (red arrow) showed a small feet protruding out of the envelope and interacting with the extension of cellular membrane.

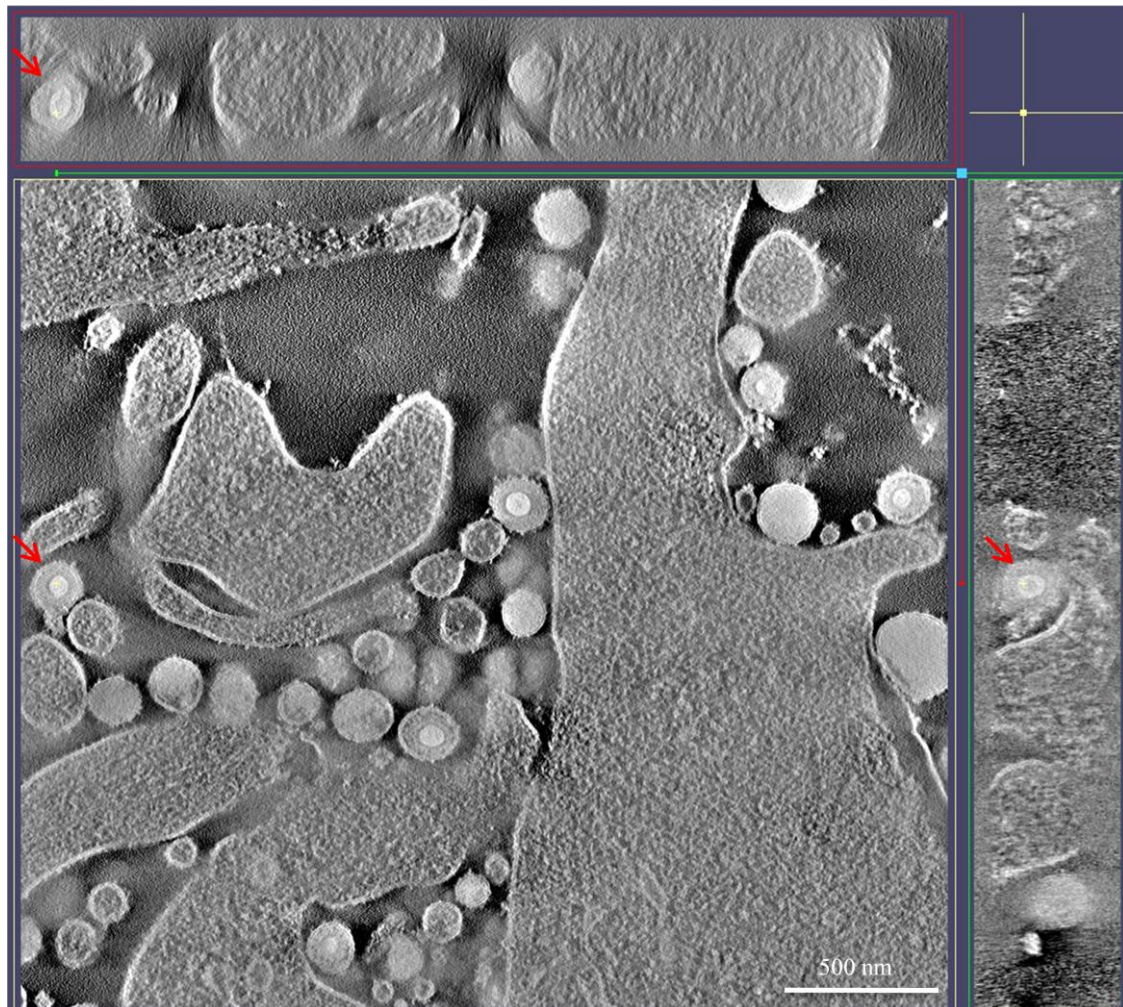


Figure 14: Image of computed sections of a tomogram of an HCMV-infected M1-M ϕ . M1-M ϕ were infected with TB40/E with an MOI of 30. At 30 minutes post infection, M ϕ were fixed by high pressure freezing and then processed for STEM tomography. The red arrows depict the same virion in the sections of the three different orientations.

By showing a direct interaction between the entire viral particles and tubular long protrusion of the M ϕ membrane (Fig.15) we could additionally support our hypothesis that the cytoskeleton remodeling is involved during HCMV entry into M ϕ .

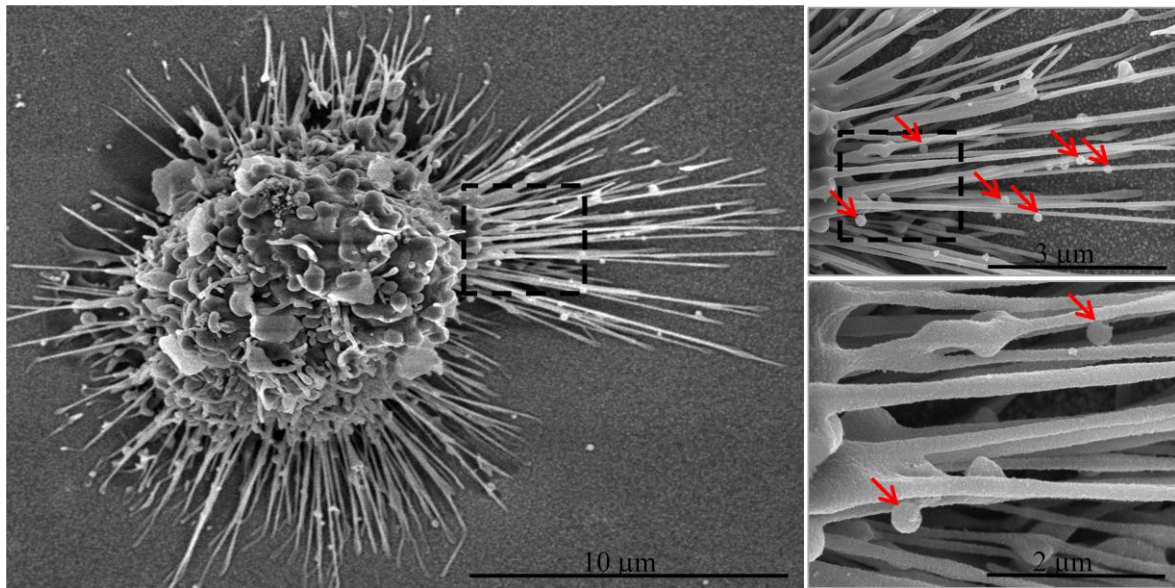


Figure 15: The attachment between HCMV and membrane protrusions containing actin. M1-M ϕ were infected with TB40/E with an MOI of 5. At 30 minutes post infection, M ϕ were fixed with 2.5% GA and processed for SEM. Red arrows point out the HCMV viral particles sitting on tubular protrusion of the cells membrane.

These data, however, are only qualitative and therefore suggest but do not prove whether the cytoskeleton remodeling plays an important role for HCMV particles entry into M1- and M2- M ϕ .

3.2.3 The viral gene expression is inhibited by actin cytoskeleton inhibitor

In order to demonstrate that cytoskeleton remodeling is required for uptake of HCMV, we assessed IE 1-2 gene expression in M1- and M2-M ϕ treated with common actin polymerization inhibitors. The cytoskeleton pharmacological inhibitor, latrunculin A, is able to prevent actin polymerization and for this property, it has been widely employed to study the entry mechanism of other viruses such as ebola virus [113]. By scanning electron microscopy, we could observe the resulting effects of inhibition of actin polymerization. M ϕ treated with 0.8 μ M latrunculin A for 30 minutes at 37 $^{\circ}$ C exhibited very smooth surface lacking almost completely the abundant protrusion typical of these cell type (Fig. 16).

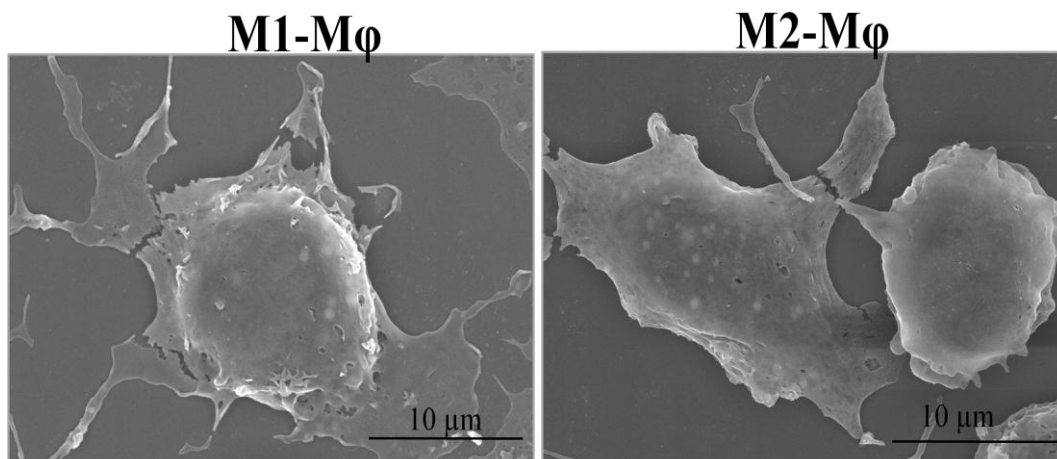


Figure 16: Morphology of M1- and M2- M ϕ treated with the actin polymerization inhibitor latrunculin A. M1- and M2- M ϕ were seeded into ibidi slides containing sapphire discs and incubated at 37 °C for overnight. The day after, M ϕ were treated with 0.8 μ M latrunculin A for 30 minutes prior to fixation by high pressure freezing and processing for SEM. These images of M1- and M2- ϕ are representative of 3 independent experiments

As shown in Fig. 16, the roughness of the surface of M1- as well as M2-M ϕ was strongly reduced. We also tested the effect exerted by latrunculin A in M1- and M2-M ϕ culture inoculated with TB40/E (MOI of 5) and we obtained comparable (data not shown) thus indicating that the treatment with 0.8 μ M latrunculin A for 30 minutes was not reverted by HCMV.

As next step, we quantified the inhibitory effect of latrunculin A on the HCMV infection of expression of the viral immediate early protein IE1-2 as a well characterized downstream event of the viral entry. M1- and M2- M ϕ were pretreated with different concentrations of latrunculin A for 30 min prior to be infected with an MOI of 5 of TB40/E. 24 hours later, treated- and control-M ϕ were stained with an antibody against HCMV IE 1-2 nuclear antigens, counterstained with DAPI and observed at the fluorescent microscope in order to quantify the percentages of IE 1-2 positive cells (Fig. 17).

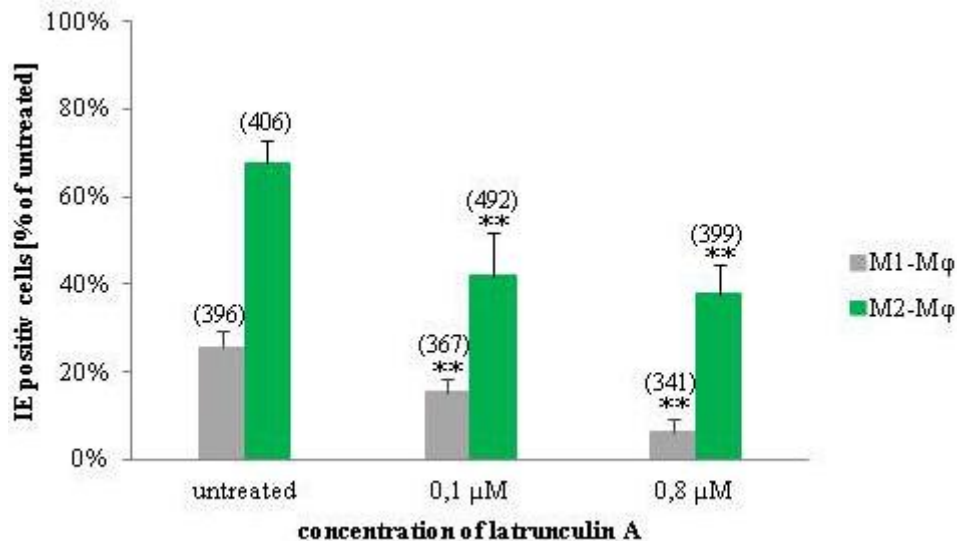


Figure 17: HCMV internalization into Mφ requires actin cytoskeleton polymerization. M1- and M2-Mφ were pretreated with the indicated concentrations of latrunculin A for 30 min, and then infected with TB40/E with an MOI of 5 for 24 hours. The infectivity of HCMV in Mφ was calculated as percentage of IE1-2 positive cells in relation to the number of DAPI positive cells. The absolute numbers of IE 1-2 positive cells is written on the top of each bar. Values are mean \pm standard deviation of 4 independent experiments. * $P < 0.05$ between treated and untreated cells.

As shown in Fig. 17, latrunculin A had a significant inhibitory effect on the HCMV infectivity in M1- and M2- Mφ. In M2- Mφ, both doses of latrunculin A had similar inhibitory effects and the IE 1-2 gene expression passed from ca. 70% in untreated cells to 40 % in cells treated either with 0.1 μ M or 0.8 μ M. On the other hand, in M1-Mφ the inhibitory effect exerted by latrunculin A was dose-dependent and an almost complete inhibition was obtained with the higher dose of latrunculin A. The total amount of cells, given by the number of DAPI positive cells, was not reduced in presence of latrunculin A thus suggesting that the drug did not lead to cell toxicity or death.

Since latrunculin A was solubilized in DMSO, we investigated whether DMSO alone had an effect on the HCMV infectivity in M1- and M2-Mφ. As shown in Fig. 18, DMSO concentration lower than 0.5%, corresponding to a 5:1000 dilution in medium did not have inhibitory effects on the percentage of IE 1-2 positive M1- and M2-Mφ.

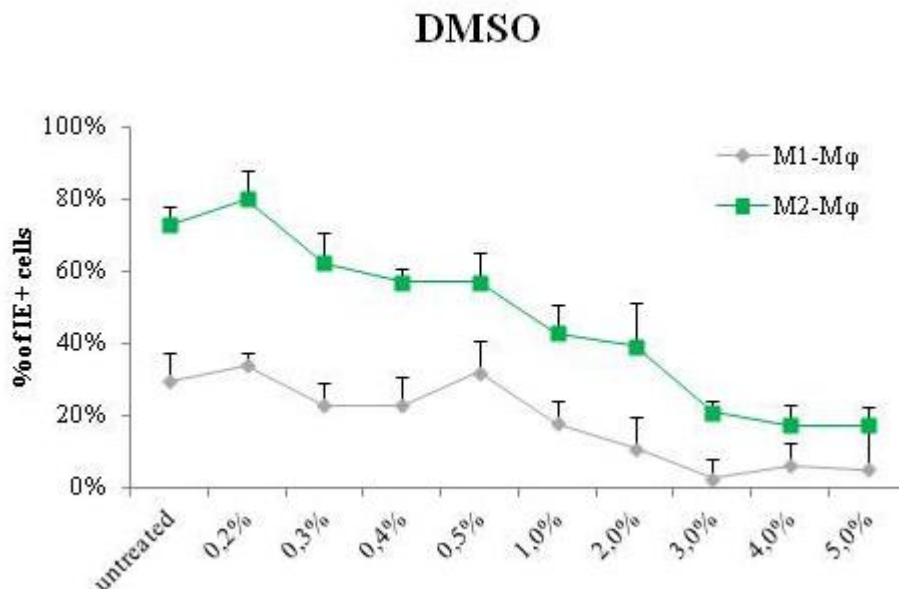


Figure 18: Effect of DMSO on HCMV infectivity in M1- and M2- Mφ. Cells were pre-incubated with indicated concentration of DMSO containing medium for 30 minutes and then infected with TB40/E with an MOI of 5 for 24 hours. The percentages of IE 1-2 positive Mφ were calculated as described in the Legend of Figure 17. Values are mean \pm SD of 5 independent experiments.

3.2.4 Latrunculin A does not interfere with the metabolic activity of M1- and M2-Mφ.

In order to exclude that latrunculin A had some negative impact on the Mφ cellular functionality, we compared the metabolic activity of treated Mφ by using the MTS (metabolization tetrazolium salt) assay. M1- and M2-Mφ were pretreated with different concentrations of latrunculin A as well as with the solvent DMSO and then infected with TB40/E (MOI of 5, w TB40/E) for another 24 hours. These conditions were similar to the infectivity measurement described in the previous chapter. As shown in Fig. 19, similar metabolic activities (quantified by the level of dehydrogenase activity and superoxide formation) were measured in mock and TB40/E-infected M1- and M2-Mφ, either with or without drug treatment. The comparable levels of metabolic activity indicated that the cells remained equally viable irrespectively on the drug or virus presence.

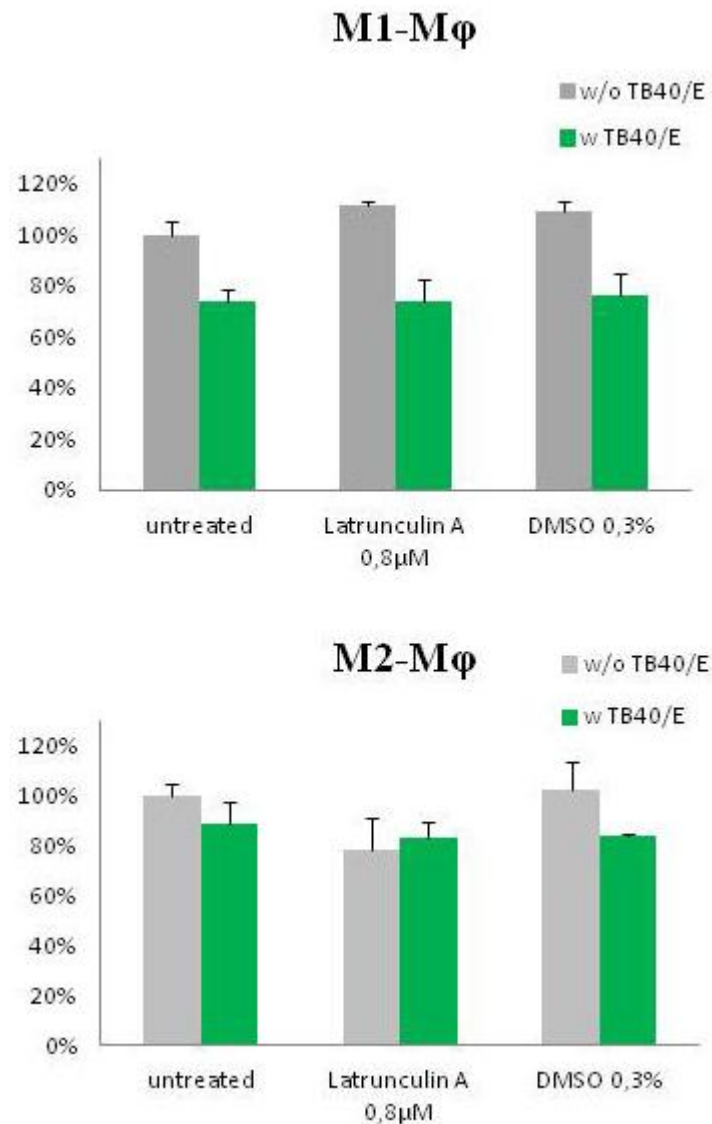


Figure 19: Effect of latrunculin A and the solvent DMSO on cell viability. M1- and M2-Mφ were pretreated with the indicated concentrations of latrunculin A or the solvent DMSO for 30 minutes and afterwards infected with TB40/E (MOI of 5) for 24 hours in presence of the chemicals. Viability was determined at 24 hours pi using the MTS cells viability assay. A single representative experiment is shown. (Error bars= S.D.)

As shown in Fig. 19, DMSO concentrations of 0.3% had no significant effect (as assessed by T-test analysis) on the metabolism of uninfected or TB40/E Mφ.

Taken together, the data obtained by electron microscopy, immune fluorescence and MTS test reveal that cytoskeleton remodeling is required for HCMV infection of both M1- and M2-Mφ.

3.3 HCMV internalization into M1- and M2-M ϕ occurs via a macropinocytosis-like pathway

3.3.1 Morphology of vesicles containing virus particles in M1- and M2- M ϕ

Considering the size of the HCMV particles (diameter between 150 and 300 nm) and that the M ϕ , take up pathogens mostly by phagocytosis or macropinocytosis, it is likely, that the virus enters into the two types of M ϕ by one of these two types of endocytosis. In addition, it has been reported that other herpes viruses such as Epstein-Barr and Herpes simplex virus are endocytosed into large uncoated vesicles via a mechanisms resembling macropinocytosis [61]. Additionally, it has been recently described that HCMV enters into dendritic cells via by a macropinocytosis-like pH – independent mechanism [28].

The distinctive features of both phagocytosis and macropinocytosis are the formation of primary endosomes with a diameter that can reach 10 μm [50] and the formation of outward directed elongations of the plasma membrane. To check whether the morphology of membranes elongations and the size of vesicles in infected M1- and M2-M ϕ satisfied these requirements, we analyzed infected M1- and M2-M ϕ by TEM at short points of time after infection. 2 minutes after infection, M1-M ϕ showed abundant membrane extension covering HCMV particles (Fig. 20). Additionally Figure 20 B demonstrates that the diameter of vesicles containing viral particles is about 1 μm . All together the morphological evidences indicated that in M1-M ϕ the uptake of HCMV took place by macropinocytosis.

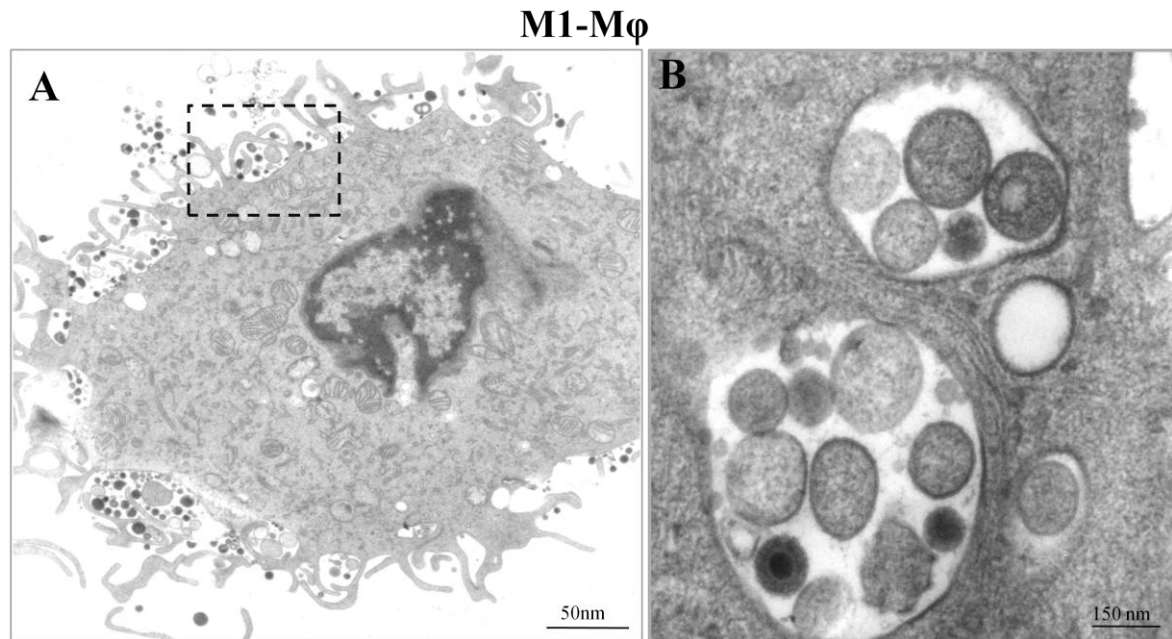


Figure 20: Ultrastructural analysis of HCMV entry into M1-M ϕ . M1-M ϕ were pre-cooled on ice, infected with TB40/E with an MOI of 30 and incubated for additional 30 minutes on ice so that the viral particles could attach to M ϕ but not penetrate them. The temperature was then shifted to 37 °C for another 2 minutes prior cell fixation by high pressure freezing. Two representative images obtained from 5 independent donors are shown.

Differently from M1-, TB40/E infected M2- ϕ showed vesicles with different shapes and sizes. As shown in Fig. 21 viral particles were visible inside big vesicle with a diameter of about 3 μm (Fig. 21A), as well as inside very small vesicles with a diameter of about 300 nm (Fig. 21C). Interestingly, naked capsids were also visible in the cytoplasm at such a short time after infection (Fig. 21B). To make sure that the round structures containing viral particles represented vesicles and not membrane invaginations, colloidal gold particles were employed as indicator. Cells were incubated with 1:50 diluted colloidal gold particles (10 nm) for 24 hours. Since the gold particles sitting in membrane invaginations communicating with the extracellular space were washed out of the samples, the persistence of the gold particles (highlighted by the green arrow) in proximity of the virion demonstrated that the circular structure were closed vesicles. The presence of both big and small vesicles could indicate that in M2-M ϕ that the uptake of HCMV took place by phagocytosis/macropinocytosis together with a different so far undefined mechanism.

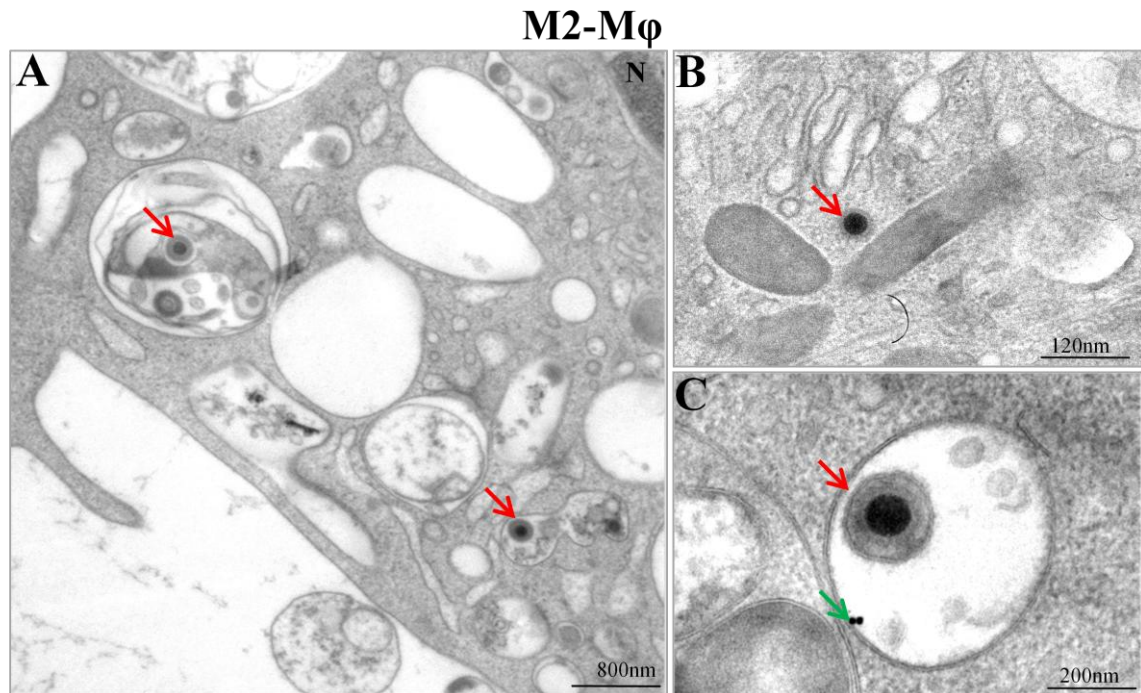


Figure 21: Ultrastructural analysis of HCMV entry into M2-M ϕ . M2-M ϕ were treated as described in the Legend of Figure 20. These images are representative of 4 independent experiments. Red arrows point in A) to big vesicles containing viral particles in B) to naked capsid, and finally in C) to small vesicles containing one viral particle. The green arrow points to colloidal gold particles. N= nucleus

In summary, while macropinocytosis seem the best candidate as HCMV entry pathway into M1-M ϕ , we suppose, that different entry mechanisms coexist in M2-M ϕ .

3.3.2 HCMV internalization into M1- and M2- M ϕ is impaired by EIPA

In order to confirm that vesicles containing viral particles in M1- and M2-M ϕ (Fig. 20 and 21) are macropinosome. we used pharmacological inhibitors of macropinocytosis prior infection with HCMV TB40/E. Amiloride, a well known Na⁺/H⁺ exchanger inhibitor, has been widely used as a selective blocker of macropinocytosis in endothelial cells and monocytes-derived dendritic cells [82]. M1- and M2-M ϕ were pretreated with increasing concentrations of the 5-(N-Ethyl-N-isopropyl) amiloride (EIPA) for 30 min prior to infection with TB40/E (MOI of 5). At 24 hours after infection, the medium containing EIPA was removed, the cells fixed/permeabilized and stained with an antibody against IE 1-2 HCMV antigens to count positive (infected) and total cells, as previously described. Fig. 22 shows that HCMV infectivity in M1- and M2- M ϕ was significantly reduced by EIPA treatment. The reduction of the number of IE 1-2 positive cells was dose dependent for both M1- and M2-M ϕ .

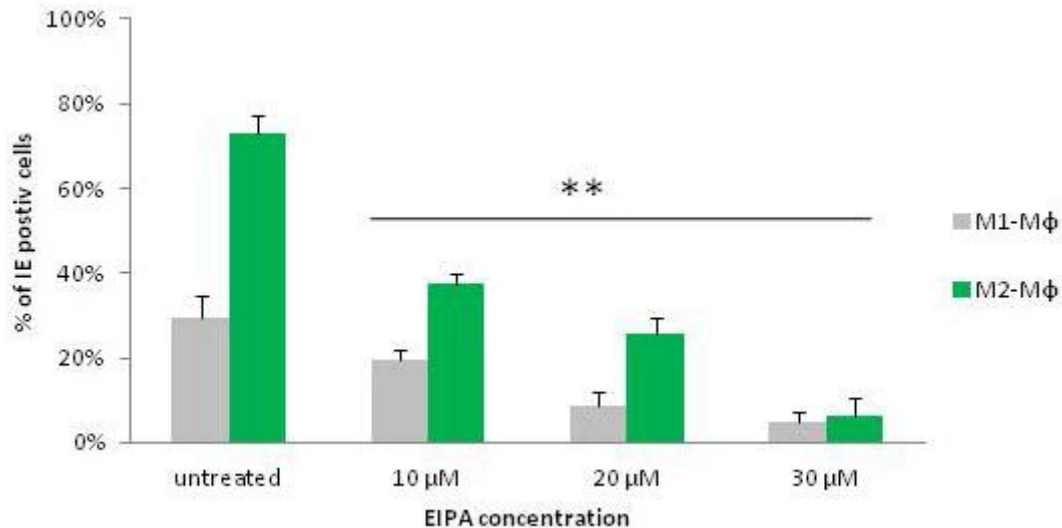


Figure 22: Effect of EIPA, a macropinocytosis inhibitor, on HCMV infection of M1- and M2- Mφ. M1- and M2-Mφ were treated with the indicated concentrations of EIPA for 30 min and then infected with TB40/E (MOI 5) for 24 h in presence of the inhibitor. Values are mean \pm SD obtained from 4 independent experiments. Individual treatment was performed in triplicate.

In order to prove that EIPA treatment was effective in blocking Mφ macropinocytosis we verified at the fluorescent microscope as well as cytofluorimeter whether the uptake of fluorescent-dextran (molecular weight 70.000 Da) was affected by the drug treatment. While untreated M1- and M2-Mφ engulfed FITC-dextran with high efficiency (Fig. 23) the pretreatment of the cells with EIPA (10 μ M EIPA, 30 minutes before of addition FITC-dextran) resulted in a complete block of macropinocytosis and lack of green fluorescence in the cytoplasm. Similar results were obtained by cytofluorimetry (Fig. 24).

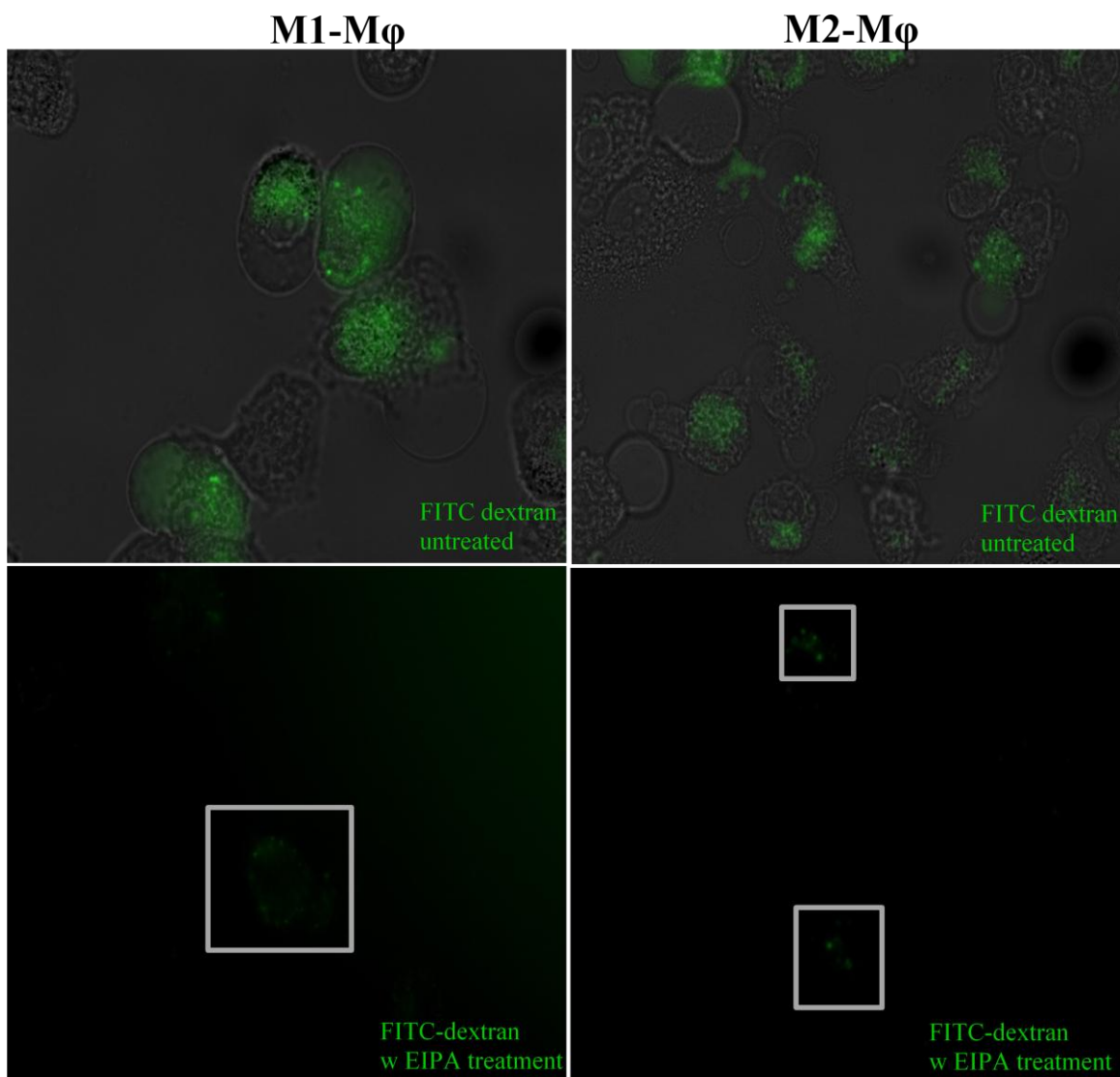


Figure 23: Effect of EIPA, a macropinocytosis inhibitor, on the uptake of FITC-dextran. M1- and M2-Mφ were pretreated with 100 μ M EIPA for 30 minutes. 2mg/ml FITC-dextran (70S) were added to the wells and the cells were incubated for 20 minutes at 37 $^{\circ}$ C.

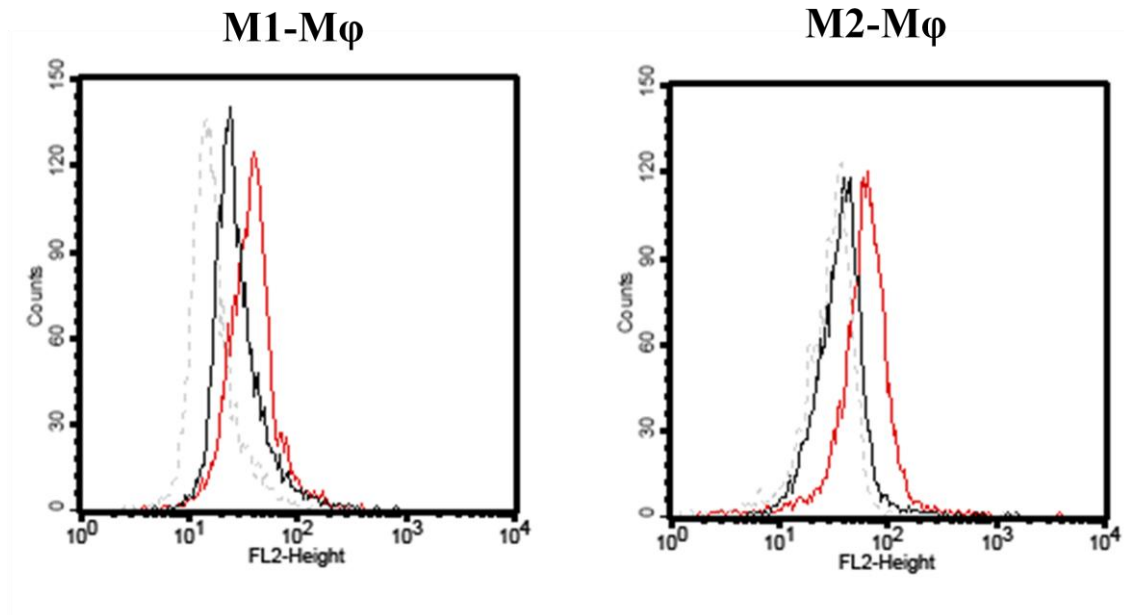


Figure 24: Effect of EIPA, a macropinocytosis inhibitor, on the uptake of TRITC-dextran. M1- and M2- Mφ were pretreated with 100 μ M EIPA for 30 minutes. 2mg/ml TRITC-dextran (70S) were added to the wells and the cells were incubated for 20 minutes at 37 $^{\circ}$ C, then FACS analysis was performed. (Dashed lines: 4 $^{\circ}$ C; red lines: 37 $^{\circ}$ C; black lines: with EIPA treatment at 37 $^{\circ}$ C)

3.4 HCMV infection of M1- and M2-Mφ depends on endosomal acidification

3.4.1 Neutralization of the endosomal pH inhibits HCMV internalization into M1- and M2- Mφ.

After penetration of HCMV into M1- and M2-Mφ by endocytosis, viral particles would require endosomal acidification to efficiently release their capsid into the cytoplasm and thus allow the injection of the genomes into the nucleus of the host cells. To address whether a low pH is required to promote the fusion between the viral envelope and the endocytotic vesicle membrane, we used pharmacological inhibitors of endosomal acidification and assessed whether the IE1-2 gene expression was affected. The drugs used had different specificity. Bafilomycin A1 (BafA1), which block the V-ATPase responsible for the endosomal pH decrease, is considered a selective inhibitor of the intravesicular pH. Ammonium chloride buffer (NH₄Cl) and monensin have more general effects and can alter the pH of the vesicles as well as the cytoplasm.

Firstly, we checked whether the three drugs effectively buffered the vesicular pH in both types of M ϕ . Acridin orange (AO), a pH-sensitive fluorescent indicator, was used to follow the acidification of the endosomal compartments. Due to the acidic pH in these organelles in untreated M ϕ , AO emitted a red fluorescence when was hit by the UV beam of the fluorescence microscope. Treatment with Baf A1, monensin or NH₄Cl led to the raise of the intraorganelle pH and to the emission of a green fluorescence. In Fig. 25, the majority of vesicles visible in untreated M1- and M2-M ϕ were red. On the contrary, the vesicles visible in M ϕ treated with Baf A1 and ammonium chloride were green. M ϕ treated with monensin that has a more unspecific mechanism of action showed an intermediate phenotype with some vesicles green and others red.

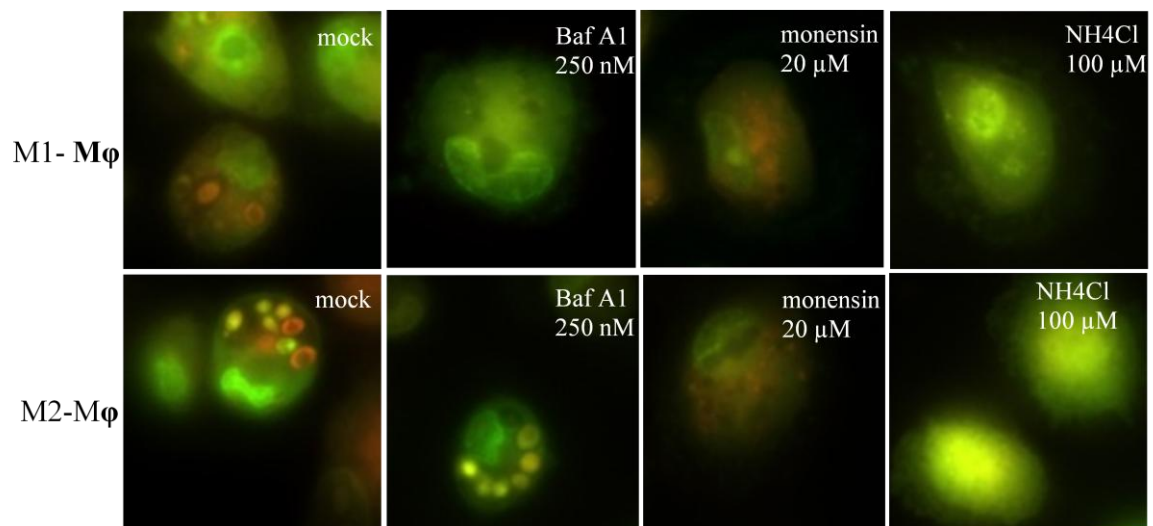


Figure 25: Effect of bafilomycin A1, monensin and NH₄Cl on M1- and M2-M ϕ . M1- and M2-M ϕ were pretreated with the indicated concentration of bafilomycin A1, monensin or NH₄Cl for 30 min at 37 °C. Control cells were left untreated (mock). 25 mM acridin orange were added for 15 minutes prior cell washing and incubation in phenol-red free medium for the imaging at fluorescent microscope. These images are representative of 3 independent experiments.

Next, we tested the inhibitory effect of the three drugs on the infectivity of HCMV. M1- and M2-M ϕ were pretreated for 30 minutes with increasing concentrations of inhibitors prior to infection with TB40/E. By counting IE1-2 positive M ϕ and DAPI positive cells (to determine the total cell number), we quantified HCMV infectivity before and after treatment with inhibitors. Fig. 26 shows that pharmacological neutralization of the endosomal pH inhibited HCMV infection in both M1- and M2-M ϕ . 50 mM and 250 mM doses of NH₄Cl could significantly inhibit the IE1-2 expression in both types of M ϕ (Fig. 26A). The effects of NH₄Cl were similar to those of Baf A1. As shown in Fig. 26 B, the IE1-2 expression was reduced in a dose dependent manner by treatment with Bafilomycin

A1. However, only the two higher doses significantly inhibited HCMV infectivity. As compared to Bafilomycin A1, monensin exerted a stronger inhibition and a roughly 50% reduction in the number of IE 1-2 positive cells was measurable already at the lowest concentration (Fig. 26 C).

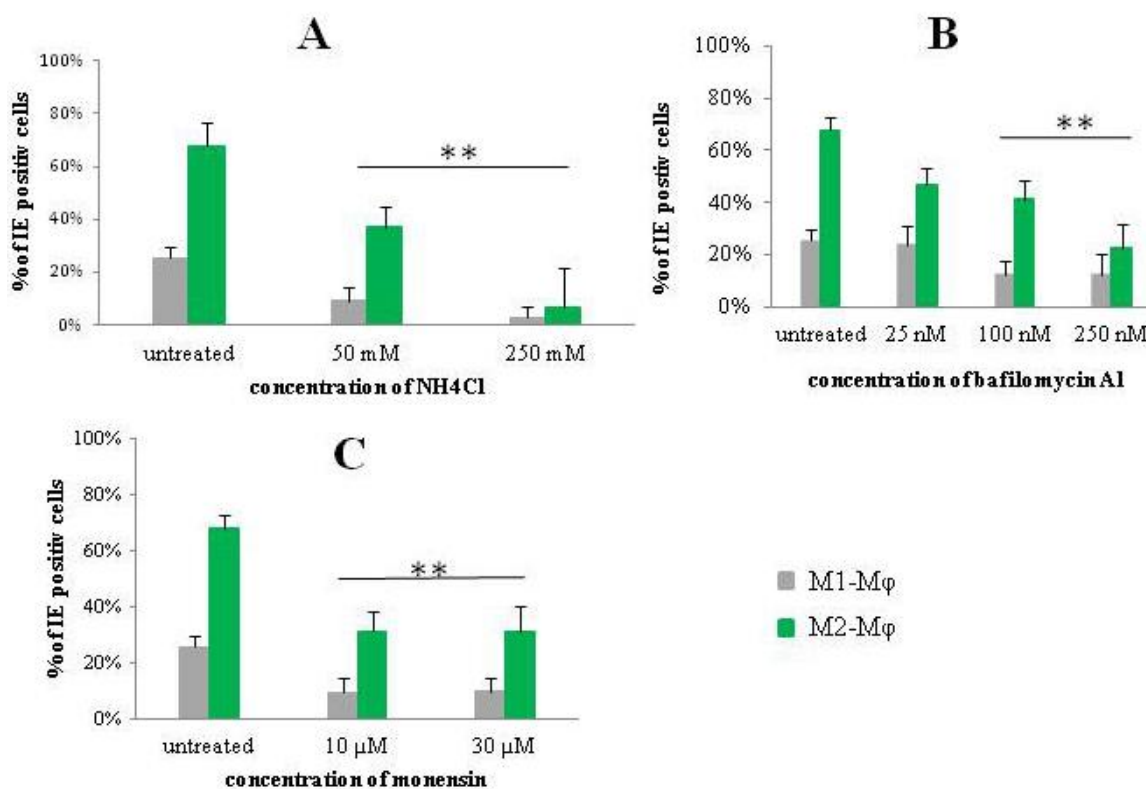


Figure 26: Endosomal pH neutralization inhibits HCMV infection in M1- and M2-Mφ. M1- and M2-Mφ were pretreated with the indicated concentration of NH₄Cl (A) bafilomycin A1 (B) or monensin (C) for 30 min at 37 °C. Then the cells were infected with TB40/E with an MOI of 5 for another 24 hours in the presence of each lysosomotropic agent. The infectivity was calculated as percentage relative to the total cell as previously described. Values are mean \pm SD obtained from 4 independent experiments. $P < 0.05$.

The total number of DAPI positive Mφ remained constant irrespectively on the type or dose of the drug used. Although this is a clear indication that the three drugs do not reduce cell viability, the Mφ metabolic activity was also measured by MTS assay.

3.4.2 Lysosomotropic agents do not alter metabolic activities of M1- and M2-M ϕ

The MTS test measures the metabolic capacity of cells to convert the not fluorescent rasazurin into a fluorescent resorufin derivate. The production of fluorescent resorufin is proportional to the number of metabolically activity cells in the culture. If a drug is toxic to the cells, the metabolic activity is reduced and less dye is converted into the fluorescent derivate. In this study we tested all drugs and their diluents, namely DMSO and ethanol. In Fig. 27, DMSO and ethanol die not show cell toxicity in M ϕ . The highest concentration of bafilomycin A1, which was used in the infectivity test (Fig. 26), did not show toxic effects, neither did it monensin.

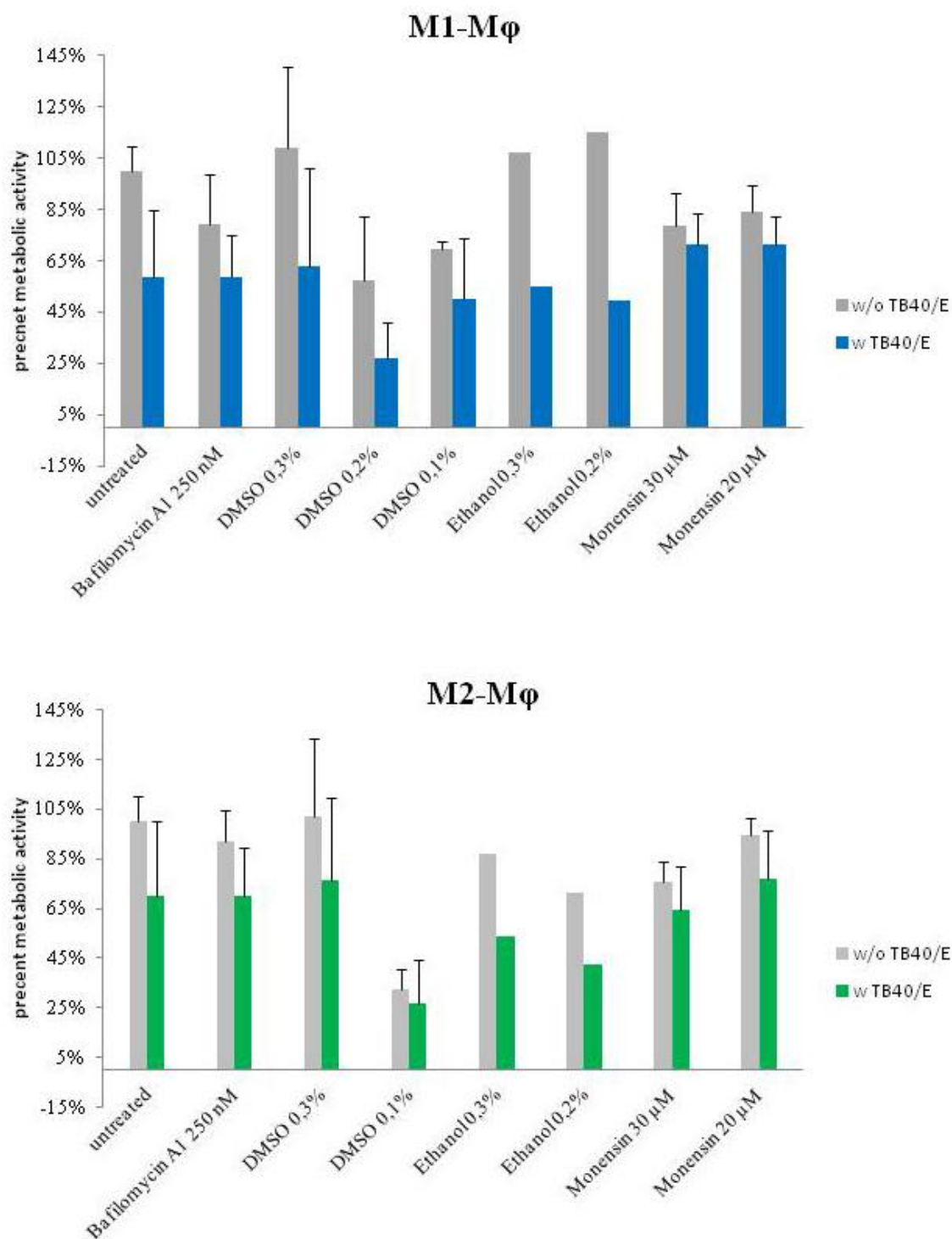


Figure 27: Effect of lysosomotropic agents on metabolic activity of M ϕ . M1- and M2-M ϕ were pretreated with the indicated concentrations of bafilomycin A1, monensin or the respective solvents (DMSO and ethanol) for 30 minutes and afterwards infected with TB40/E (MOI of 5) for 24 hours in presence of the chemicals. Viability was determined at 24 hours pi using the MTS cells viability assay. Values are mean \pm SD from 4 independent experiments.

In summary, our results show a significant reduction of the number of IE1-2 positive M ϕ after treatment of the cells with lysosomotropic agents in a dose-dependent manner for all drugs tested. The inhibitory effects is not due to reduction of M ϕ viability because the drugs nor the respective diluents show toxic effects on M ϕ .

3.5 HCMV viral particles do not co-localize with late endosomes but only with early endosomes

3.5.1 HCMV do not co-localize with late endosomes in M1- and M2-M ϕ .

As shown in Fig. 20 and 21, few minutes after infection are sufficient to allow the visualization of several HCMV particles in big vesicles in both types of M ϕ . Moreover, 3 hours after inoculation of M ϕ with HCMV, there are many vesicles containing virus particles in M2-M ϕ and few vesicles in M1-M ϕ (Fig. 7). Since the feature of these vesicles containing viral particles were unclear, the fate of the viral particles during the infection process could not be determined. In order to characterize the location of HCMV in different organelles, M ϕ were infected with the recombinant virus HCMV pUL32-EGFP, which possess the enhanced green fluorescent protein (EGFP) fused to the C terminus of the capsid-associated tegument protein pUL32 (pp150) [98]. At different points of time after infection, M ϕ were stained with antibodies against EEA1 or LAMP1, which are preferentially expressed by early or late endosomes/lysosome, respectively. The pictures obtained with a confocal fluorescence microscopy displayed aggregates of viral particles as green dots and the early and late endosomes as red bigger dot. At 30 minutes post infection, the early endosomes could be found closed to the plasma membrane in both types of M ϕ , because this corresponds to the general localization of early endosomes in the cytoplasm. Moreover, only few early endosomes co-localize with HCMV particles. As shown by the white arrows in Fig. 28, the proximity of HCMV particles and early endosomes was more frequently observed in M2- than in M1-M ϕ . At 24 hours post infection late endosomes distributed preferentially close to the nucleus, which also corresponds to the general late endosome distribution in cells. Interestingly we were unable to find any co-localization between HCMV particles and late endosomes in M1- and M2-M ϕ at any time point, thus suggesting that the viral particles do not enter into late endosomes nor in lysosomes.

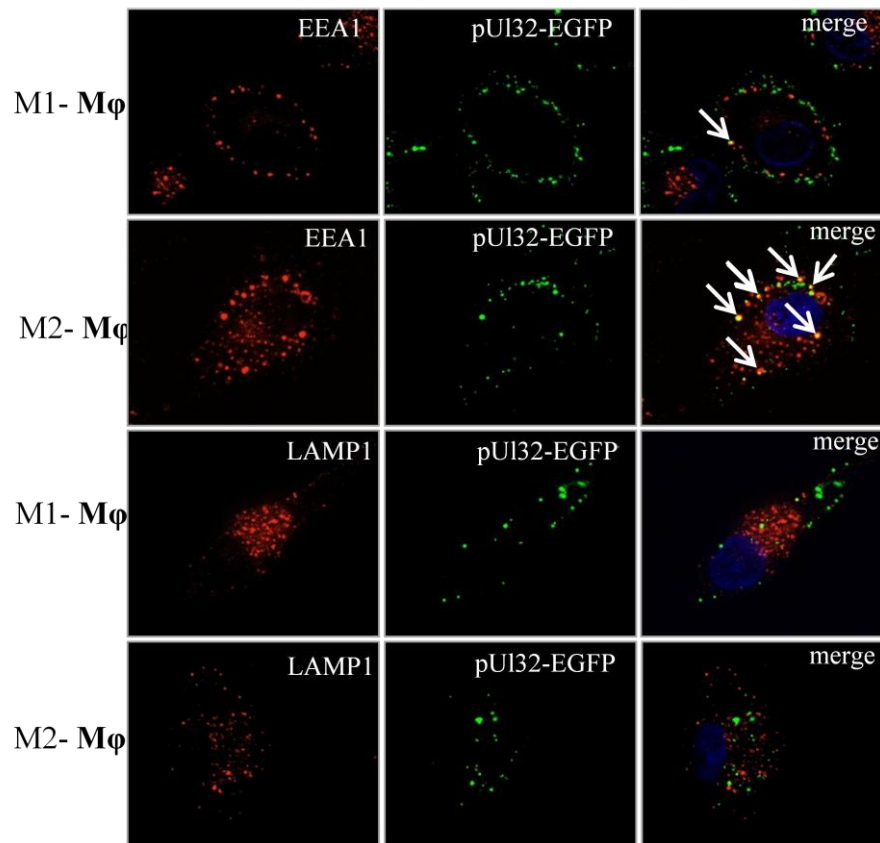


Figure 28: Internalized HCMV partially co-localize with EEA1 but not with LAMP1 in M1- and M2-M ϕ . M1- and M2-M ϕ were infected with the recombinant HCMV pUL32-EGFP (green) for 30 min (Upper two rows) and for 24 hours (lower two rows). Cells were then permeabilized and immunostained with anti-EEA1 or anti- LAMP1 antibodies (red). EEA1, an early endosome marker was imaged at 30 min while the late endosome (LAMP1) was tested. At 24 hours post infection Images were obtained by Apo tome analysis on a Zeiss Observer, Z1 microscope, so that optical sections in the depth of the cell are visualized. White arrowheads in the merged images indicate the co-localization between virus and cellular endosome marker in both types of macrophages. Pictures are representative of 4 independent experiments

3.5.2 HCMV does not co-localize with gold labeled vesicles representing late endosomes

The limited resolution of light microscopy (about 200 nm) impairs co-localization experiments. Therefore, we use transmission electron microscopy. M1- and M2-M ϕ were seeded in ibidi slides with sapphire discs. After one day attachment, cells on sapphire discs were feeded with 10 nm colloidal gold particles (diluted 1 to 50) for another 24 hours, so that the gold labeled vesicles could proceed into late endosomes or lysosomes. Then, M ϕ

were infected with TB40/E with an MOI of 30 prior for two hours to fixation by high pressure freezing.

Firstly we observed the pattern acquired by late endosomes or lysosomes labeled with the gold particles in mock-infected M ϕ . The position of the gold labeled vesicles resembles the pattern of LAMP1 staining observed at the fluorescent microscope (Fig. 29)

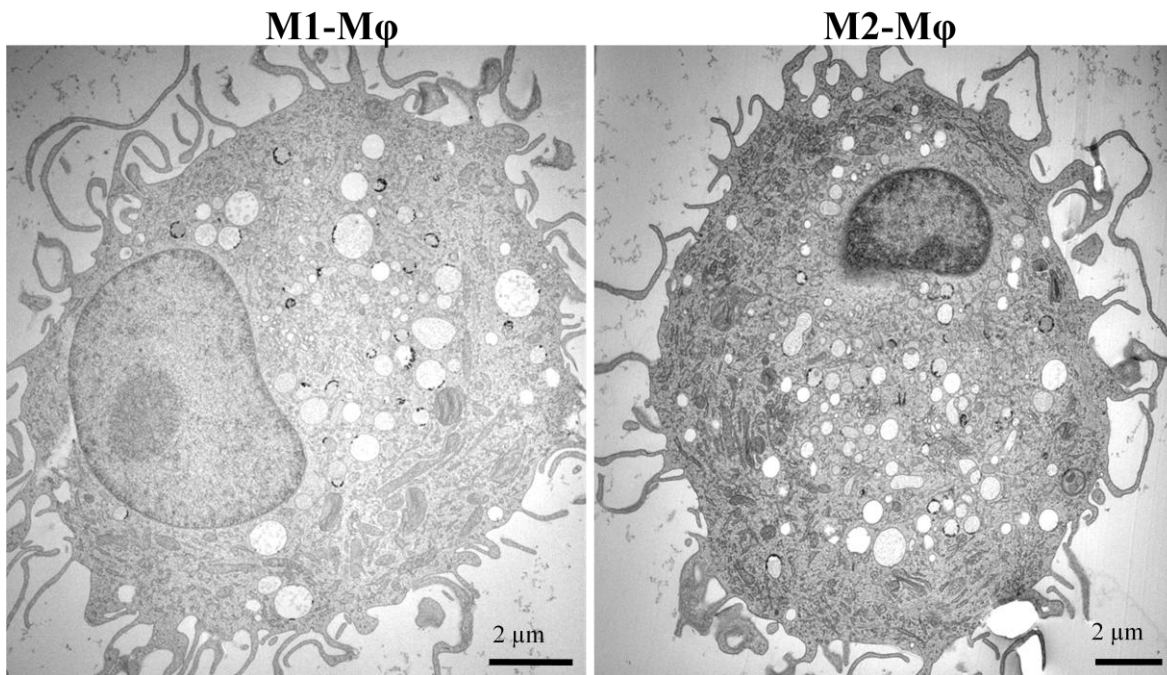


Figure 29: Mock-infected M1- and M2-M ϕ with 15 nm colloidal gold labeling. M1- and M2-M ϕ were seeded in ibidis slides containing sapphire discs for 3 hours attachment. Then 1:50 diluted colloidal gold solution was added to the M ϕ and maintained in incubator for 24 hours. At this time point M1-M ϕ were fixed by high pressure freezing. These images are representative of 3 independent experiments.

After M1- and M2-M ϕ were infected with TB40/E for two hours, we investigated whether viral particles reached gold labeled vesicles (considered as late endosome/lysosome) or gold free vesicles (considered as early endosomes)

As shown in Fig. 30 A, in M1-M ϕ only few viral particles were detected intracellularly and mainly located in vesicles (red arrows) without colloidal gold. The vesicles had mainly a diameter of ca. 250 nm to 1 μ m. A single virion was endocytosed into a ca. 250 nm diameter vesicle and additionally one naked capsid was visible in the cytoplasm. The virus containing vesicles spread only in the periphery of M1-M ϕ , while the gold labeled vesicle were closed to the nucleus and did not contain viral particles. In Fig. 30 B, another infected M1-M ϕ is shown. There is also one naked capsid (red arrow) in the cytoplasm. Another virion is located in one vesicle with dense bodies and NIEPs, this vesicle contains no

colloidal gold. There are some vesicles with 2 μm diameter, in which cell debris and few dense bodies of HCMV are located. Since the colloidal gold particles are also found in these vesicles, it could indicate that these viral particles might traffic to the lysosomes for degradation.

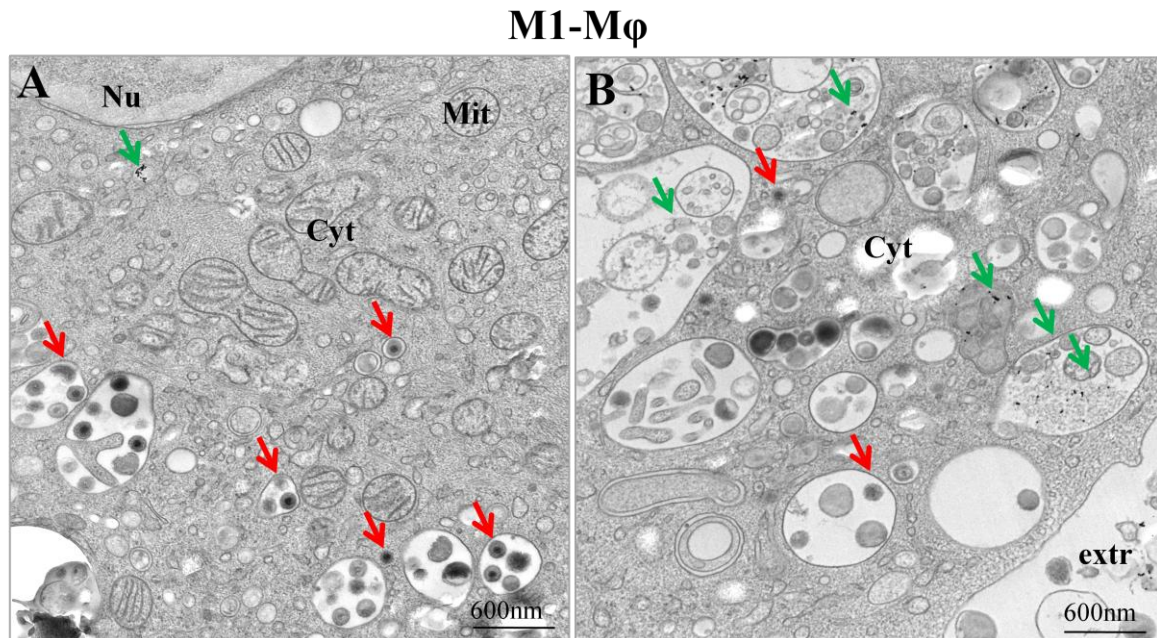


Figure 30: Virions do not co-localize with colloidal gold labeled vesicles. M1-M ϕ were seeded in ibidis slides with sapphire discs and incubated overnight to attach. Then the cells were feeded with 15 nm colloidal gold particles and incubated for 24 hours at 37 $^{\circ}\text{C}$. On the third day, M1-M ϕ were infected with TB40/E for 2 hours prior fixation by high pressure freezing. These images are representative of 3 independent experiments.

Fig. 31 (A, B) shows the HCMV infected M2-M ϕ . The procedure was the same as for M1-M ϕ in Fig. 28. panel A exhibits an overview of M2-M ϕ . The red arrows depict naked capsids and vesicles containing HCMV virions. Panel B shows the marked area at higher magnification. Single virions are located in vesicles without gold particles. And another vesicle (green arrows) contains colloidal gold particles but no virions.

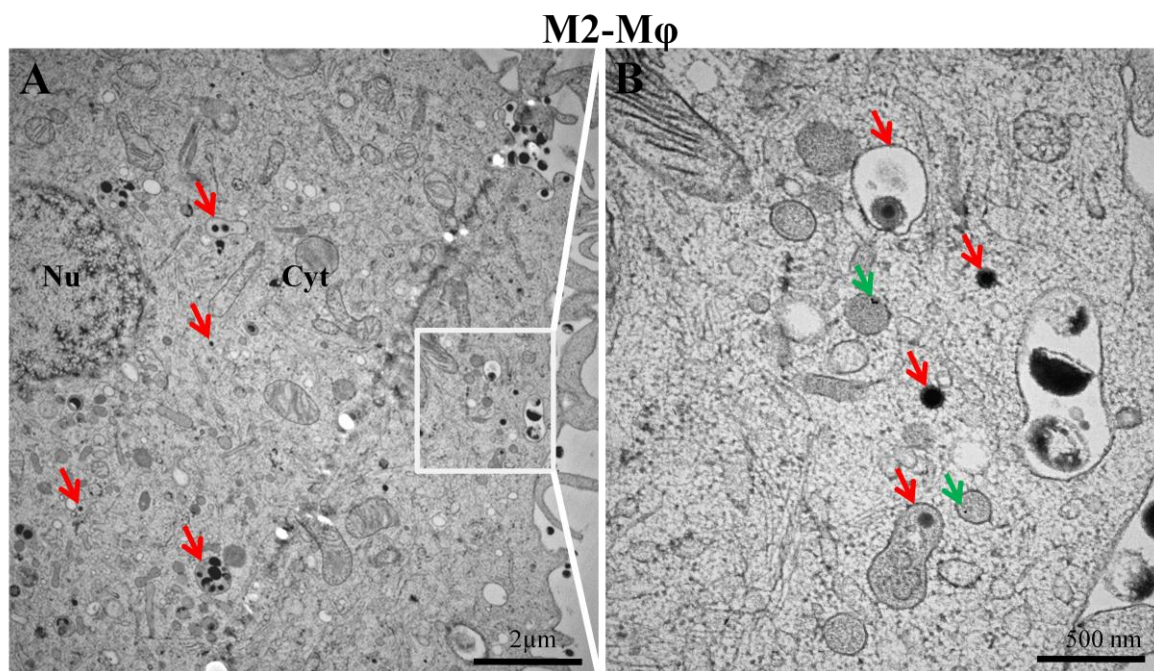


Figure 31: HCMV do not co-localize with colloidal gold labeled vesicles. M2-Mφ were seeded in ibidi slides with sappire discs and incubated for 1day to get attached. Then the cells were feeded with 15 nm colloidal gold particles and incubated for additional 24 hours at 37 °C. On the third day, M2-Mφ were infected with TB40E for 2 hour prior fixation by high pressure freezing. These images are representative of 3 independent experiments.

Interestingly, we did not observe any co-localization between virions and vesicles containing colloidal gold particles. In some extent, dense bodies and other debris entered into gold labeled vesicles, can indicates that only virions apparently are not enter late endosome or lysosome and thus are protected from degradation.

To summarize the data from TEM and IIF, we can conclude that HCMV virions do not co-localize with late endosomes at any time point. The few co-localizations of viral particles and early endosomes give us indirect information that HCMV is endocytosed into M1- and M2-Mφ.

4. Discussion

Human cytomegalovirus (HCMV) establishes with the cells of the hematopoietic system a very peculiar relationship: it can infect monocytes and their stem cell precursors but it remains for the most part transcriptional inactive [101]. However, stimulation of these cells by inflammatory or allogeneic stimuli triggers the monocytes to macrophages (M ϕ) differentiation and the reactivation of HCMV [32,90,94]. Viral particles produced by tissues M ϕ can disseminate in the tissues/organs as well as within the circulation. In *in vivo*, the infection of monocytes and M ϕ has been implicated in clinical manifestations such as hepatitis, nephritis and bronchiolitis [15,84]. Since monocytes and M ϕ are important cells of this innate immune system, it is still unknown whether the deleterious effect for the host is due to a viral or immune mediated process. Additionally, it is still not understood how HCMV can escape this innate defense mechanisms of M ϕ and establish a productive infection inside one of the most hostile cellular environment in the human body. Due to their high content of lytic enzymes and granules, their adjustable expression of histocompatibility and costimulatory molecules M ϕ , normally contribute to host defense and pathogen elimination [69,73]. Before complete sequencing of the viral genome and for long time, the laboratory HCMV strain AD169 has been used in *in vitro* to study how HCMV does use M ϕ as target. The complete sequencing of the viral genome and the availability of new clinical isolates such as the strain TB40/E [81,88], have revealed the existence of great differences between the genomes of viruses adapted to growth into fibroblasts as compared to those strains still able to replicate into endothelial cells. It was therefore not surprising that AD169 could only infect a small proportion of M ϕ and express a limited range of viral products. By using endotheliotropic HCMV strains such as TB40/E (or VHLE, VR1418, etc) it was possible to infect high percentages of M ϕ and to observe the production of all classes of viral gene products. Preliminary data of our laboratory shows that two distinct types of M ϕ can be obtained in *in vitro*, namely pro-inflammatory M1- and anti-inflammatory M2-M ϕ . The interaction between these two types of M ϕ and HCMV is in most case unclear. Recent data [71,79] confirmed our observations that HCMV infectivity in M2-M ϕ is very high and it is in contrast very low in M1-M ϕ . Since the entry mechanisms used by HCMV in the two types of M ϕ might be the key to explain the difference of infectivity we decided to characterize the mechanisms of HCMV internalization in M1- and M2-M ϕ .

So far, it has been shown that HCMV can enter different cell types using different mechanisms, in fibroblast HCMV uses predominantly the direct fusion of the viral envelope with the cell plasma membrane while in endothelial cells HCMV enters via a pH independent type of endocytosis [7,13]. The differential analysis of these entry pathways in M1- and M2-M ϕ could provide a deeper understanding of the different infections rate in two types of M ϕ and contribute to the identification of potentially new targets of antiviral drugs. Our study was performed by integrating different tools and technical approaches such as innovative imaging techniques and classical biochemical/functional analysis using pharmacological inhibitors.

M ϕ are a very heterogeneous cell population. Since to our knowledge, the morphology of M1- and M2-M ϕ was not described yet, we initiated our study by a detailed characterization of the morphology of the two types of M ϕ . During monocytes to M ϕ differentiation, we observed dramatic morphological changes. Under light microscope, the size and shape of mature M1-M ϕ was smaller and rounder as compared to M2-M ϕ , although both types of M ϕ were bigger than monocytes. Interestingly, after detachment and seeding onto ibidi slide for examination under scanning electron microscope, M1- and M2-M ϕ appeared similar. Both types of M ϕ exhibited a relatively complex surface. After infection, both of them resulted activated and showed much more complex and rough surface. Owing to the high resolution, we could observe tubular extension of the cell membrane protruding towards and interacting with HCMV particles. Formation of long protrusion or filopodia could increase the area of the plasma membrane and so guarantee more opportunities to uptake viral particles. Because the membrane extensions are supported by actin filaments, this observation indirectly suggested, that M ϕ may use macropinocytosis or phagocytosis to uptake HCMV.

An entry pathway such as endocytosis might offer some advantages to HCMV as described in the introduction. Till now it is well characterized that endothelial cells take up HCMV by endocytosis, there are no data describing whether a proportion of the incoming viral particles are lysed within lysosomes. Our indirect immune fluorescence pictures showing the localization of HCMV particles in M1- and M2-M ϕ at 90 minutes post infection, suggest that the incoming HCMV particles enter in both types of M ϕ by endocytosis but reach different destinations. HCMV particles accumulate on the periphery of M1-M ϕ , whereas they spread in the entire cytoplasm of M2-M ϕ and at later times even accumulated in proximity of the nucleus. This different localization of HCMV particles could reflect an

important difference between the mechanisms of entry into M1- or M2-M ϕ . For endothelial cells, it has already been demonstrated that while the highly endotheliotropic HCMV strains such as VHL/E and TB40/E are efficiently translocated in proximity of the nucleus [91], fibroblast-adapted strains such as AD169 and TB40/F, even though internalized, remain in the periphery of the cell and are not able to migrate towards the nucleus where the viral genomes needs to be delivered in order to start the viral gene expression [91,93]. The observation that HCMV localized much closer to the nucleus in M2-M ϕ than in M1-M ϕ would indicate that the delivery of viral particles to the nucleus of M1-M ϕ is less efficient than in M2-M ϕ . Therefore we can suppose that the inefficient translocation from the cell periphery to the nucleus in M1-M ϕ might be the causes of the low infectivity in M1-M ϕ while the efficient translocation in M2-M ϕ explains their high susceptibility. The ultrastructural analysis performed by TEM, confirmed the different localization of the viral particles and additionally demonstrated that the majority of viral particles remained inside vesicles at least until 3 hours post infection in M2-M ϕ . In M1-M ϕ , the majority of HCMV particles remained very close to the plasma membrane accumulating below complex membrane extensions. In an attempt to address whether these structures were closed vesicles or deep invaginations still communicating with extracellular space, we performed 3D electron microscopy tomography. Due to the considerable thickness of the section, this method is more informative and allows the distinction between internalized (“in”) and still external (“out”) HCMV particles. Fig. 11 shows the 3D reconstruction of a whole endosome. It is evident, that the spherical structure is closed and has no opening toward the extracellular space.

According to the complexity of M ϕ surface and to the size of the vesicles containing HCMV particles, we hypothesized that the uptake of HCMV into M1- and M2-M ϕ occurred via macropinocytosis. A similar mechanism has been shown for HCMV entry into human retinal pigment epithelial cells [7] and dendritic cells [28]. Using transmission electron microscopy, we observed open or closed filopodia-like structures establishing close contact with HCMV particles. Since it is common opinion that filopodia protrusions of plasma membrane require an actin scaffold, we investigated the importance of actin during HCMV infection of M ϕ by treating the cells with chemical inhibitors of actin polymerization. Our results show that M ϕ treated with latrunculin A lack the filopodia and present a drastic reduction in the percentage of IE 1-2 positive cells. Actin-polymerization has been described as an important cellular factor involved in the entry of several enveloped viruses e.g, HIV-1, HSV-1 and vaccinia virus. For HCMV it is known that actin

dependent infection takes place in retinal pigment epithelia cells, endothelial cells and dendritic cells, while in fibroblasts the infection process does not require actin [13]. On the other hand, our data showed that HCMV entry and the subsequent event, the immediate early gene expression involved an active and actin dependent remodeling of the plasma membrane in both types of M ϕ . However since the inhibitory effect of latrunculin A was not complete nor dose dependent in M2-M ϕ and additionally few naked capsids were visible by TEM in the cytoplasm of M2-M ϕ , we can conclude that at least in this M2- M ϕ . HCMV enters via macropinocytosis and also by another mechanism that could be direct fusion at the plasma membrane.

During macropinocytosis, the extracellular material is surrounded by circular ruffles and protrusions of the plasma membrane, and then it is engulfed into large vesicles called macropinosomes which have usually a size of 500-2000 nm [6,19]. According to the size of HCMV virion of roughly 200-300 nm in diameter [55], the macropinosomes should be large enough to contain even more than one HCMV particle. Additionally macropinocytosis has been considered a possible entry route for other herpesviruses such as herpes simplex virus and Epstein-Barr virus that have been detected inside 300-1000 nm or 300-500 nm large uncoated vesicles, respectively [61,63]. The images we obtained by ultra structural analysis of from HCMV infected M1- and M2 –M ϕ showed big vesicles containing more than one viral particles of with diameter of ca 1 μ m. Additionally, the use of specific macropinocytosis inhibitors confirmed the importance of this pathway during HCMV infection of M ϕ . The HCMV entry and the following expression of the immediately early HCMV antigens were indeed significantly reduced by M ϕ pre-treatment with the amiloride EIPA. The inhibition of HCMV infectivity as well as of FITC-dextran uptake was dose-dependent in the two types of M ϕ .

Because the contents of macropinosomes can either be degraded at the late endosome/lysosome stage or recycled at the plasma membrane [45,50], we analyzed the location and the fate of internalized HCMV particles. To lead to a productive infection, the endocytosis of enveloped viruses must be followed by the fusion of the viral envelope with the membrane of the endocytotic vesicles. This fusion event, responsible of the release of the viral capsid in proximity of the nucleus, is often triggered by a drop of the endosomal pH that occurs when, the early endosomes has already translocated towards the cell center and the proteolytic enzymes haven been activated [47]. The drop of the endosomal pH can either promote the conformational changes required for the fusion process itself or expose

the viral particles to a process of degradation. The requirement for a low pH can be a dangerous choice for the virions and it has been shown that while TB40/E infects endothelial cells and epithelial cells in a pH-dependent way [81], the infection of dendritic cells is pH-independent [28]. A crucial factor defining the virions's fate could be the duration of the virions persistence inside low pH compartments. Our working hypothesis was that due to a longer persistence or trapping of the viral particles into acidic compartments, HCMV underwent a preferential destruction inside M1-M ϕ as compared to M2-M ϕ . To address whether the M ϕ infection required a low pH, we used different pharmacological inhibitors in order to drop the endosomal acidification. Inhibition of endosomal acidification by bafilomycin A1 reduced infectivity efficiently reduced HCMV infectivity in a dose-dependent fashion in both types of M ϕ but not in fibroblast or dendritic cells. Ammonium chloride and monensin, the less specific pH inhibitors induced significant reduction of HCMV infectivity in the two types of M ϕ but without clear close-dependent relation. All together these data demonstrate that HCMV infection of M ϕ requires low pH. Additionally, the lack of a complete inhibition of HCMV infectivity event at the higher doses of these drugs suggests a very fast transit of the viral particles from the low pH compartment to the cytoplasm. This pH-dependent entry mechanism might be another example of HCMV adaptability to into host. Inside the highly phagocytic and lytic M ϕ , HCMV seems to use the endocytotic machinery to penetrate into M1- and M2-M ϕ without being entirely destroyed. Interestingly while we could observe a particles co-localization between HCMV particles and early endosome vesicles, we did not find evidence of viral accumulation inside or in proximity of late endosomes. The viral persistence into cytoplasmic vacuoles could be explained as a mechanism developed by HCMV to remain compartmentalized and protected inside the cells even in absence of a productive infection. A similar mechanism has been described for human immune – deficiency virus (HIV) that also appears to accumulate in M ϕ vacuoles [64] derived from the Golgi complex [64]. On the view, it is intriguing the old report demonstrating that the Golgi marker mannosidase II associates with HCMV particles in infected M ϕ [21]

The data presented so far do not reveal major differences between M1- and M2-M ϕ and therefore are not sufficient to explain at the molecular level the different susceptibility of the two types of M ϕ . Keeping on mind that the TB40/E we used in our experiments, is not a genetically pure virus but contains heterogeneous particles, some of them containing the UL128 to UL150 genes and other missing these genes, we can't exclude that the entry mechanisms we attempted to dissect were multiple due to the presence of different types of

particles. As example it is possible to imagine that while some particles are well equipped to rapidly enter and infect the M ϕ , others are prone to accumulate in the macropinosome-like vesicles where they undergo eventually degradation. Maybe there are more fusion receptors on the surface of M2-M ϕ than on M1-M ϕ , thus leading to a receptor-mediated internalization into M2-M ϕ and a receptor-independent process in M1-M ϕ .

On the other side, it is possible that the particles contained into vesicles are not those responsible for the deposition of the viral genomes into the nucleus and for the expression of the viral genes. In the TEM images we have observed that the amount of naked capsids is higher in the cytoplasm of M2-M ϕ as compared to M1-M ϕ at all points of time. On this line, it is possible that independently on the great amount of endocytosed viral particles, the “truly” infectious particles are only the few naked capsids that have fused at the plasma membrane or that have quickly escaped from the endosomes. In this case, there would be a clear correlation between the ultrastructural data and the different percentage of IE 1-2 positive M1- and M2-M ϕ .

The mechanism used by the viral particles to escape from the endosomes could then be a more important factor than the mechanisms used to enter inside them. If it would be confirmed that in M2-M ϕ the truly infectious HCMV particles are quickly released from the endosome by a pH-dependent mechanism while they are retained for longer times in M1-M ϕ we could explain the basics of the different susceptibility of M1- and M2-M ϕ .

5. Summary

Human cytomegalovirus (HCMV) is a ubiquitous Herpesvirus causing morbidity under conditions of impaired immune control. Even though HCMV can virtually infect any cells of the human body, the processes of viral proliferation transmission and systemic spread mainly occur in fibroblasts, epithelial/ endothelial cells and cells of the hematopoietic system. In previous studies it has been shown that i) HCMV-infected macrophages (M ϕ) can contribute to hematogenous spread of the virus, and that ii) although M ϕ play important roles in the host's antiviral immune reaction these cells seem to support viral immune evasion. Previous data of our laboratory demonstrated that both, pro-inflammatory M1-M ϕ and anti-inflammatory M2-M ϕ could be infected by the endotheliotropic HCMV strain TB40/E. However, the susceptibility to HCMV infection, quantified as the percentage of cells expressing the immediate early gene products IE 1-2 at 24 hours post infection, was dramatically different: very low (roughly 30%) into M1-M ϕ , and in contrast very high (roughly 70%) in M2-M ϕ . Because it was still not known how HCMV enters and establishes infection into M ϕ , we decided to investigate HCMV the entry mechanisms into these two types of M ϕ . In order to explain the difference of HCMV susceptibility and shed some light on the molecular mechanism of HCMV entry into M ϕ we performed sub-cellular and ultrastructural analysis by applying a great range of light microscopic and electron microscopic techniques.

The first data obtained by light and electron microscopy clearly showed that shortly after infection (from 2-3 minutes until 3 hours) HCMV particles acquired different cellular distribution in M1- and M2-M ϕ . While the majority of vesicles containing viral particles remained in the cell periphery in M1-M ϕ , they accumulated in proximity of the nucleus in M2-M ϕ thus suggesting a more efficient intracellular translocation in this cell type. Even though these techniques do not allow the quantification of the absolute number of internalized particles, we believe that the amount of virions inside M2-M ϕ is higher than in M1-M ϕ .

One of the main processes used by M ϕ to internalize fluids and particles is macropinocytosis, an actin-dependent endocytotic process involving plasma membrane ruffles and large uncoated vesicles. Since the size of HCMV particles is compatible with the average size of macropinosomes, we considered macropinocytosis as a mechanism used by HCMV to enter M ϕ . Ultrastructural analysis and light microscopic pictures

showed that HCMV vesicles localize preferentially in close proximity of membrane extensions morphologically reminiscent of macropinocytic ruffles. In addition, since the actin polymerization inhibitor Latrunculin A caused a significant reduction of the IE 1-2 expression in M1- and M2-M ϕ , we could demonstrate that actin polymerization, a process required for the extension and movements of the macropinocytic ruffles, was also required for HCMV infection. Finally, keeping on mind that macropinosome formation appears to be uniquely susceptible to inhibition by amiloride and its analogues, by using EIPA (ethylisopropylamiloride) we could show that both the expression of IE 1-2 viral proteins and the formation of HCMV containing vesicles was inhibited in both M1-and M2-M ϕ . All together our data provided strong evidence that the HCMV infection process in M1- and M2-M ϕ fulfills the criteria that define macropinocytosis as previously defined by others.

Another peculiar feature of macropinocytosis is the high sensitivity to pH variation. By using bafilomycin A, monensin and ammonium chloride as lysosomotropic agents inhibiting the endosomal and cytoplasm acidification, respectively we obtained strong reduction in the percentage IE 1-2 positive cells thus demonstrating that HCMV infection of M1- and M2-M ϕ takes place by a pH-dependent pathway. The lack of physical proximity between viral particles and markers of late endosomes suggests that the vesicles containing HCMV particles do not undergo along the degradative pathway. Instead, shortly after pH acidification of the vesicles HCMV capsids are released from the endosome by fusion of the viral envelope with the endosomal membrane.

In summary, our data indicate that HCMV is internalized in M1- and M2-M ϕ by a macropinocytosis pathway followed by a pH-dependent release of the capsids.

6. Reference

1. **Aderem, A. and D. M. Underhill.** 1999. Mechanisms of phagocytosis in macrophages. *Annu. Rev. Immunol.* **17**:593-623.
2. **Adler, B., L. Scrivano, Z. Ruzcics, B. Rupp, C. Sinzger, and U. Koszinowski.** 2006. Role of human cytomegalovirus UL131A in cell type-specific virus entry and release. *J. Gen. Virol.* **87**:2451-2460.
3. **Akagawa, K. S.** 2002. Functional heterogeneity of colony-stimulating factor-induced human monocyte-derived macrophages. *Int. J. Hematol.* **76**:27-34.
4. **Akagawa, K. S., I. Komuro, H. Kanazawa, T. Yamazaki, K. Mochida, and F. Kishi.** 2006. Functional heterogeneity of colony-stimulating factor-induced human monocyte-derived macrophages. *Respirology.* **11 Suppl**:S32-S36.
5. **Becker, L. B., D. W. Smith, and K. V. Rhodes.** 1993. Incidence of cardiac arrest: a neglected factor in evaluating survival rates. *Ann. Emerg. Med.* **22**:86-91.
6. **Bishop, N. E.** 1997. An Update on Non-clathrin-coated Endocytosis 1. *Rev. Med. Virol.* **7**:199-209.
7. **Bodaghi, B., M. E. Slobbe-van Drunen, A. Topilko, E. Perret, R. C. Vossen, M. C. van Dam-Mieras, D. Zipeto, J. L. Virelizier, P. LeHoang, C. A. Bruggeman, and S. Michelson.** 1999. Entry of human cytomegalovirus into retinal pigment epithelial and endothelial cells by endocytosis. *Invest Ophthalmol. Vis. Sci.* **40**:2598-2607.
8. **Bullough, P. A. and P. A. Tulloch.** 1991. Spot-scan imaging of microcrystals of an influenza neuraminidase-antibody fragment complex. *Ultramicroscopy* **35**:131-143.
9. **Campadelli-Fiume, G., L. Menotti, E. Avitabile, and T. Gianni.** 2012. Viral and cellular contributions to herpes simplex virus entry into the cell. *Curr. Opin. Virol.* **2**:28-36.
10. **Chan, G., M. T. Nogalski, and A. D. Yurochko.** 2009. Activation of EGFR on monocytes is required for human cytomegalovirus entry and mediates cellular motility
1. *Proc. Natl. Acad. Sci. U. S. A* **106**:22369-22374.
11. **Chen, J., K. H. Lee, D. A. Steinhauer, D. J. Stevens, J. J. Skehel, and D. C. Wiley.** 1998. Structure of the hemagglutinin precursor cleavage site, a determinant of influenza pathogenicity and the origin of the labile conformation. *Cell* **95**:409-417.
12. **Compton, T. and A. Feire.** 2007. Early events in human cytomegalovirus infection.

13. **Compton, T., R. R. Nepomuceno, and D. M. Nowlin.** 1992. Human cytomegalovirus penetrates host cells by pH-independent fusion at the cell surface. *Virology* **191**:387-395.
14. **Conner, S. D. and S. L. Schmid.** 2003. Regulated portals of entry into the cell. *Nature* **422**:37-44.
15. **Crough, T. and R. Khanna.** 2009. Immunobiology of human cytomegalovirus: from bench to bedside. *Clin. Microbiol. Rev.* **22**:76-98, Table.
16. **Damm, E. M., L. Pelkmans, J. Kartenbeck, A. Mezzacasa, T. Kurzchalia, and A. Helenius.** 2005. Clathrin- and caveolin-1-independent endocytosis: entry of simian virus 40 into cells devoid of caveolae. *J. Cell Biol.* **168**:477-488.
17. **Doherty, G. J. and H. T. McMahon.** 2009. Mechanisms of endocytosis. *Annu. Rev. Biochem.* **78**:857-902.
18. **Dohner, K. and B. Sodeik.** 2005. The role of the cytoskeleton during viral infection. *Curr. Top. Microbiol. Immunol.* **285**:67-108.
19. **Falcone, S., E. Cocucci, P. Podini, T. Kirchhausen, E. Clementi, and J. Meldolesi.** 2006. Macropinocytosis: regulated coordination of endocytic and exocytic membrane traffic events 1. *J. Cell Sci.* **119**:4758-4769.
20. **Feire, A. L., H. Koss, and T. Compton.** 2004. Cellular integrins function as entry receptors for human cytomegalovirus via a highly conserved disintegrin-like domain. *Proc. Natl. Acad. Sci. U. S. A* **101**:15470-15475.
21. **Fish, K. N., W. Britt, and J. A. Nelson.** 1996. A novel mechanism for persistence of human cytomegalovirus in macrophages. *J. Virol.* **70**:1855-1862.
22. **Fleetwood, A. J., H. Dinh, A. D. Cook, P. J. Hertzog, and J. A. Hamilton.** 2009. GM-CSF- and M-CSF-dependent macrophage phenotypes display differential dependence on type I interferon signaling. *J. Leukoc. Biol.* **86**:411-421.
23. **Frascaroli, G., S. Varani, C. Bayer, L. Wang, S. X. Zhou, S. Straschewski, P. Walther, M. Bacher, C. Soderberg-Naucler, and T. Mertens.** 2012. Human cytomegalovirus infection of M1 and M2 macrophages triggers inflammation and autologous T-cell proliferation. *J. Virol.*
24. **Gerna, G., E. Percivalle, F. Baldanti, S. Sozzani, P. Lanzarini, E. Genini, D. Lilleri, and M. G. Revello.** 2000. Human cytomegalovirus replicates abortively in polymorphonuclear leukocytes after transfer from infected endothelial cells via transient microfusion events. *J. Virol.* **74**:5629-5638.
25. **Ghigo, E., J. Kartenbeck, P. Lien, L. Pelkmans, C. Capo, J. L. Mege, and D. Raoult.** 2008. Ameobal pathogen mimivirus infects macrophages through phagocytosis 20. *PLoS. Pathog.* **4**:e1000087.

26. **Giugni, T. D., C. Soderberg, D. J. Ham, R. M. Bautista, K. O. Hedlund, E. Moller, and J. A. Zaia.** 1996. Neutralization of human cytomegalovirus by human CD13-specific antibodies. *J. Infect. Dis.* **173**:1062-1071.
27. **Harrison, S. C.** 2008. The pH sensor for flavivirus membrane fusion. *J. Cell Biol.* **183**:177-179.
28. **Haspot, F., A. Lavault, C. Sinzger, S. K. Laib, Y. D. Stierhof, P. Pilet, C. Bressolette-Bodin, and F. Halary.** 2012. Human cytomegalovirus entry into dendritic cells occurs via a macropinocytosis-like pathway in a pH-independent and cholesterol-dependent manner. *PLoS. One.* **7**:e34795.
29. **Helenius, A., J. Kartenbeck, K. Simons, and E. Fries.** 1980. On the entry of Semliki forest virus into BHK-21 cells. *J. Cell Biol.* **84**:404-420.
30. **Hewlett, L. J., A. R. Prescott, and C. Watts.** 1994. The coated pit and macropinocytic pathways serve distinct endosome populations. *J. Cell Biol.* **124**:689-703.
31. **Homman-Loudiyi, M., K. Hultenby, W. Britt, and C. Soderberg-Naucler.** 2003. Envelopment of human cytomegalovirus occurs by budding into Golgi-derived vacuole compartments positive for gB, Rab 3, trans-golgi network 46, and mannosidase II. *J. Virol.* **77**:3191-3203.
32. **Jarvis, M. A. and J. A. Nelson.** 2002. Human cytomegalovirus persistence and latency in endothelial cells and macrophages. *Curr. Opin. Microbiol.* **5**:403-407.
33. **Johannsdottir, H. K., R. Mancini, J. Kartenbeck, L. Amato, and A. Helenius.** 2009. Host cell factors and functions involved in vesicular stomatitis virus entry. *J. Virol.* **83**:440-453.
34. **Johnson, R. A., X. Wang, X. L. Ma, S. M. Huong, and E. S. Huang.** 2001. Human cytomegalovirus up-regulates the phosphatidylinositol 3-kinase (PI3-K) pathway: inhibition of PI3-K activity inhibits viral replication and virus-induced signaling. *J. Virol.* **75**:6022-6032.
35. **Kerr, M. C. and R. D. Teasdale.** 2009. Defining macropinocytosis. *Traffic.* **10**:364-371.
36. **Kielian, M. C., M. Marsh, and A. Helenius.** 1986. Kinetics of endosome acidification detected by mutant and wild-type Semliki Forest virus. *EMBO J.* **5**:3103-3109.
37. **Kinzler, E. R. and T. Compton.** 2005. Characterization of human cytomegalovirus glycoprotein-induced cell-cell fusion. *J. Virol.* **79**:7827-7837.
38. **Kirkham, M. and R. G. Parton.** 2005. Clathrin-independent endocytosis: new insights into caveolae and non-caveolar lipid raft carriers 3. *Biochim. Biophys. Acta* **1746**:349-363.
39. **Koivusalo, M., C. Welch, H. Hayashi, C. C. Scott, M. Kim, T. Alexander, N. Touret, K. M. Hahn, and S. Grinstein.** 2010. Amiloride inhibits

- macropinocytosis by lowering submembranous pH and preventing Rac1 and Cdc42 signaling. *J. Cell Biol.* **188**:547-563.
40. **Kremer, J. R., D. N. Mastronarde, and J. R. McIntosh.** 1996. Computer visualization of three-dimensional image data using IMOD 1. *J. Struct. Biol.* **116**:71-76.
 41. **Kumari, S., S. Mg, and S. Mayor.** 2010. Endocytosis unplugged: multiple ways to enter the cell. *Cell Res.* **20**:256-275.
 42. **laib Sampaio, K., Y. Cavignac, Y. D. Stierhof, and C. Sinzger.** 2004. Human cytomegalovirus labeled with green fluorescent protein for live analysis of intercellular particle movements. *Virology* **79**:2754-2767.
 43. **Lakadamyali, M., M. J. Rust, and X. Zhuang.** 2006. Ligands for clathrin-mediated endocytosis are differentially sorted into distinct populations of early endosomes. *Cell* **124**:997-1009.
 44. **Li, L., J. A. Nelson, and W. J. Britt.** 1997. Glycoprotein H-related complexes of human cytomegalovirus: identification of a third protein in the gCIII complex. *J. Virol.* **71**:3090-3097.
 45. **Lim, J. P. and P. A. Gleeson.** 2011. Macropinocytosis: an endocytic pathway for internalising large gulps 2. *Immunol. Cell Biol.* **89**:836-843.
 46. **Mantovani, A., T. Schioppa, C. Porta, P. Allavena, and A. Sica.** 2006. Role of tumor-associated macrophages in tumor progression and invasion. *Cancer Metastasis Rev.* **25**:315-322.
 47. **Marsh, M. and A. Helenius.** 2006. Virus entry: open sesame. *Cell* **124**:729-740.
 48. **Mayor, S. and R. E. Pagano.** 2007. Pathways of clathrin-independent endocytosis. *Nat. Rev. Mol. Cell Biol.* **8**:603-612.
 49. **McKeating, J. A., J. E. Grundy, Z. Varghese, and P. D. Griffiths.** 1986. Detection of cytomegalovirus by ELISA in urine samples is inhibited by beta 2 microglobulin. *J. Med. Virol.* **18**:341-348.
 50. **Mercer, J. and A. Helenius.** 2009. Virus entry by macropinocytosis. *Nat. Cell Biol.* **11**:510-520.
 51. **Mercer, J., M. Schelhaas, and A. Helenius.** 2010. Virus entry by endocytosis. *Annu. Rev. Biochem.* **79**:803-833.
 52. **Mettenleiter, T. C.** 2002. Herpesvirus assembly and egress 9. *J. Virol.* **76**:1537-1547.
 53. **Mettenleiter, T. C.** 2004. Budding events in herpesvirus morphogenesis 1. *Virus Res.* **106**:167-180.
 54. **Minami, K., Y. Tambe, R. Watanabe, T. Isono, M. Haneda, K. Isobe, T. Kobayashi, O. Hino, H. Okabe, T. Chano, and H. Inoue.** 2007. Suppression of

- viral replication by stress-inducible GADD34 protein via the mammalian serine/threonine protein kinase mTOR pathway. *J. Virol.* **81**:11106-11115.
55. **Mocarski, E. S.** 1996. Cytomegaloviruses and their replication, p. 2447-2492. *In* B. N. Fields, D. M. Knipe, and P. M. Howley (eds.), *Fields Virology*, vol. 1. Lippincott-Raven, Philadelphia.
56. **Mocarski, J.** 2007. Betaherpes viral genes and their functions.
57. **Modrow S, Falke D, and Truyen U.** 2003. *Molekulare Virologie*. Akademischer Verlag GmbH Heidelberg.
58. **Mukherjee, S. and F. R. Maxfield.** 2004. Lipid and cholesterol trafficking in NPC. *Biochim. Biophys. Acta* **1685**:28-37.
59. **Mukhopadhyay, S., B. S. Kim, P. R. Chipman, M. G. Rossmann, and R. J. Kuhn.** 2003. Structure of West Nile virus. *Science* **302**:248.
60. **Murphy, E., I. Rigoutsos, T. Shibuya, and T. E. Shenk.** 2003. Reevaluation of human cytomegalovirus coding potential. *Proc Natl Acad Sci USA* **100**:13585-13590.
61. **Nemerow, G. R. and N. R. Cooper.** 1984. Early events in the infection of human B lymphocytes by Epstein-Barr virus: the internalization process 3. *Virology* **132**:186-198.
62. **Nichols, B. J. and J. Lippincott-Schwartz.** 2001. Endocytosis without clathrin coats
1. *Trends Cell Biol.* **11**:406-412.
63. **Nicola, A. V., J. Hou, E. O. Major, and S. E. Straus.** 2005. Herpes simplex virus type 1 enters human epidermal keratinocytes, but not neurons, via a pH-dependent endocytic pathway. *J. Virol.* **79**:7609-7616.
64. **Orenstein, J. M. and F. Jannotta.** 1988. Human immunodeficiency virus and papovavirus infections in acquired immunodeficiency syndrome: an ultrastructural study of three cases
23. *Hum. Pathol.* **19**:350-361.
65. **Parihar, A., T. D. Eubank, and A. I. Doseff.** 2010. Monocytes and macrophages regulate immunity through dynamic networks of survival and cell death. *J. Innate. Immun.* **2**:204-215.
66. **Parton, R. G. and A. A. Richards.** 2003. Lipid rafts and caveolae as portals for endocytosis: new insights and common mechanisms. *Traffic.* **4**:724-738.
67. **Pelkmans, L. and A. Helenius.** 2002. Endocytosis via caveolae. *Traffic.* **3**:311-320.
68. **Pelkmans, L., J. Kartenbeck, and A. Helenius.** 2001. Caveolar endocytosis of simian virus 40 reveals a new two-step vesicular-transport pathway to the ER. *Nat. Cell Biol.* **3**:473-483.

69. **Peluso, R., A. Haase, L. Stowring, M. Edwards, and P. Ventura.** 1985. A Trojan Horse mechanism for the spread of visna virus in monocytes
1. *Virology* **147**:231-236.
70. **Pietropaolo, R. and T. Compton.** 1999. Interference with annexin II has no effect on entry of human cytomegalovirus into fibroblast cells. *J. Gen. Virol.* **80** (Pt 7):1807-1816.
71. **Poglitsch, M., T. Weichhart, M. Hecking, J. Werzowa, K. Katholnig, M. Antlanger, A. Krmpotic, S. Jonjic, W. H. Horl, G. J. Zlabinger, E. Puchhammer, and M. D. Saemann.** 2012. CMV late phase-induced mTOR activation is essential for efficient virus replication in polarized human macrophages
1. *Am. J. Transplant.* **12**:1458-1468.
72. **Porcheray, F., S. Viaud, A. C. Rimaniol, C. Leone, B. Samah, N. reuddre-Bosquet, D. Dormont, and G. Gras.** 2005. Macrophage activation switching: an asset for the resolution of inflammation. *Clin. Exp. Immunol.* **142**:481-489.
73. **Price, R. W., B. Brew, J. Sidtis, M. Rosenblum, A. C. Scheck, and P. Cleary.** 1988. The brain in AIDS: central nervous system HIV-1 infection and AIDS dementia complex
1. *Science* **239**:586-592.
74. **Racoosin, E. L. and J. A. Swanson.** 1993. Macropinosome maturation and fusion with tubular lysosomes in macrophages. *J. Cell Biol.* **121**:1011-1020.
75. **Raghu, H., N. Sharma-Walia, M. V. Veettil, S. Sadagopan, and B. Chandran.** 2009. Kaposi's sarcoma-associated herpesvirus utilizes an actin polymerization-dependent macropinocytic pathway to enter human dermal microvascular endothelial and human umbilical vein endothelial cells. *J. Virol.* **83**:4895-4911.
76. **Reddehase, M. J. and Lemmermann N.** 2006. Cytomegalovirus *Molecular Biology and Immunology.*
77. **Roche, S. and Y. Gaudin.** 2002. Characterization of the equilibrium between the native and fusion-inactive conformation of rabies virus glycoprotein indicates that the fusion complex is made of several trimers. *Virology* **297**:128-135.
78. **Roizman, B., L. E. Carmichael, F. Deinhardt, G. de-The, A. J. Nahmias, W. Plowright, F. Rapp, P. Sheldrick, M. Takahashi, and K. Wolf.** 1981. Herpesviridae. Definition, provisional nomenclature, and taxonomy. The Herpesvirus Study Group, the International Committee on Taxonomy of Viruses. *Intervirology* **16**:201-217.
79. **Romo, N., G. Magri, A. Muntasell, G. Heredia, D. Baia, A. Angulo, M. Guma, and M. López-Botet.** 2011. Natural killer cell-mediated response to human cytomegalovirus-infected macrophages is modulated by their functional polarization. *Journal of Leukocyte Biology* **90**:1-10.

80. **Rust, M. J., M. Lakadamyali, F. Zhang, and X. Zhuang.** 2004. Assembly of endocytic machinery around individual influenza viruses during viral entry. *Nat. Struct. Mol. Biol.* **11**:567-573.
81. **Ryckman, B. J., M. A. Jarvis, D. D. Drummond, J. A. Nelson, and D. C. Johnson.** 2006. Human cytomegalovirus entry into epithelial and endothelial cells depends on genes UL128 to UL150 and occurs by endocytosis and low-pH fusion. *J. Virol.* **80**:710-722.
82. **Sarkar, S. and D. A. Fox.** 2005. Dendritic cells in rheumatoid arthritis 4. *Front Biosci.* **10**:656-665.
83. **Scrivano, L., C. Sinzger, H. Nitschko, U. H. Koszinowski, and B. Adler.** 2011. HCMV spread and cell tropism are determined by distinct virus populations. *PLoS. Pathog.* **7**:e1001256.
84. **Shimamura, M., M. Mach, and W. J. Britt.** 2006. Human cytomegalovirus infection elicits a glycoprotein M (gM)/gN-specific virus-neutralizing antibody response. *J. Virol.* **80**:4591-4600.
85. **Sieczkarski, S. B. and G. R. Whittaker.** 2002. Dissecting virus entry via endocytosis. *J. Gen. Virol.* **83**:1535-1545.
86. **Simons, K. and D. Toomre.** 2000. Lipid rafts and signal transduction. *Nat. Rev. Mol. Cell Biol.* **1**:31-39.
87. **Sinzger, C.** 2008. Entry route of HCMV into endothelial cells. *J. Clin. Virol.* **41**:174-179.
88. **Sinzger, C., M. Digel, and G. Jahn.** 2008. Cytomegalovirus cell tropism. *Curr. Top. Microbiol. Immunol.* **325**:63-83.
89. **Sinzger, C., K. Eberhardt, Y. Cavnac, C. Weinstock, T. Kessler, G. Jahn, and J. L. Davignon.** 2006. Macrophage cultures are susceptible to lytic productive infection by endothelial-cell-propagated human cytomegalovirus strains and present viral IE1 protein to CD4+ T cells despite late downregulation of MHC class II molecules. *J. Gen. Virol.* **87**:1853-1862.
90. **Sinzger, C., A. Grefte, B. Plachter, A. S. Gouw, T. H. The, and G. Jahn.** 1995. Fibroblasts, epithelial cells, endothelial cells and smooth muscle cells are major targets of human cytomegalovirus infection in lung and gastrointestinal tissues. *J. Gen. Virol.* **76 (Pt 4)**:741-750.
91. **Sinzger, C., M. Kahl, K. Laib, K. Klingel, P. Rieger, B. Plachter, and G. Jahn.** 2000. Tropism of human cytomegalovirus for endothelial cells is determined by a post-entry step dependent on efficient translocation to the nucleus. *J Gen Virol* **81**:3021-3035.
92. **Sinzger, C., J. Knapp, K. Schmidt, M. Kahl, and G. Jahn.** 1999. A simple and rapid method for preparation of viral DNA from cell associated cytomegalovirus. *J. Virol. Methods* **81**:115-122.

93. **Slobbe-van Drunen, M. E., A. T. Hendrickx, R. C. Vossen, E. J. Speel, M. C. van Dam-Mieras, and C. A. Bruggeman.** 1998. Nuclear import as a barrier to infection of human umbilical vein endothelial cells by human cytomegalovirus strain AD169. *Virus Res.* **56**:149-156.
94. **Smith, A. E. and A. Helenius.** 2004. How viruses enter animal cells. *Science* **304**:237-242.
95. **Smith, M. S., G. L. Bentz, J. S. Alexander, and A. D. Yurochko.** 2004. Human cytomegalovirus induces monocyte differentiation and migration as a strategy for dissemination and persistence. *J. Virol.* **78**:4444-4453.
96. **Sodeik, B., M. W. Ebersold, and A. Helenius.** 1997. Microtubule-mediated transport of incoming herpes simplex virus 1 capsids to the nucleus. *J. Cell Biol.* **136**:1007-1021.
97. **Soderberg, C., T. D. Giugni, J. A. Zaia, S. Larsson, J. M. Wahlberg, and E. Moller.** 1993. CD13 (human aminopeptidase N) mediates human cytomegalovirus infection
5. *J. Virol.* **67**:6576-6585.
98. **Straschewski, S., M. Patrone, P. Walther, A. Gallina, T. Mertens, and G. Frascaroli.** 2011. Protein pUL128 of human cytomegalovirus is necessary for monocyte infection and blocking of migration
1. *J. Virol.* **85**:5150-5158.
99. **Sun, M. L., J. H. Piao, C. C. Yin, G. S. Yang, and H. L. Huang.** 2005. [A preliminary study of the structure prediction and expression of SARS-CoV spike protein]. *Yi. Chuan* **27**:623-628.
100. **Swanson, J. A. and C. Watts.** 1995. Macropinocytosis. *Trends Cell Biol.* **5**:424-428.
101. **Taylor-Wiedeman, J., J. G. Sissons, L. K. Borysiewicz, and J. H. Sinclair.** 1991. Monocytes are a major site of persistence of human cytomegalovirus in peripheral blood mononuclear cells. *J. Gen. Virol.* **72 (Pt 9)**:2059-2064.
102. **Tiwari, V., C. Clement, P. M. Scanlan, D. Kowlessur, B. Y. Yue, and D. Shukla.** 2005. A role for herpesvirus entry mediator as the receptor for herpes simplex virus 1 entry into primary human trabecular meshwork cells. *J. Virol.* **79**:13173-13179.
103. **Tomtishen, J. P., III.** 2012. Human cytomegalovirus tegument proteins (pp65, pp71, pp150, pp28)
1. *J. Virol.* **9**:22.
104. **Tooze, J., M. Hollinshead, B. Reis, K. Radsak, and H. Kern.** 1993. Progeny vaccinia and human cytomegalovirus particles utilize early endosomal cisternae for their envelopes. *Eur. J. Cell Biol.* **60**:163-178.
105. **Ungewickell, E. J. and L. Hinrichsen.** 2007. Endocytosis: clathrin-mediated membrane budding. *Curr. Opin. Cell Biol.* **19**:417-425.

106. **Waldman, W. J., D. A. Knight, E. H. Huang, and D. D. Sedmak.** 1995. Bidirectional transmission of infectious cytomegalovirus between monocytes and vascular endothelial cells: an in vitro model. *J Infect Dis* **171**:263-272.
107. **Walther, P. and J. Hentschel.** 1989. Improved representation of cell surface structures by freeze substitution and backscattered electron imaging 1. *Scanning Microsc. Suppl* **3**:201-210.
108. **Wang, D. and T. Shenk.** 2005. Human cytomegalovirus UL131 open reading frame is required for epithelial cell tropism. *J. Virol.* **79**:10330-10338.
109. **Wang, F., H. W. Wang, D. R. Lu, J. L. Xue, and X. Zhang.** 2003. [Vesicular stomatitis virus G-protein retrovector mediated a herpes simplex virus thymidine kinase gene transduction and expression in the human retinal pigment epithelial cells]. *Zhonghua Yan. Ke. Za Zhi.* **39**:201-205.
110. **Wiley, D. C., I. A. Wilson, and J. J. Skehel.** 1981. Structural identification of the antibody-binding sites of Hong Kong influenza haemagglutinin and their involvement in antigenic variation. *Nature* **289**:373-378.
111. **Wilson, I. A., J. J. Skehel, and D. C. Wiley.** 1981. Structure of the haemagglutinin membrane glycoprotein of influenza virus at 3 Å resolution. *Nature* **289**:366-373.
112. **Wright, J. F., A. Kurosky, E. L. Pryzdial, and S. Wasi.** 1995. Host cellular annexin II is associated with cytomegalovirus particles isolated from cultured human fibroblasts
1. *J. Virol.* **69**:4784-4791.
113. **Yonezawa, A., M. Cavrois, and W. C. Greene.** 2005. Studies of ebola virus glycoprotein-mediated entry and fusion by using pseudotyped human immunodeficiency virus type 1 virions: involvement of cytoskeletal proteins and enhancement by tumor necrosis factor alpha
1. *J. Virol.* **79**:918-926.

Acknowledgements

Firstly I would like to give my great thanks to Prof. Mertens and Prof. Walther. Thank you both for giving me the opportunity to continue with my PhD study in the institute of virology and the central electron microscopy facility after my diploma study. I am always feeling free and independent with getting supports on time during my study. Special thanks to my supervisor, Dr. Giada Frascaroli, for the constitutive supports and discussions over the years. During my work as well as in my private life, she is always thoughtful and outstanding intelligent with sharing me her expert experiences.

I thank all my colleagues in both the virology and the EM laboratories for their support. Special thanks to Eberhard Schmid for his expert technical assistance and a big thank goes to Carina Bayer, Zeguang Wu, and Sarah Straschewski, the colleagues in our work group. In the time I am pregnant, they are always helping me at experiments in the labor and encouraging me to finish my thesis during the last year of my PhD study.

At the end, I would like to give many thanks to my family. They are always supporting me and encouraging me in all time. Thanks Papa and Mama for always supporting me in any phase of my life. Pengjie, my husband, thanks for your love. You are always standing beside me and do not complain anything to support my work on the weekend, for example, fixing the cells by high pressure freezing. They are going to be your few of biology laboratory experiences.

Curriculum Vitae

Li Wang

E-mail: liwang@gmx.de

Date of birth: 11.08.1977 in Hebei, China

Education

- 09/2009-present Institute of Virology, University Hospital Ulm
Dissertation in Human Biology
- 10/2005-08/2009 Ulm University
Course of studies: Biology (molecular biology, endocrinology, microbiology, cell biology, mathematics, pharmacology)
Degree awarded: Diplom-Biologie
- 10/2003-09/2005 Ulm University
Course of studies: Biology
Degree awarded: Vordiplom in Biologie
- 04/2003-09/2003 Goettingen University
German language course
DSH test passed
- 10/2002-03/2003 Ulm University
German language course
- 10/2001-09/2002 Goethe Institut in Beijing
German language course, mittel-stufe reif
- 08/2000-09/2001 Naqiu dentistry praxis in Beijing
Work as assistant dentist

09/1997-07/2000 Beijing University
Dental medicine
Degree awarded: 3 years degree

09/1994-08/1997 The No. 55 school in Beijing
Abitur

Language and IT-Skills:

Languages: Chinese: native language

German: fluent in writing and speaking

English: fluent in writing and speaking

IT-skills: Microsoft Office, Adobe Photoshop

Methodical skills:

Molecular biology: Infection and cultivation of human cells (primary macrophages, fibroblast, endothelia cells); DNA-preparation and –purification; protein purification and characterization; Immunoassay

Electron microscopy: Scanning electron microscopy; Transmission electron microscopy; Immunofluorescence microscopy; light microscopy; high-pressure freezing and freeze substitution

Virology: Cultivation, concentration, purification and titration of human pathogenic viruses; Regular working under safety conditions (S1, S2)

Profound knowledge in blood; handling of blood samples.

Additional information:

Hobbies: Reading; painting; cooking; Aerobics; dancing; swimming

Peer reviewed papers:

- Höhn K, Sailer M, Wang L, Lorenz L, Schneider EM, Walther P. (2011) *Preparation of cryofixed cells for improved 3D ultrastructure with scanning transmission electron tomography*. Histochem Cell boil. 135, 1-9
- Bayer C, Varani S, Wang L, Walther P, Zhou S, Straschewski S, Bachem M, Söderberg-Naucler C, Frascaroli G. (2012) *Human cytomegalovirus infection of M1 and M2 macrophages triggers inflammation and autologous T-cell proliferation*. J Virol. 87(1): 67-79
- Wu Z, Sinzger C, Frascaroli G, Reichel J, Bayer C, Wang L, Schirmbeck R, Mertens T. (2013) *HCMV induced NKG2ChiCD57hi natural killer cells are effectors depending on humoral antiviral immunity*. J Virol. 01096-13

Book article:

- Walther P, Wang L, Ließem S, and Frascaroli G. (2010) *Viral infection of cells in Culture- Approaches for Electron Microscopy*. In (Mueller-Reichert T. Ed) METHODS IN CELL BIOLOGY, VOL, 96. Pp 603-618. Copyright 2010 Elsevier Inc. (book article)

Manuscript in preparation:

- Wang L., Walther P, Mertens T, Frascaroli G. *Human cytomegalovirus enter into M1- and M2- macrophages by macropinocytosis in a low pH-dependent manner*

Diploma thesis:

- Wang L. (2009): *Eintrittsmechanismen des humanen Cytomegalievirus in M- und GM- Makrophagen untersucht mit modernen mikroskopischen Methode*

Diploma thesis, Electron Microscopy Facility, Ulm University

Abstracts with poster presentation:

- Wang L, Mertens T, Walther P, Frascaroli G (2012): *The entry route of HCMV in M1 and M2 macrophages*. 22nd Annual Meeting of the GfV, March 14-17 2012, Essen, Germany.
- Wang L., Walther P, Mertens T, Frascaroli G (2011): *Human cytomegalovirus (HCMV) enter into M1- and M2- monocyte derived macrophages through a*

macropinocytosis and low pH dependent mechanism. 21st Annual Meeting of the Society for Virology, March 23-26, Freiburg, Germany

- Wang L., Walther P., Mertens T., Frascaroli G. (2011): *Human cytomegalovirus (HCMV) enter into M1- and M2- monocyte derived macrophages through a macropinocytosis and low pH dependent mechanisms.* 13th international CMV/BetaHepersvirus Workshop, May 14-17, Nuremberg, Germany.
- Wang L., Walther P., Mertens T., Frascaroli G. (2010): *Entry mechanisms of human cytomegalovirus (HCMV) into M1- and M2- monocyte derived macrophages.* 4th European Congress of Virology, Society for Virology, March 7-11 2010, Cernobbio, Italy.

Abstracts with oral presentation:

- Wang L., Mertens T, Walther P, Frascaroli G (2011): *Ultra structural analysis of HCMV infection in M1 and M2 macrophages.* Microscopy Congress, 28 August-02 September 2011, Kiel, Germany
- Wang L., Walther P., Walther P., Frascaroli G. (2009): *Entry mechanisms of human cytomegalovirus (HCMV) into GM- and M-monocyte derived macrophages.* Microscopy Conference, 30 Aug- 4 Sept 2009, Graz, Austria.

Ulm, 22.11.2012 Li Wang